REPORT

Tonkin+Taylor

Manukau Harbour Port Feasibility Study

Coastal - Final Technical Working Paper

Prepared for

Ministry of Transport | Te Manatū Waka

Prepared by

Tonkin & Taylor Ltd

Date

June 2024

Job Number

1018198-CPR v1.0

Together we create and sustain a better world

www.tonkintaylor.co.nz

Document control

Title: Manukau Harbour Port Feasibility Study					
Date	**Version**	**Description**	**Prepared by:**	**Reviewed by:**	**Authorised by:**
23/02/24	0.1	Final Technical Working Paper (draft)	Tom Shand Peter Quilter	Andrew Brown Mal Green	Richard Reinen-Hamill
11/05/24	1.0	Final Technical Working Paper (final)	Tom Shand Peter Quilter	Andrew Brown Mal Green	Richard Reinen-Hamill

Distribution:

Ministry of Transport | Te Manatū Waka — 1 PDF copy

Beca — 1 PDF copy

HR Wallingford — 1 PDF copy

Tonkin & Taylor Ltd (FILE) — electronic copies

Table of contents

Executive summary

This Technical Working Paper 03 Coastal has been prepared by Tonkin & Taylor Ltd and accompanies the study Final Report. This Paper synthesises existing coastal, geological, and environmental knowledge of the Manukau Harbour and supplements this knowledge with results from the field data collection (refer *TWP02*), bar morphology analysis (refer *TWP03a*) and numerical modelling relating to the existing conditions and processes (refer *TWP03b* and *TWP03c*). This paper then summarises the likely implications of the proposed dredged navigation channel (*TWP04*) works in terms of channel stability, sediment infill and impacts on coastal and harbour processes. Implications on navigational operability and dredging are presented in *TWP05* an *TWP06*.

The Manukau Harbour is a drowned river valley and is New Zealand's second largest estuary. The harbour is located to the southwest of the Auckland isthmus and discharges between the Awhitu Peninsula to the south and Waitākere Ranges to the north to the Tasman Sea. The harbour covers 344 km^2 and comprises shallow, intertidal banks interspersed with deeper channels. The spring tidal range varies from around 3 m at the entrance to 3.6 m in the upper reaches giving a spring tidal prism of around 918M m^3. Currents reach up to 3 m/s within the constricted inlet between the Awhitu Peninsula and Waitākere Ranges.

At the entrance to the Manukau Harbour is a large tidal delta complex, comprising the flood tide delta at the landward end of the entrance channel, and an ebb tidal delta (or *Manukau Bar*) at the seaward end of the channel where it discharges into the Tasman Sea. The deltas are formed as tidal currents moving quickly through the narrow inlet slow down as they enter/exit the inlet and deposit entrained sediment. On the ebb tidal delta, opposing waves from the Tasman Sea move sediment onshore building a shallower area. The Manukau Bar is a very large geomorphological feature containing approximately 1,250M m^3 of sand that is also notable for its dynamic nature with changes in seabed level in the order of 10 to 15 m as the position of the main channel migrates. The Manukau Bar was the scene of New Zealand's worst maritime accident with the HMS Orpheus being wrecked after striking a shallow bar in 1863 resulting in 189 deaths.

As part of the establishment of a port within Manukau Harbour, a navigation channel would be required to be dredged through the Manukau Bar. This study does not compare potential port sites, but rather the most landward location at Puhinui was chosen as a representative port location due to its longer required dredging length compared to other potential sites. Channel design (*TWP 04*) indicates the navigation channel would be dredged to a maximum depth of around -19 m below Chart Datum across the bar, with an additional over-dredge allowance of 1 m, (up to 15 m below current seabed levels depending on the bar configuration), with a width of some 295 m (plus side batters) with dredging across a distance of some 4 km between the deeper offshore areas and the deeper channel between the heads. Inside the harbour the navigation channel extends another 25 to 30 km to reach the potential port location with dredging occurring within the inner 10 to 15 km to a depth of -16 m CD, with an additional over-dredge allowance of 0.5m (up to 10 m below current seabed levels).

Key findings of this coastal process part of the study related to the proposed work are:

- The Manukau Bar is a very large (~1,250M m^3) and very dynamic geomorphological feature. The position of the main outlet channel appears to undergo a semi-regular (~30 year) cyclic process of movement towards the northwest and then breaching through the swash bars to the south. This process appears to have been ongoing since records began in the early 19th century with the present channel (as of 2023) having recently breached to the south (around 2017-18) and is slowly moving towards the west.
- The configuration of the channel and shallow adjacent bars make a considerable difference to the required dredge volumes to establish a channel and plant requirements (refer TWP06). The

present channel configuration represents a ‘lower volume’ state along the proposed channel alignment, with future movement towards the northwest likely to increase the volume of the bars along the alignment (i.e. these will build up as the channel moves off the alignment to the north).

- Sediments on the bar are generally fine to medium sands and inside the harbour are interbedded sands and silts with rare gravel and shell lenses. Existing side slopes vary depending on exposure to tidal currents but in areas of high tidal flow can reach 10° (1V:6H) in the inner harbour and 4° (1V:15H) near the bar. Preliminary geotechnical modelling indicates the proposed channel side slopes are generally stable under static conditions with potential for small displacements in the inner harbour during seismic activity.
- Sediment transport on the open coast is driven by the wave climate out of the Tasman Sea, with waves predominantly arriving from the south-west, arriving slightly oblique to the coastline and driving sediment to the north. Less frequent, but at times highly energetic and highly oblique, waves from the northwest can drive sediment in a southerly direction. Longshore transport rates south of the Manukau Bar have been calculated in the order of 1 to 2M m^3/year (gross) and 0.75 to 1.9M m^3/year (net towards the north). Similar volumes are found by survey to be infilling the entrance channel from the southern bar, likely responsible for moving it to the north.
- Sediment transport patterns around the Manukau Bar are influenced by tidal currents as well as waves. It is characterised by sediment being transported along the coast from the south and deposited into the main entrance channel during flood tides. This material is then transported into the harbour and onto the flood tide delta during flood tides, or offshore during ebb tides, being deposited onto the ebb tide delta as tidal currents dissipate. During wave events, sediment is then transported onshore, building the height of the bar, and north and south onto the adjacent shallower bars due to gradients in radiation stress. Material on these adjacent bars is then moved onshore over the shallow bar system and eventually back into the main channel forming a semi-closed system. Some material is likely lost from this system to the open coast to the north.
- The volume of sediments being transported on the Manukau Bar is considerably higher than on the open coast with modelling showing volumetric transport during high energy events an order of magnitude greater than occurring in the same area on the open coast. This is likely due to a combination of waves mobilising sediment over large areas and strong radiation-stress driven and tidal currents able to transport this material. Similar large gross volumetric changes (with smaller net changes) were identified in analysis of sequential Port of Auckland surveys (TWP03a). As described above, the semi-closed nature of the system means that much larger volumes can be moving around the ebb tidal delta system while lower volumes move along the open coast to the north and south (an analogy being a large mobile reservoir with smaller inflows and outflows).
- The proposed dredged navigation channel may modify hydrodynamic and sediment transport processes on the Manukau Bar and within the harbour as follows:
  - The navigation channel allows the tide to more efficiently enter Manukau Harbour, slightly increasing tidal prism (by around 0.5% during spring tides) and advancing the rate of tidal propagation.
  - Currents are slightly increased within the dredged navigation channel both on the bar and within the harbour, and decreased in adjacent areas. The most notable effect is over the Manukau Bar where the flows are increased by over 1 m/s (or around 50%) higher owing to the greater flow efficiency and less friction provided by the deeper channel.

- Waves tend to refract in the deeper channel and, during outgoing tides around the tidal jet and become focussed on either side, to the south during southwest waves and to the north during northwest waves.
- Sediment transport tends to be increased over the bar with greater scour occurring within the middle parts of the dredged channel and material being deposited further offshore as a more seaward bar develops and at landward end of the dredged channel along with on the adjacent batter slopes. It is likely, though not certain that much of this accumulated material is derived from the eroded area within the channel. Therefore, this rate of change may slow over time as the eroded area reaches a deeper, more stable depth. Sediments accumulating on the side batter would likely persist as currently occurs.
- Slightly increased onshore transport occurs on the shallow bar adjacent to the channel due to the increased wave refraction/focussing. However, this may change in the longer-term as a more seaward bar is developed.
- Dredging inside the harbour in the upper reaches of the Papakura Channel will likely increase flood-tidal (shoreward) transport of fine to medium sands from lower reaches/seaward extents of this channel into the dredged area.

- While the net change in sediment transport within the dredged channel tends to be negative, material does begin to accumulate along the side slope batters and in the inner part of the dredged channel as a bar. If the channel was left for a prolonged period, this bar would develop until it is removed by dredging or a new morphology establishes. This is not compatible with a shipping channel and so material that accumulates above the design depth would need to be removed by dredging.
- A modelling approach that assumes that this material is constantly removed has been adopted to estimate the total material infilling the dredged channel above the design depth. This approach is found to slightly over-estimate infill rates during longer storm events and may over-predict in the longer-term if rates of accumulation decrease as the eroding area within the channel reach a more stable depth. However, based on current understanding of the processes, it is a reasonable representation for a maintained navigation channel in the long-term.
- Total material infilling the dredged channel above the design depth is found to range from 5M to 7.7M m^3/year with an average of 6.55M m^3/year with increased wave climate due to climate change increasing this by around 10% by 2070-2099. This is considerably higher than the longshore transport rates on the adjacent open coast, or the material currently moving into the entrance channel from the south. This is due to the higher volumes of material in circulation on the bar as mentioned above, with much of the material accumulating due to onshore and offshore movement of sediment rather than lateral movement from the adjacent bars. The net change is relatively small by comparison indicating that this change is substantially a readjustment of the profile within the dredged channel.
- Much of this infill occurs in high-energy winter months. The ability to maintain the channel to a design depth will be dependent on the upper working limit (wave height) of the dredging equipment and dredging capacity per day. These are set out within *TWP06* with analysis showing that the proposed equipment can generally maintain a channel dredged to the design depth, but accumulation over the winter months can take some weeks to months to completely remove. Sensitivity testing indicates if the daily production rate is not sufficient or the wave height threshold to enable working is too low, then the channel will be difficult to clear before the next large infill period.
- A high-level assessment of infill rates for a southern channel was undertaken. This channel is in the lower energy flood channel, or 'South Channel' and required a substantially longer length of dredging. Results indicate less infill into the base of the channel compared to the southwest

channel (likely due to lower flows and less readjustment within the channel), but higher infill onto the side batters owing to their longer length.

- The placement of capital and maintenance dredge spoil will affect the geomorphology of the bar and adjacent beach systems. The calculated dredge volumes are substantially larger than the calculated longshore transport rates on adjacent beaches so if the material were all placed downdrift it may affect existing coastal processes on adjacent beaches and, over time, shrink the bar system (though the annual infill and dredge rate is 0.4 to 0.5% of the total ebb tidal delta volume). A reduction in the ebb tidal delta volume may have adverse effects on adjacent coastlines and/or the flood tide delta as sand is 'sourced' from elsewhere to bring the system back to equilibrium. Placement of spoil would need to be designed to maintain the existing sediment transport circulation patterns on the bar and generally keep these circulation patterns in balance.
- During certain stages of the channel and bar evolution, large volumes of sediment (several M m^3) are forced by waves and currents across the proposed channel alignment. However, these changes are likely dependent on sufficient material accumulating on the southern banks to interrupt the strong tidal flows and force the channel to the north. By selective placement of the maintenance dredge spoil, the accumulation of sediment can be likely managed and this process controlled. If this was not the case and sediment continued to accumulate on the south bank and be forced into the channel, either rapid dredging would be required (ideally before the event), or potentially managed by training structures. However, as discussed below, such structures would not likely be suitable in this environment due to the very large scale of the area and dynamic and high energy environment.
- However, the ability of placed sediment to move onshore and be retained in the active littoral system is dependent on the depth it is placed in. Based on the size of the currently proposed dredger, it is unlikely that material would be placed in shallow enough depth to propagate onto the bar and open coast beach in a reasonable (months rather than years) timeframe. Additional investigation would be required to determine whether sediments can be placed in a such a way that they can migrate onto the bar and remain in the littoral system, but may require smaller vessels or other infrastructure.
- Sensitivity assessments have been undertaken using a range of sediment sizes and using a continuous modelling approach with updating morphology compared to the 12-hour scenario approach. These indicate variations in total transport in the order of ± 20% is reasonable. Verification data is, however, limited to limited sediment flux samples and empirical predictions of longshore sediment transport. If stress testing is undertaken, adopting a ± 50% to account for uncertainty in model accuracy due to the lack of verification data and long-term system behaviour is likely prudent at this stage of assessment.
- A range of engineering measures were explored to reduce the volume of maintenance dredge material, provide greater capacity for sediment infill to occur before maintenance dredging would be required, or potentially train the channel if stability of the channel alignment cannot be maintained by dredging alone. The only suitable measure is likely to be dredged sediment traps with other structures unlikely to be effective, or suitable in this environment due to the very large scale of the area and dynamic and high energy environment.
- Inside the harbour, the majority of sand transport is considered to occur along harbour channels in response to tidal currents that are typically ebb-dominant. We estimate around 400,000 to 450,000 m^3/year of sand infill entering the dredged channel base and side batter slopes, although material deposited on side batter slopes may reduce following initial adjustment. These values exclude fine silts and clays which are not modelled and are subject to different transport processes that typically involve resuspension due to wind wave actions and currents in the shallow intertidal areas with movement into the deeper areas due to tidal currents, only settling in deeper areas or where currents are low. Background sedimentation rates of fine silts

and clays of ~5 mm/year measured in nearby sheltered areas have been applied over the proposed dredge area as a check with rates found to be in the order of 5,000 m^3/year - much lower than sand infill - and have therefore been omitted from overall dredge volume estimation.

- New Zealand in general and the Auckland region including Manukau Harbour is exposed to numerous natural hazards. The potential exposure and level of impact to establishing and operating a port in the Manukau Harbour has been considered at a high level. Findings include:
  - Tsunami hazard on the west coast is less than on the east coast. The high velocities resulting from a major tsunami are likely to result in large scale movements within the sandy systems of the nearshore, ebb tide delta, coastline and inner harbour. The dredged navigation channel could be subject to both rapid deposition and erosion in different locations and would need inspection and likely some maintenance dredging to resume operability. However, this is unlikely to result in prolonged closure due to the large amount of maintenance dredging being undertaken and dredging equipment on hand.
  - Earth shaking, ground displacement, and liquefaction can be experienced during seismic events and can cause damage and losses to infrastructure, property, and lives as well as the economy and environment. The National Seismic Hazard Model (NSHM) shows generally low ground accelerations in the southern Auckland region. Given the location of any port will be in the Coastal Marine Area, the risk of earthquake impacts will need to be considered in design of the port and navigation channels. Preliminary assessment of the seismic stability of the dredged navigation side slopes indicates these are generally stable with some limited lateral movement possible within the harbour.
  - The Auckland Volcanic Field (AVF) is located in the central part of the Auckland region and is an active volcanic centre. Any eruption in Auckland will likely cause significant widespread disruption to the region, possibly for an extended time although the initial phase of the activity is likely to be the most catastrophic. Consideration of volcanic hazard risk to a port would need to be carried out in detailed design.
  - Climate change may result in increases in sea level by up to 1.6 m over the next 100 years. The potential effects of this sea level rise may be to increase the amount of water entering and leaving the harbour, tidal current velocity and potentially sedimentation rates. However, these effects are likely to be subtle and gradual providing opportunity to gradually increase dredging regimes and are therefore unlikely to pose a major issue for port operation. Increased wind strength and offshore wave climate may likewise affect navigational operability and sedimentation but should likewise be able to be accommodated by changes in the dredging regimes or navigational operations over time.

1 Introduction

Te Manatū Waka / the New Zealand Ministry of Transport has appointed Tonkin & Taylor Ltd and their subconsultants (Royal HaskoningDHV, MetOcean Solutions, Pacific Marine Management, the University of Auckland, Discovery Marine Limited, and RMA Science) to undertake a feasibility study to understand whether it would be technically possible to locate a port in the Manukau Harbour from a navigation and operational reliability perspective.

The Manukau Harbour has previously been identified as a potential port location (Figure 1.1), however there are unanswered questions around the technical feasibility of this given the complex and dynamic nature of the harbour entrance along with other factors associated with greenfield port development. This is an engineering study, and environmental, social, and economic factors are not part of the current scope of work.

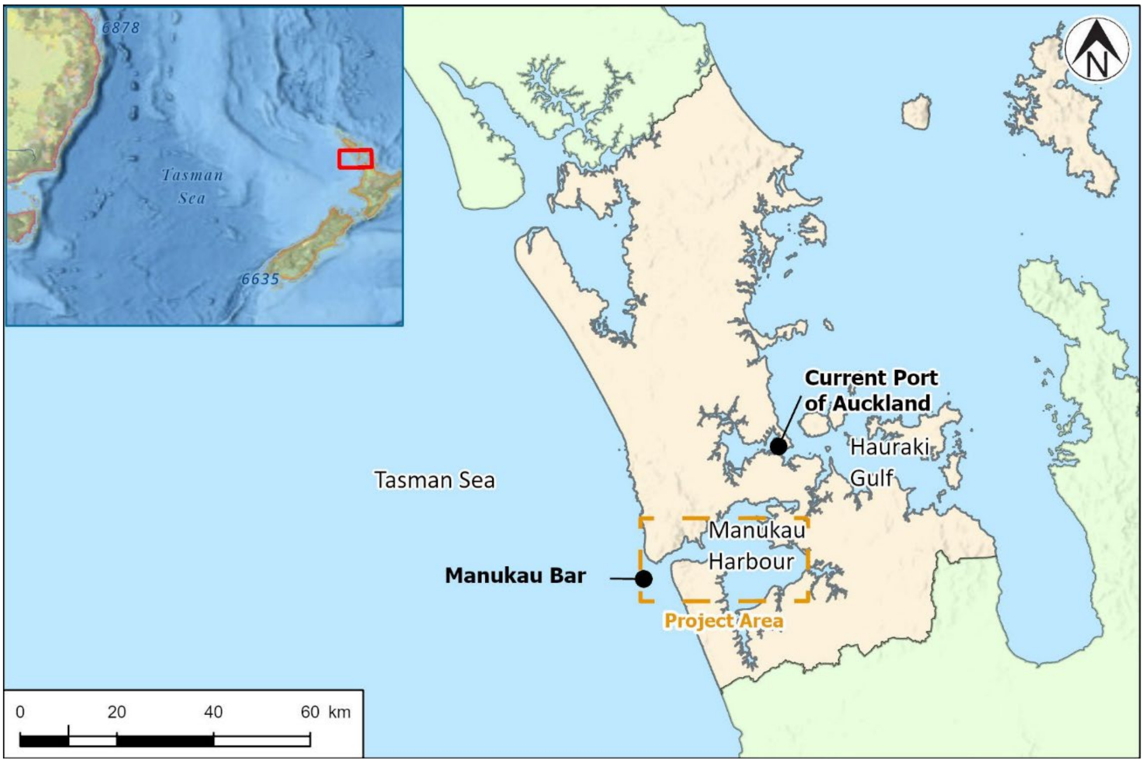

Figure 1.1 Location figure

1.1 Purpose of the document

This Coastal Technical Working Paper (TWP03) has been prepared by Tonkin & Taylor Ltd. (T+T) and accompanies the study Final Report.

This Technical Working Paper is intended to:

a Provide a synthesis of the existing coastal, geological, and environmental knowledge of the Manukau Harbour to inform other assessments.

b Summarise results from the field data collection, bar morphology analysis and numerical modelling relating to the existing conditions and processes.

c Summarise the likely implications of the proposed dredging works in terms of channel stability, sediment infill and impacts on bar and harbour processes.

This paper draws heavily on:

- *TWP03a Historic bar and channel dynamics of the Manukau Harbour entrance by Murray Ford (University of Auckland)*
- *TWP03b Manukau Harbour Numerical Modelling - Metocean Study by Metocean Solutions Ltd. and*
- *TWP03c Manukau Harbour Numerical Modelling – Sediment Transport by Metocean Solutions Ltd.*

and these Technical Papers should be referred to for further detail.

This paper does not include a formal effects assessment of the proposed works, which is outside the scope of this study, but rather presents the results of modelling which has focussed on changes in hydrodynamic, wave, and sediment transport processes and channel infilling rates as a result of proposed works. These changes have been used to inform a risk assessment and can be used as a basis for a future effects assessment.

1.2 Datums and coordinates

The project datum and coordinate system are as follows:

- Vertical datum: Chart Datum (CD) Onehunga.
- Coordinate: NZTM2000 (EPSG: 2193).

The relationship of the selected vertical datum to other commonly used datums is set out below.

Table 1.1: Vertical datum relationship, using LINZ geodetic marker at Onehunga Port

	Chart Datum (m CD)	**Auckland Vertical Datum (m AVD46)**	**New Zealand Vertical Datum (m NZVD16)**
B.N CC 65 (LINZ code ADLT)	5.593	3.389	3.10

1.3 Proposed works

A navigation channel is proposed to be dredged through the Manukau ebb tide delta, or entrance bar, to a port located in the inner harbour. Defining a specific port location is beyond our scope of work. To test feasibility, a representative site (Site B, refer Figure 1.2) has been chosen as it has the longest channel and shortest land connection of the three Port Future Study (2015) sites.

Channel design (refer *Technical Working Paper 04 Navigation and Channel Design*) indicates the navigation channel would be dredged to a maximum depth of around -19 m CD across the bar (plus 1 m for over-dredge allowance), with a width of some 295 m (plus side batters). Two options have been initially considered across the bar including a Southwest channel with dredging across a distance of some 4 km between the deeper offshore areas and the deeper channel between the heads and a South Channel with dredging across 9 km (refer Figure 1.3). Vessels would navigate this dredged channel to reach deeper natural water in the harbour entrance. The navigation channel then extends another 25 to 30 km to reach a potential port location within the Manukau Harbour with dredging occurring within the inner 10 to 15 km to a depth of -16m CD (plus 0.5m over-dredge allowance) to reach a dredged port basin.

Ongoing maintenance dredging is then proposed to maintain a navigable channel.

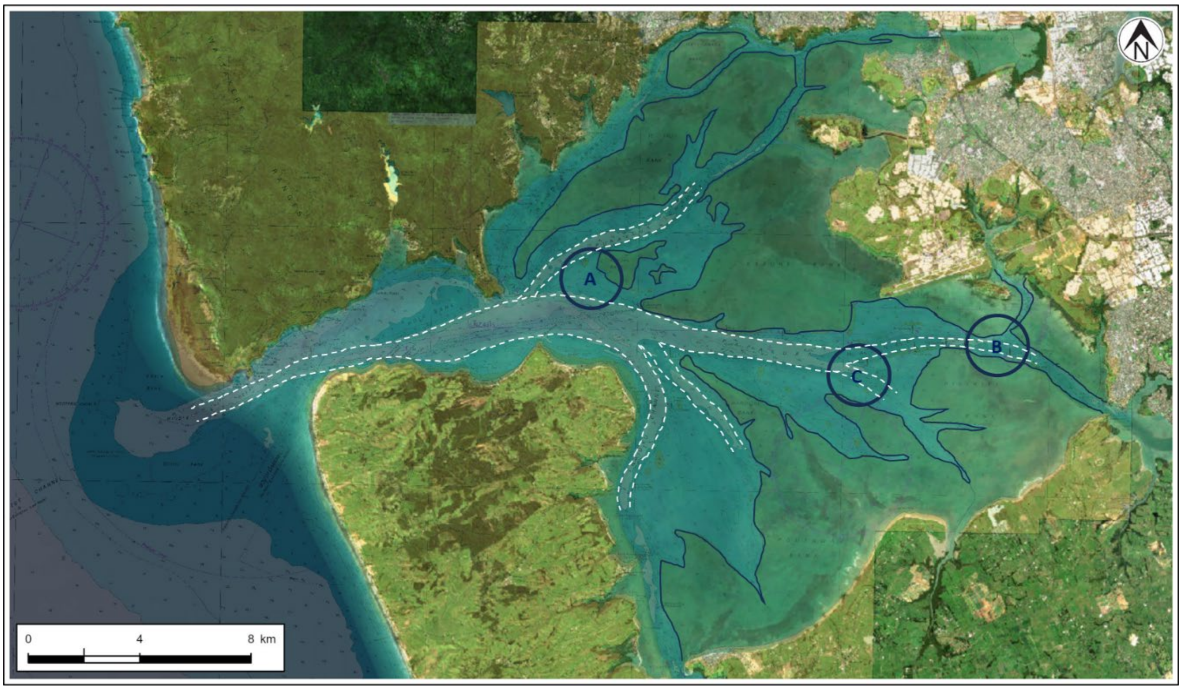

Figure 1.2: The Manukau Harbour with the main naturally deep tidal channels shown by white dashed lines, and indicative port locations identified by the Port Future Study (2015) and carried through to the Sapere (2020) studies shown with blue circles labelled A, B, and C.

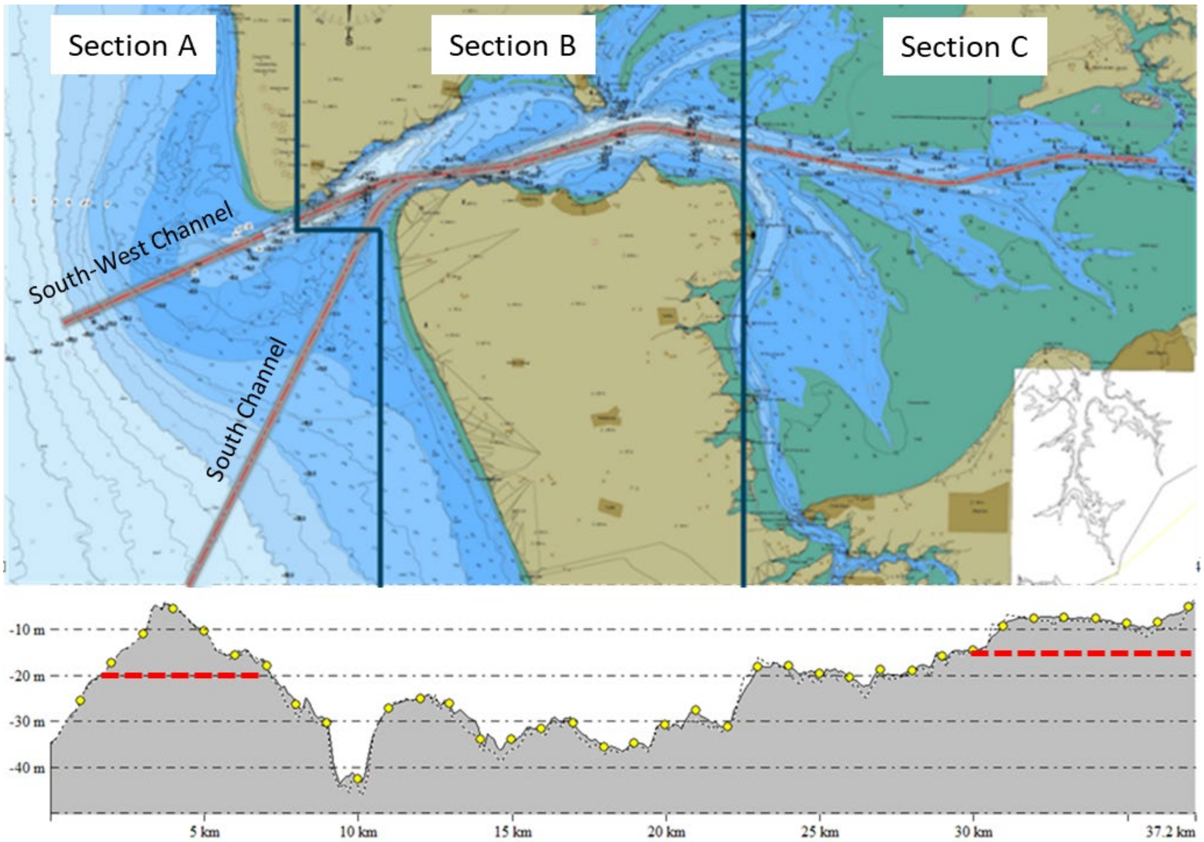

Figure 1.3: Indicative navigation channel alignments, and likely dredge extents based on existing bathymetry (long section taken through the southwest orientated Section A)

Part I – Existing Environment

2 Physical environment

2.1 Location and landforms

The Manukau Harbour is New Zealand's second largest estuary located to the southwest of the Auckland isthmus (refer Figure 2.1). The Harbour extends across 344 km^2 and comprises shallow, intertidal banks across approximately 42% (144 km^2) of its total area interspersed with deeper channels. It has a catchment size of 1,100 km^2, and three main inlets that freshwater and fine sediments are sourced: the Māngere Inlet, the Pāhurehure Inlet, and the Waiuku Inlet. Each inlet feeds into deep tidal channels which are the primary routes for sediment transport and tidal flow. These tidal channels are subtidal and reach depths of 20 – 30 m below Chart Datum.

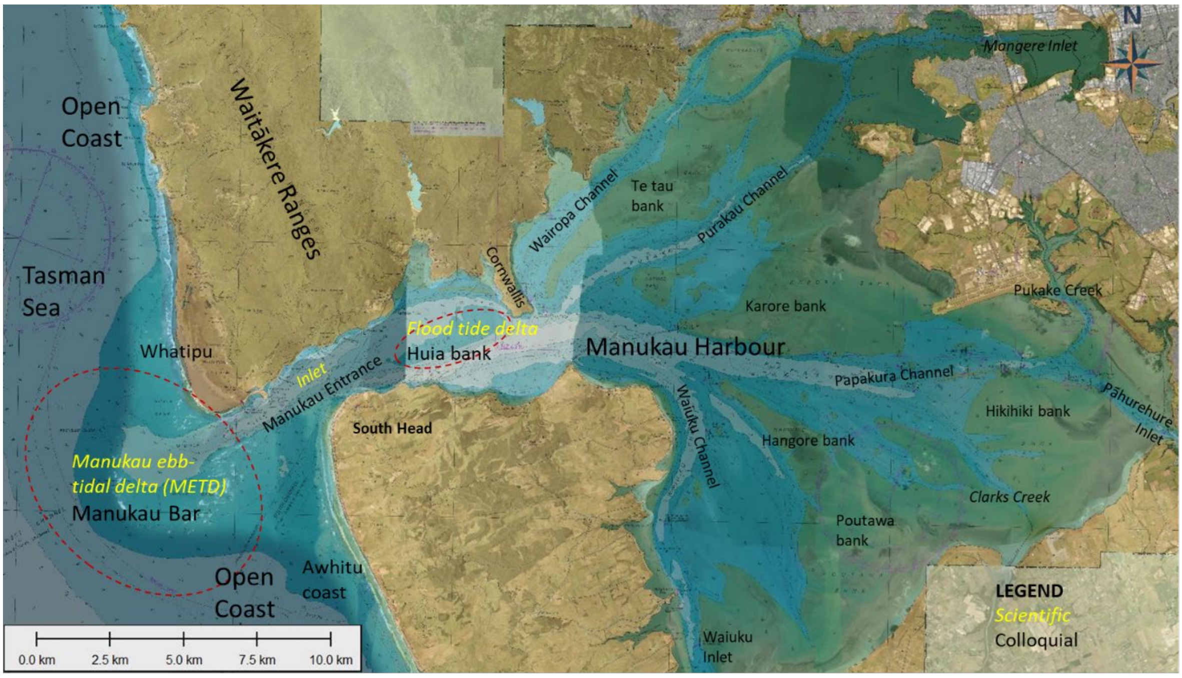

Figure 2.1: Key features of the Manukau Harbour

The inner Manukau Harbour (defined as area inside of approximately Cornwallis Peninsula) coastline is characterised by a mixture of sandy beaches and intertidal flats on the western and southern edges, a developed coastline to the north and east, and a forested cliff coastline to the northwest. A visual overview of the inner Harbour coastline is shown in Figure 2.2. The harbour narrows between Cornwallis Peninsula and the Āwhitu Peninsula with the Huia Bank forming a shallow area before a deeper and narrow Manukau Entrance.

The open coast where the harbour outlet discharges is characterised by large dissipative beaches characteristic of Auckland's large wave west coast beaches. Figure 2.3 shows the three main components of the open coastline; the north head (Whatipū), the South head (Āwhitu Peninsula) and the ebb tidal delta, or Manukau Bar. The north head, Whatipū, is a volcanic headland (Waitākere Ranges) fronted by a large swath of sand that extends out some 1,000 m at its maximum width. The sand is rich in iron and volcanic in origin. The south head, Āwhitu Peninsula, is an eroding cliff coastline consisting of poorly composited and consolidated sand deposits.

The Manukau Bar or Manukau ebb-tidal delta (METD) is a complex geomorphic feature (Figure 2.4) including deeper channels and shallower shoals or bars. These are dynamic features as described in

Section 2.6.3 but often comprise a 'South Channel' and a 'South-West' or 'North Channel' depending on configuration. 'South' and 'North Banks' run alongside the deeper middle channel.

Figure 2.2: Manukau Harbour inner Harbour coastline, top left image sourced from NZ Geographic, other three images sourced from T+T

Figure 2.3: Notable geomorphological features (1-3) at the entrance to the Manukau Harbour

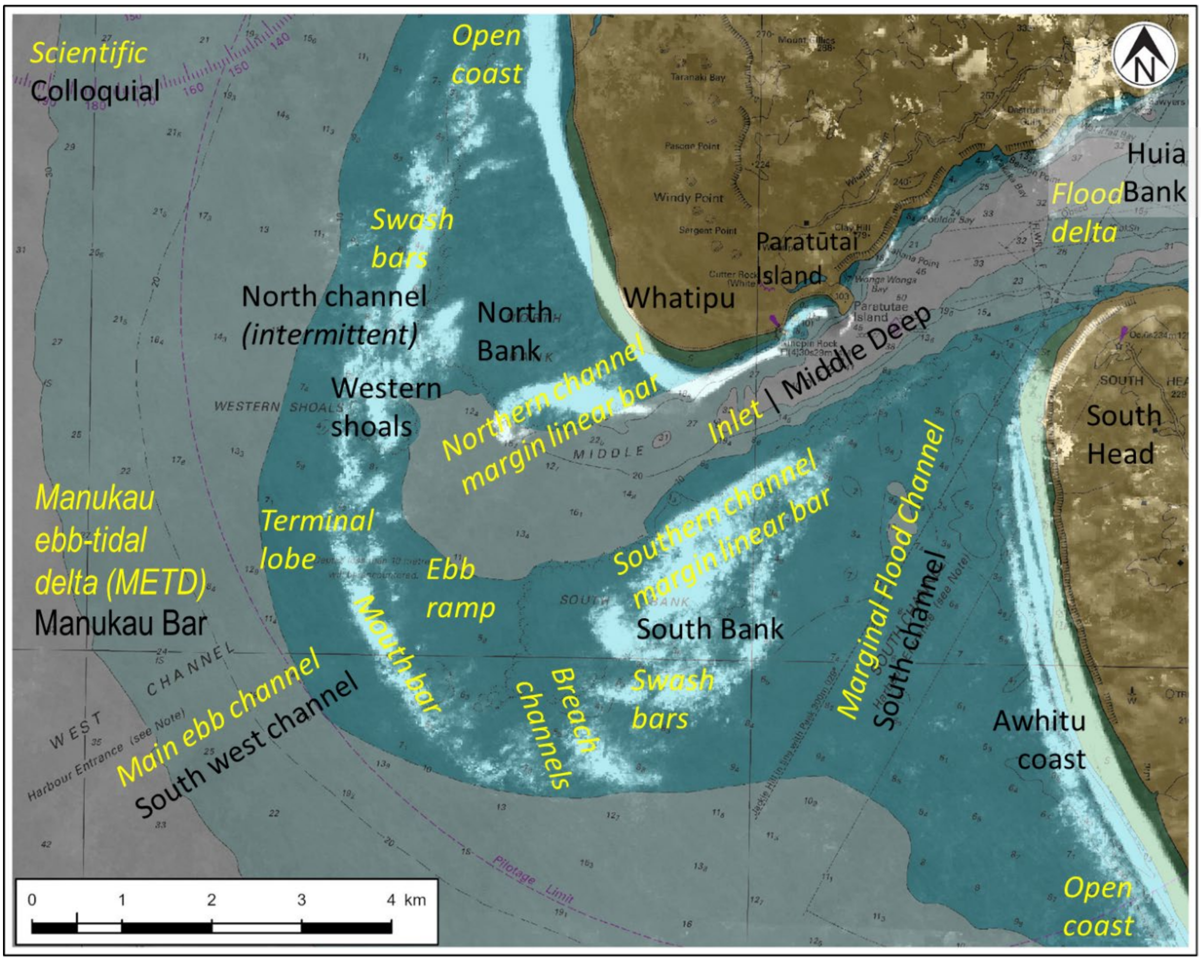

Figure 2.4: Key features of the Manukau Bar

2.2 Topography and bathymetry

The inner Manukau Harbour (Figure 2.5) comprises shallow banks (Motukaraka, Te Tau and Karore in the north and Hangore, Hikihiki and Poutawa in the south) which dry at low tides. These are intersected by deeper channels – Wairopa and Purakau in the north and Papakura and Waiuku in the south which reach depths of -20 m Chart Datum, decreasing as they progress into tributaries around the harbour edges. The land surrounding the harbour varies between steep cliffs in the north, lower lying, unconsolidated shorelines in the south and sloping backshore in the southwest onto the Āwhitu Peninsula.

The entrance channel between the Cornwallis Peninsula has depths typically between 30 and 40 m below CD as flows are compressed between the Waitākere Ranges and Āwhitu Peninsula. The Huia Bank, part of the flood tide delta is located next to the inner portion of entrance channel with depths of -4 to -10 m CD.

The primary ebb tidal channel reaches a maximum depth of ~ 50 m below CD to the south of Ninepin rock, but this depth decreases offshore as the entrance channel widens and tidal flow velocities are reduced. The location and depth of the entrance bars vary considerably depending on the form and location of bar and channel at that time (refer Section 2.6.3), but in general relatively stable North and South Banks confine the main (SW) channel for a distance of some 3 to 4 km offshore. These banks are not generally surveyed due to depth and may have depths at or just below low tide. The location and depth of the SW channel fluctuates but generally rises to a depth of -5 m CD as it crosses the entrance bar. Note the depth across the inner portion of the bar can decrease during certain bar configurations (refer Section 2.6.3). The distance between -20 m CD depths offshore and in the entrance channel is some 4 to 5 km depending on configuration. The South Channel is located to the south of the South Bank and is more consistent in location with minimum depths of -5 to -10 m CD, though the distance between -20 m CD contours is some 10 km. Offshore of the entrance bar, the seabed slopes down at ~1V:100H before flattening at around -60 m CD.

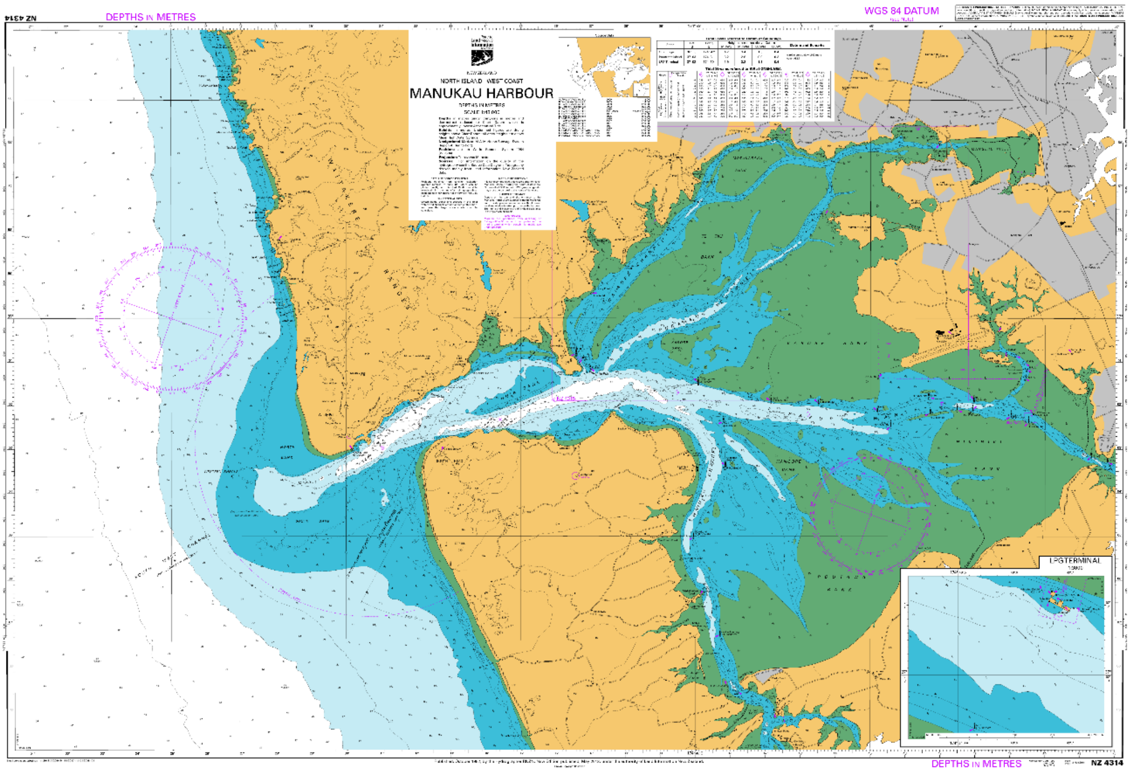

Figure 2.5: LINZ Chart 4313 (source Toitū Te Whenua Land Information New Zealand) https://charts.linz.govt.nz/charts/paper-chart/nz4314 accessed 5 February 2024.

Manukau Harbour and in particular the entrance bar has been formally surveyed since 1862 with several comprehensive surveys undertaken between 1961 and 1989 (Figure 2.6). Surveys have been undertaken more recently (between 2001 and 2016) by Port of Auckland Ltd (POAL), though have tended to focus on the location of the SW and S channel across the bar and the Papakura Channel and Waiuku Creek. These have been for specific navigation purposes with surveys ceased as the Port of Onehunga closed in 2016. Most recently (between 2018 and 2020), limited surveys focussing on the South Channel have been undertaken by POAL on behalf of Sanford Ltd., again for specific navigation purposes. The extent of these surveys is shown in Figure 2.7 including a cross-section through the bar including all POAL surveys, 1989 and 2023 surveys. Considerable variation is evident across the Manukau Bar between surveys with the outer (seaward) portions of the bar observed to vary by 5-10 m and inner (landward) portions by 10-15 m. The reason for these variations is further discussed in Section 2.6.3. The difference in volume on the bar between the comprehensive 1989 and 2023 surveys was found to be in the order of 50M m^3. However, it should be noted that given the extremely large area that bar encompasses, small changes in bar elevation where survey points were sparse could contribute to this difference.

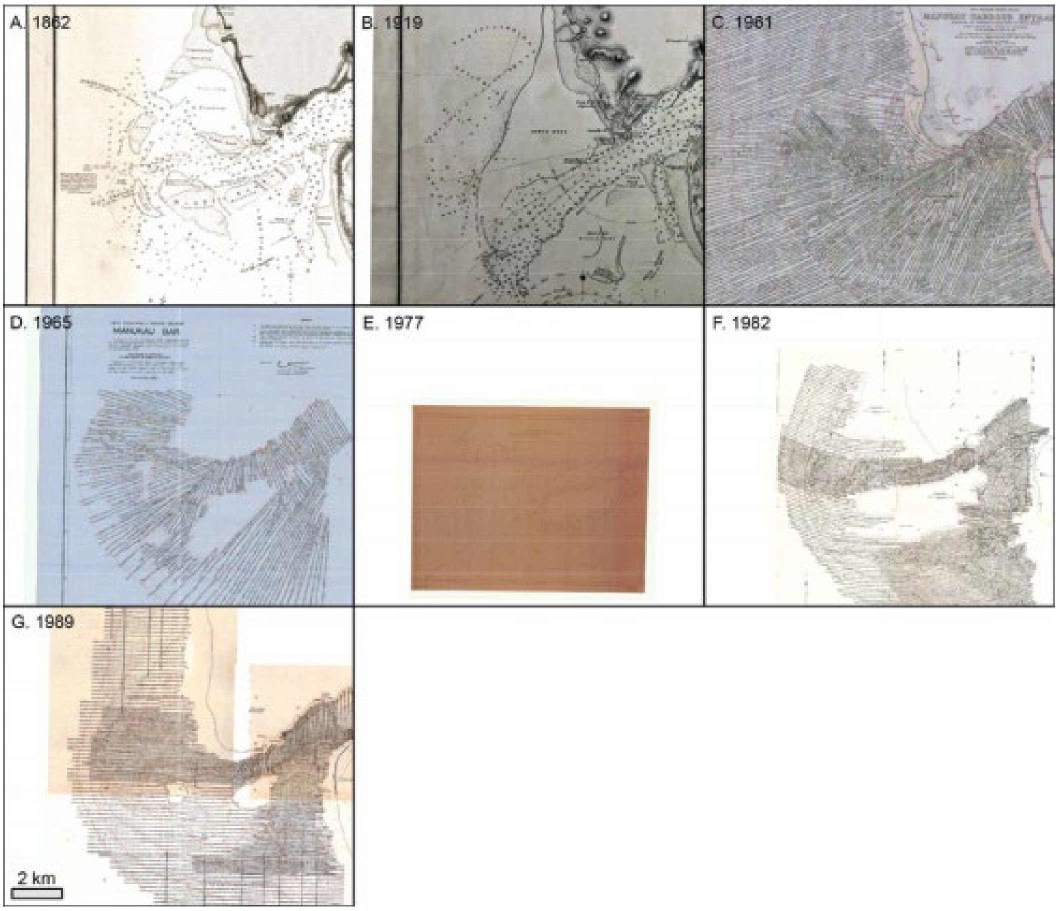

Figure 2.6: Scans of historic charts and sounding sheets of the Manukau Harbour entrance (refer TWP03a Historic bar and channel dynamics of the Manukau Harbour entrance for further information)

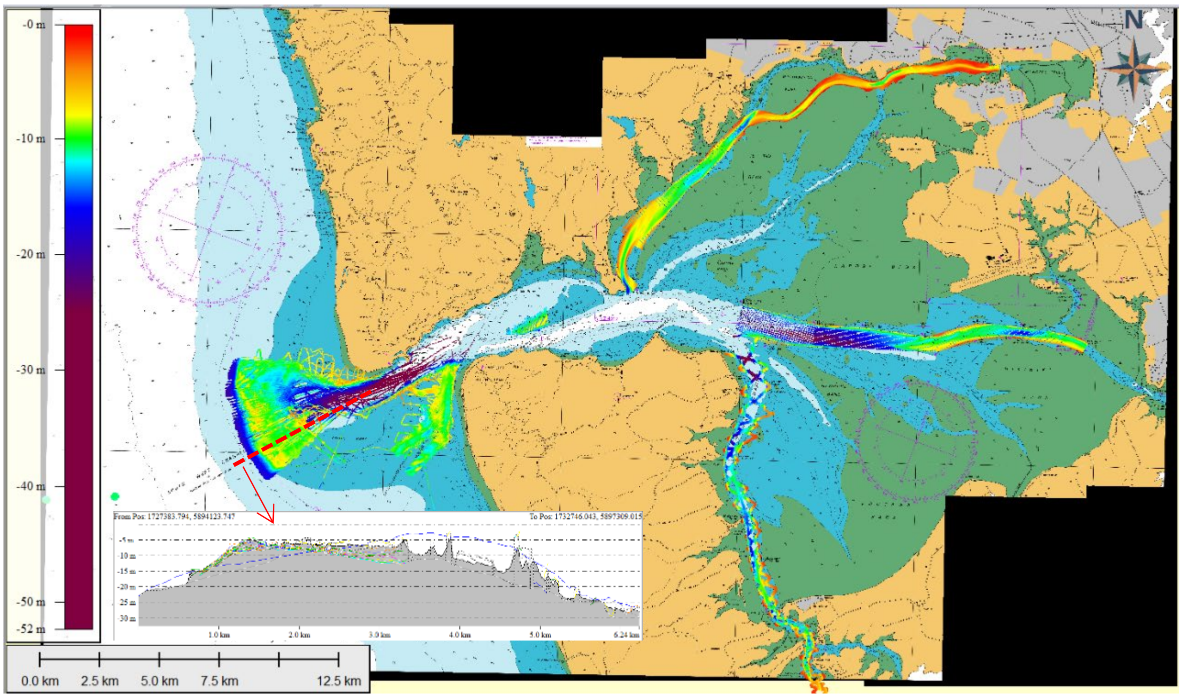

Figure 2.7: Surveys by Port of Auckland Ltd and Sanford Ltd. between 2001 and 2020 overlying the LINZ Chart 4314 with a cross-section through the bar and surveys overlain

LINZ Chart 4314 covers the entire Manukau Harbour, entrance bar and offshore (Figure 2.5). The chart was developed using a combination of previous surveys with the most recent version (2018) including surveys from 1961 to 2009. As the charts are developed using a combination of sources, they are not necessarily representative of a specific point in time and are instead intended to provide conservative depths for navigation.

Therefore, a new survey focussing on the bar, entrance and Papakura was collected for this study between May and June 2023 using single-beam sonar and a pressure transducer dipped from a helicopter for shallow, exposed areas on the bar. Extents for the survey are shown in Figure 2.8 and described in detail within *Technical Working Paper 02 – Fieldwork*.

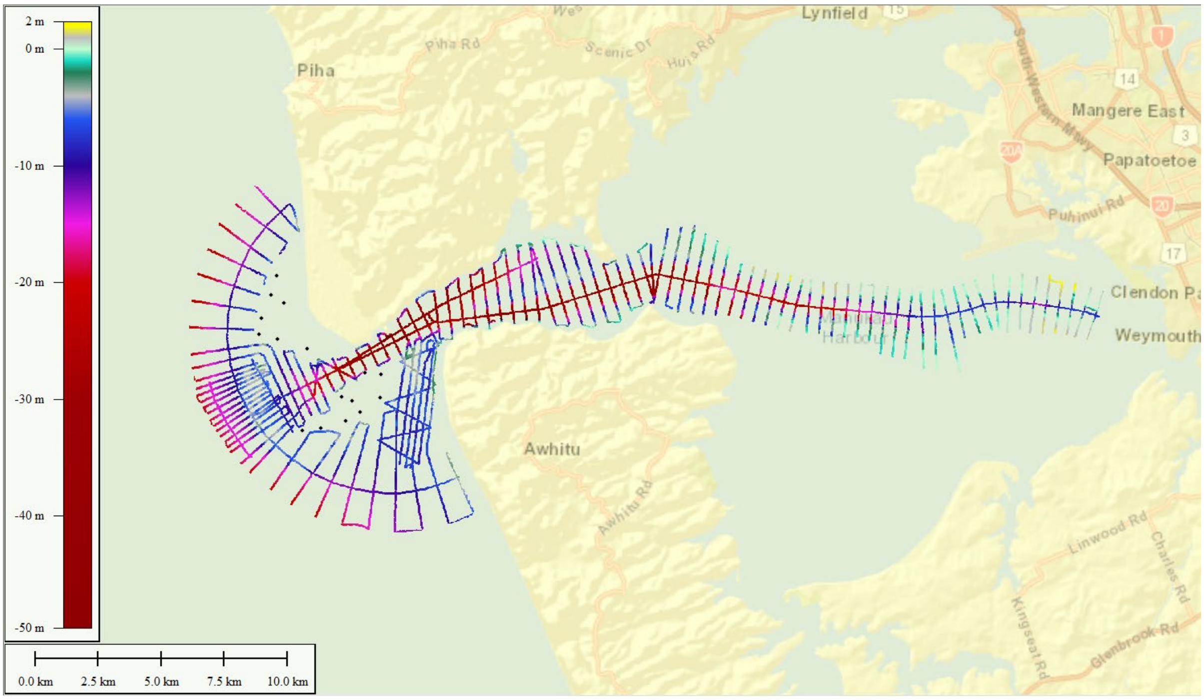

Figure 2.8: Survey data of the Manukau Bar, entrance, Huia Bank and the Papakura channel collected between May and June 2023 using a vessel and single-beam sonar (lines) and dipped pressure transducer (points). Refer Technical Working Paper 02 – Fieldwork for further detail

A ***composite bathymetry*** has been developed for use in concept channel design and modelling. This composite bathymetry (Figure 2.9) is based on combining the best available sources of data with preference given to the most accurate, comprehensive, and recent data. Refer to *TWP03b Numerical Modelling – Metocean Study Report* for further detail but the sources used to develop this composite bathymetry (in order of preference) include:

1. LIDAR (2016-2018) Auckland north and LiDAR (2016-2017) Auckland south
2. DML 2023 survey across the Manukau Bar
3. Helicopter dip bathy points on shallower banks on the bar
4. Previous Port of Auckland bathymetry in some Manukau Harbour channels
5. 1961 sounding sheets offshore
6. LINZ ENCs for general infill within harbour (between LiDAR and bathymetric survey)
7. Contours produced by hand to aid gridding between survey run lines.

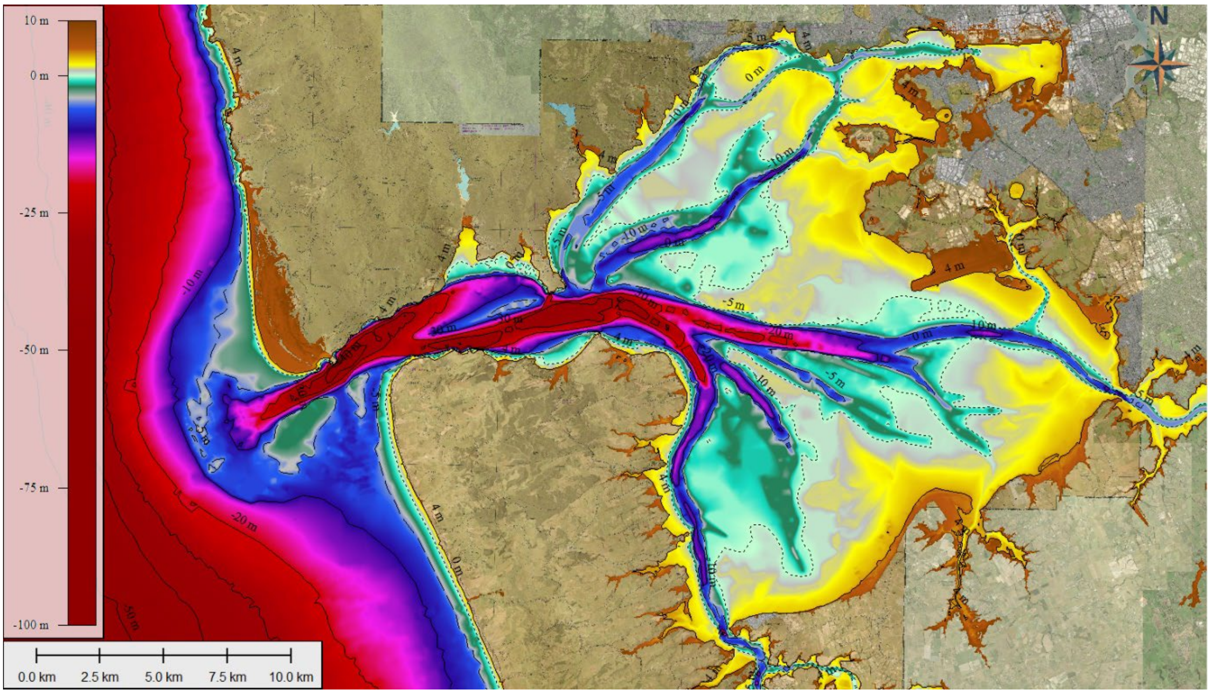

Figure 2.9: Composite bathymetry from combined sources (depths in CD).

2.3 Built environment and human geography

The Manukau Harbour has a complex history. It is host to some of Auckland's largest infrastructure projects; the Auckland Airport, the Mangere Wastewater Treatment plant (MWTP), and the smaller Onehunga Wharf (Figure 2.10).

The northern and eastern coastline is well developed, with large industrial areas within the Manukau catchment that add to the historic pollution and human activities: Manukau City, Māngere, Onehunga, Penrose. Flatland farming on the southern Manukau lowlands has contributed to the presence of fine sediments and contaminants via stormwater runoff.

The Onehunga Wharf and the LPG terminal are known examples of marine freight into and through the Manukau Harbour. Currently there are restrictions on commercial fishing within the harbour as per the Fisheries Regulations 1986; however, commercial boats use the Onehunga Wharf as a home port for fishing activities on the open west coast. The harbour is also used recreationally for sailing and fishing.

Figure 2.10 Critical Infrastructure located within the Manukau Harbour: Auckland Airport (top left – NZ Herald), Mangere Wastewater Treatment plant (top right – Fletcher Trust Archives), Onehunga Wharf (bottom – Auckland Council)

2.4 Geology

2.4.1 Geological history

New Zealand has a complex geological history given its volcanic activity and mobile plate tectonics. Most of the present-day harbour geology can be described by events that have occurred in the last 5 million years, or epochs: Plio-Pleistocene (~5 ma to 1.64 ma), Pleistocene (~1.64 ma to 0.1 ma), and the Holocene (11,700 ya to present day).

2.4.1.1 Waitākere Ranges

The present-day Waitākere Ranges are remnants of an ancient volcanic massif that formed ~ 22 ma through a series of volcanic activities that likely ceased ~ 16 ma. This submarine volcanic mass, identified as the Manukau Massif by Herzer (1995) and Isaac et al. (1994), formed a plain close to sea level and was capped at many times by small islands inferred by reef structures within rock facies. This volcanic massif subsided becoming largely buried by sediment and was planed by wave action. Volcanic debris from this erosive process is visible along the west coast. Some of these rounded volcanic rocks form the conglomerates visible at Piha and Karekare, refer to Figure 2.11.

Figure 2.11: Smoothed volcanic rock interlaced with marine sands at Piha

2.4.1.2 Manukau Basin

At the beginning of the Plio-Pleistocene period, the North Island was uplifting through tectonic movement and volcanic uplift and continued to uplift into the late Pleistocene. At this point in time, the (relative) sea level varied from between 12 and 32 m above the present-day coastline, with Northland separated from the North Island. During this period, the Manukau Harbour area was infilled with shelly marine sediments and volcanic conglomerates. This sediment was later buried by sandy and silty river sediments from the Waikato River and Coromandel regions. This Manukau lowland is assumed to have been a structural lowland, a former delta for the Waikato River until it was re-directed by volcanic activity and uplift from the South Auckland volcanic field ~ 1.5 – 2 ma. This activity is shown in Figure 2.12.

Once redirected, sediment from the Waikato River exited in the Port Waikato region and fed the west coast under a prevailing south-westerly wind and wave attack, in combination with iron rich sands sourced from the geologically recent Taranaki eruptions. This sediment accumulated in the lee of the Port of Waikato area to form the Āwhitu Peninsula over the last ~ 2 ma. Sand travelled along the coast via longshore drift to form other major coastal sand barriers, the Kaipara Harbour South and North Head.

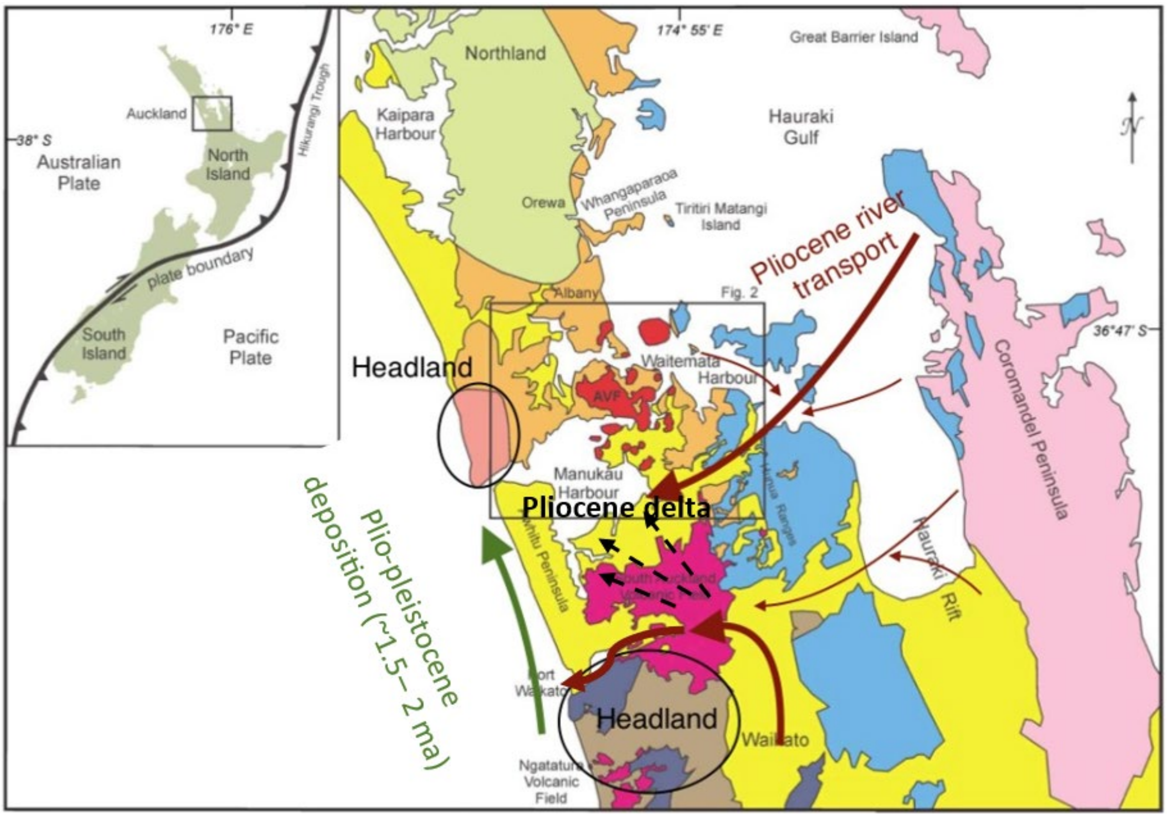

Figure 2.12: Excerpt from (Kenny, Lindsay, & Howe, 2012) of Manukau geology, overlaid with arrows to show Pliocene and Plio-Pleistocene sediment transport to form the Manukau area

During glacial periods, the most recent (and most severe) of which was 20,000 years ago, the mean sea level was more than 100 m below present-day sea level. River channels were much longer, and thus flows were much greater leading to deep incised valleys in pre-existing riverine systems. As sea level rose from around 12,000 to 7,000 years ago, the valley systems quickly infilled with marine sediment, forming a drowned valley estuarine environment.

2.4.2 Published geology

The published geology (ref. Figure 2.13) and research papers (Balance, 1965 & Searle, 1981), of the Geology of the Auckland area shows the Manukau Harbour is an infilled paleo valley. The Harbour deposits consist of Quaternary age marine, estuarine and terrestrial sediments which have infilled a down-thrown block associated with the inferred Manukau Fault (ref Figure 2.14). The elevated Auckland Isthmus lies to the north and the Manukau Lowlands are to the south.

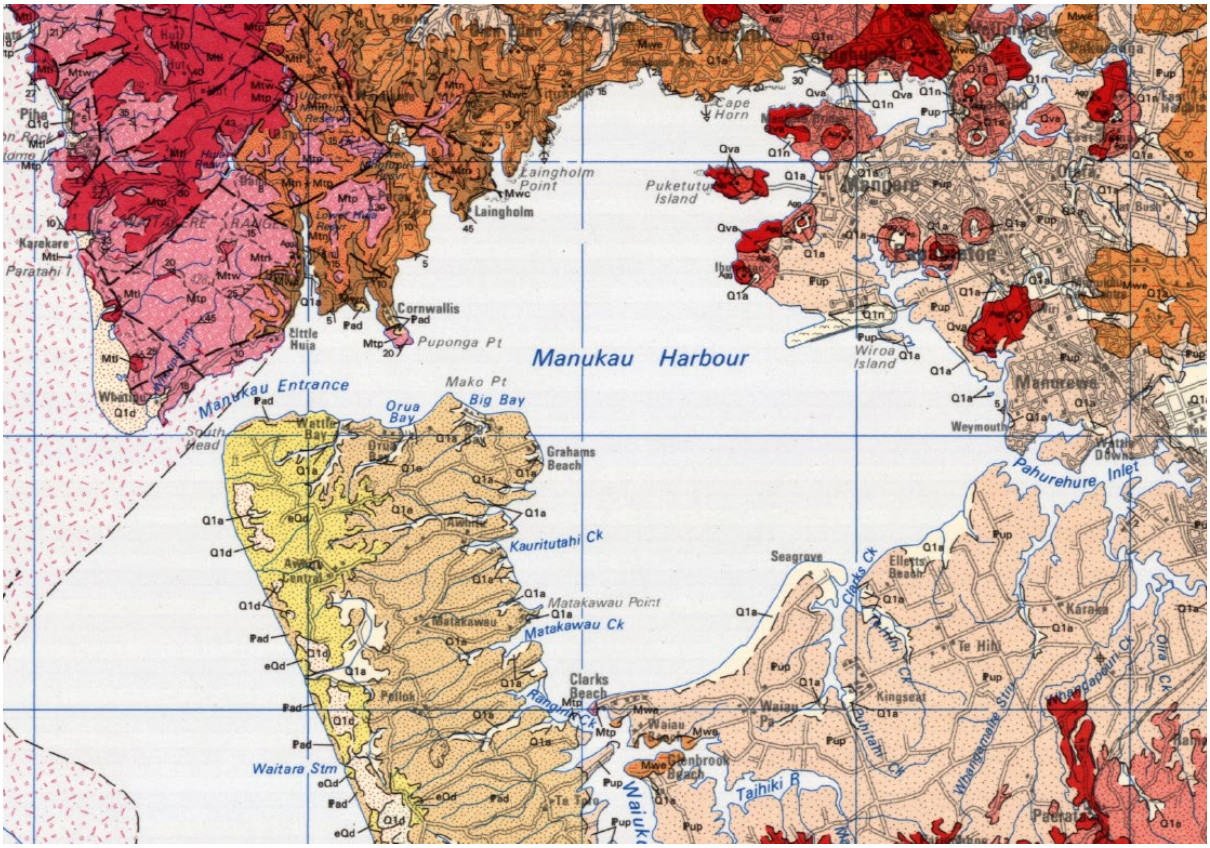

Figure 2.13: Edbrooke, S.W. (compiler) 2001: Geology of the Auckland area. Institute of Geological & Nuclear Sciences 1:250,000 geological map 3. 1 sheet + 74 p. Lower Hutt, New Zealand. Institute of Geological & Nuclear Sciences Limited.

The geology of the northern extents of the Manukau Harbour entrance is dominated by Miocene age Piha Formation, comprising stratified submarine andesitic breccia-conglomerate with minor sandstone and siltstone. The southern extents are underlain by Pleistocene to Holocene age formations. Between South Head and Wattle Bay, weakly cemented coastal foredunes of the Kariotahi Group Formation occur. From Wattle Bay to Big Bay, cemented dune sand of the Āwhitu Group occurs with some inclusions of pumice sands, silts and gravels of the Taupō Pumice Alluvium (Tauranga Group). The Tauranga Group sediments extends to the east, underlying the Manukau Harbour. The northern and north-eastern extent of the upper harbour comprises alternating sandstone and mudstone of the East Coast Bays Formation of the Waitemata Group as well as basalt, scoria, volcanic ash and tuff associated with the Auckland Volcanic Field.

Kenny (2011) shows the indicative location of the Manukau Fault which is inferred to transect the harbour in a north-east to southwest direction, as shown on Figure 2.14. This structural feature has formed the disassociation between the Auckland Isthmus to the north and the Manukau Harbour to the south and underlies the infilled paleo valley underlying the harbour. The Cornwallis Fault transects the harbour entrance channel in a similar orientation to the Manukau Fault.

The likely navigation channel alignment is along the boundary between the Manurewa Horst and the Otahuhu Graben. These faults are not considered 'active', meaning that they have not moved in the last 125,000 years. Studies undertaken by Kenny et al. (2011) indicates fault offsets in shell beds, suggesting that the earliest rifting could have occurred along the ENE-trending block faults 3 Ma. By the Pleistocene, coastal and non-marine sediments were being deposited in faulted depressions. These sediments have not been offset, suggesting that regional tectonism had abated by c. 1.5 Ma ago and the pattern of fault-bounded blocks across the Auckland region, as appears today, had already been established.

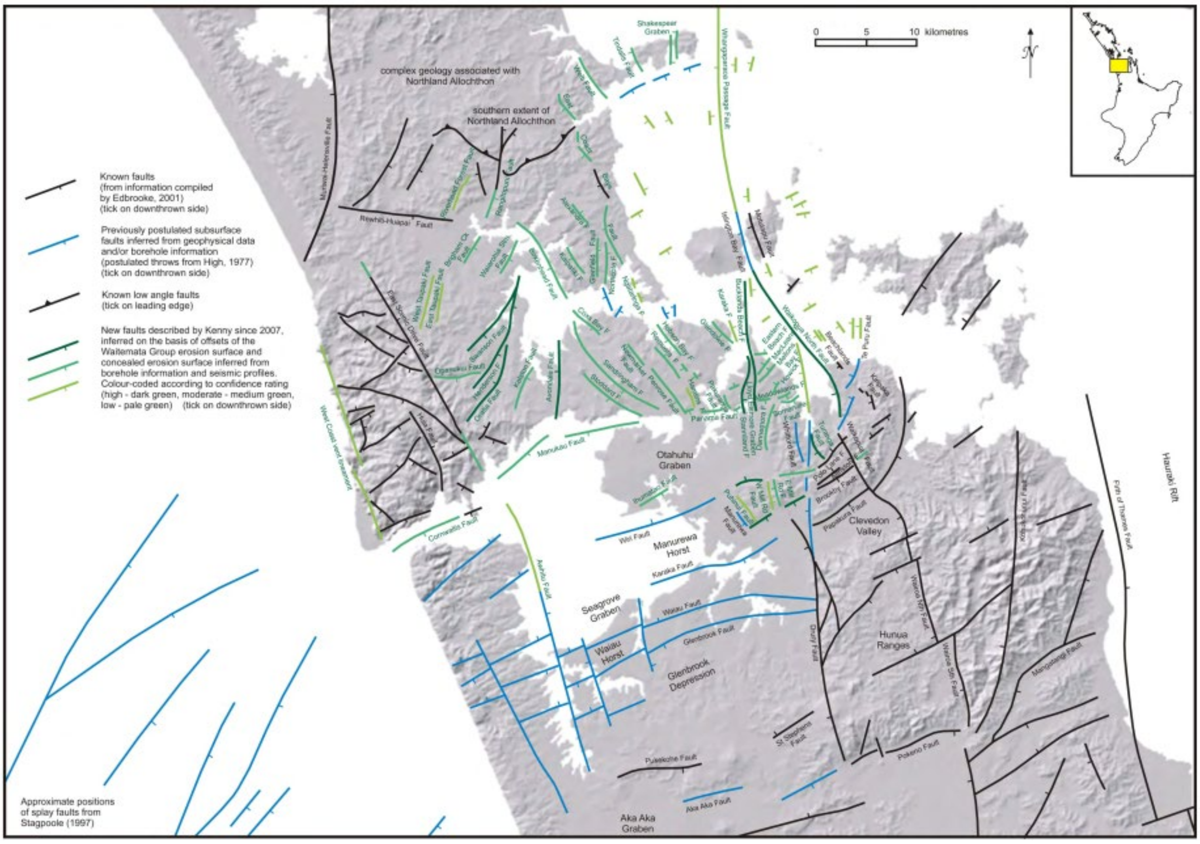

Figure 2.14: Locations of the Manukau and Cornwallis Faults (ref. J.A Kenny, J.M. Lindsay, and T.M. Howe "Large Scale Faulting in the Auckland Region", IESE, August 2011)

The emergence of the Auckland Volcanic Field over the last 200 thousand years has resulted in the formation of significant volcanic landforms that surround the Manukau Harbour that include Mangere Lagoon, Maungataketake, Pukati, Manurewa etc., that are likely to have resulted in changes to these catchment areas and the location of tributaries where they enter the harbour. Volcanic material is also likely to have either entered the harbour as airfall or transported into the harbour as suspended sediment via tributaries.

2.4.3 Subsurface conditions

Both the recent volcanic history discussed above and changes in historical sea level are considered to be significant influences and drivers of alluvial material deposited within the Manukau Harbour.

Ghada (2005) presented a schematic model of an infilled valley as a possible mechanism for infilling and formation of the Tāmaki River that feeds into the Waitematā Harbour on the opposite side of the Auckland isthmus. This model highlights the importance of historical sea levels, driving repeat erosion and re-deposition within Tauranga Group and recent alluvium within the Manukau Harbour. This provides some explanation for the interbedded nature of sand and silt deposits, their discontinuity and the differing depths at which successive transitions between these materials are encountered.

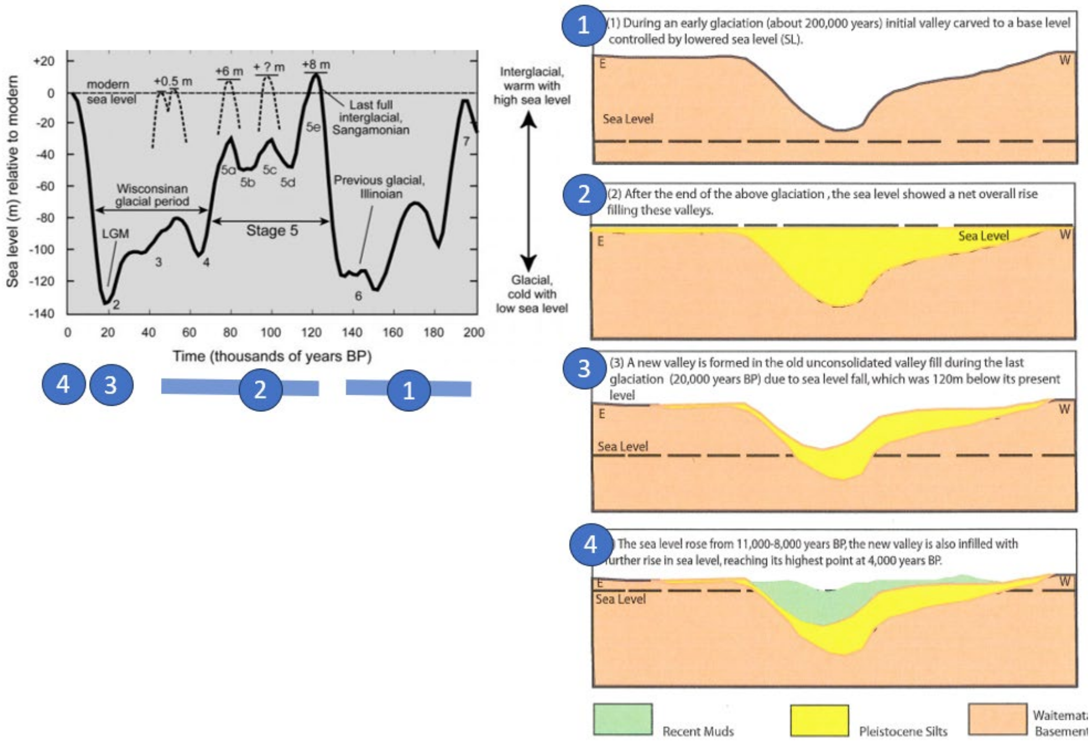

Figure 2.15 schematic model of an infilled valley as a possible mechanism for infilling and formation of the Tamaki River that feeds into the Waitemata Harbour on the opposite side of the Auckland isthmus (Ghada, 2005)

2.4.3.1 Previous borehole investigations

Available borehole data from both our T+T database and the New Zealand Geotechnical Database has been compiled as part of our desk study. A summary of relevant borehole information is presented in Appendix A. These show marine boreholes existing within the Manukau Harbour. While there are no known marine boreholes within the entrance, reference has been made to nearby land-based boreholes as part of our interpretation of the likely range of geotechnical conditions.

This information has been used to infer subsurface conditions along the proposed alignment as described in Section 4.2.1.

2.5 Sediments

2.5.1 Sources of sediment

As discussed in 2.4.1.2 the geological history of the Manukau basin accounts for large volumes of sediment that make up the harbour seabed today. Since this historical deposition, new sources of sediment in the Manukau Harbour are predominantly sourced from the open coast, harbour shoreline and cliff erosion, marine biogenic processes, and sediment runoff from surrounding catchment areas. Figure 2.16 outlines key sediment sources.

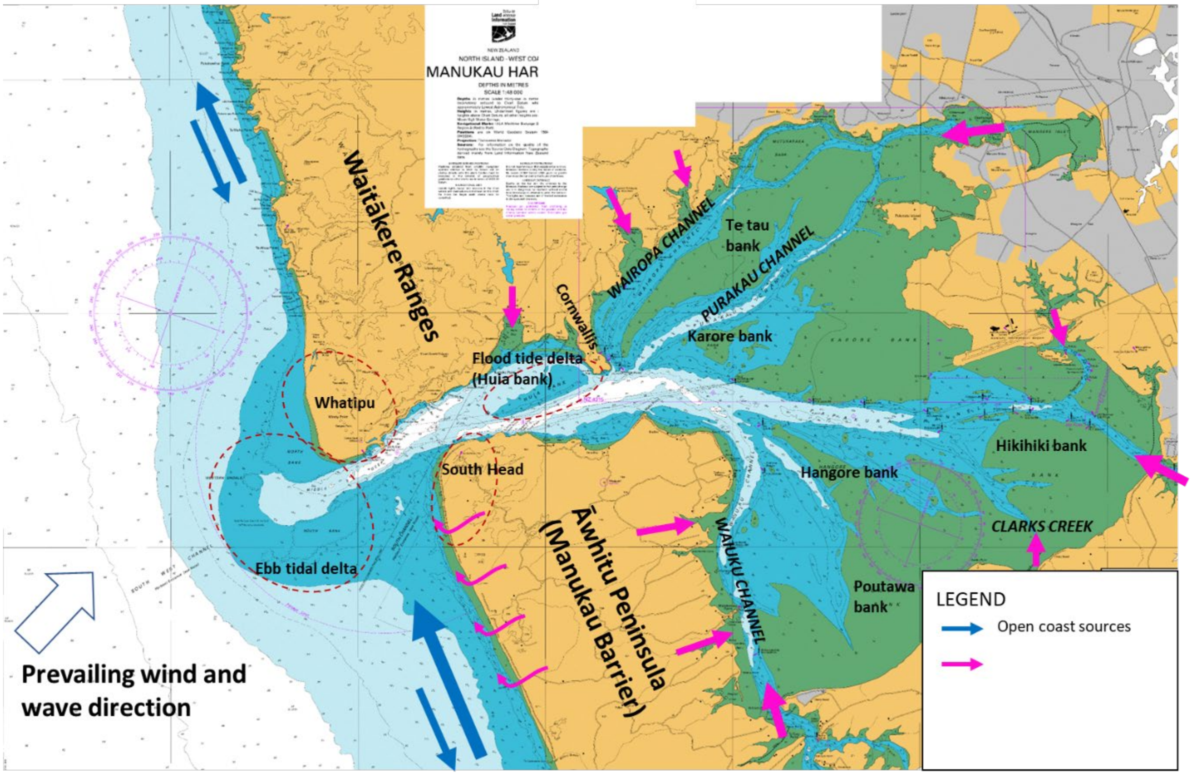

Figure 2.16: Conceptual model of key sediment sources within and outside of the Manukau Harbour

2.5.1.1 Harbour

Sediments on the Huia Bank, part of the flood tide delta are likely predominantly sourced from the open coast and exchange with the ebb tidal delta. Further east, within the harbour (areas inside of the Huia Bank), the geological history of the Manukau basin accounts for large volumes of existing sediment that make up the harbour seabed today.

Around the extents of the harbour, narrow sandy beaches typically line the backshore, examples visible in Figure 2.17 and in the photo of Clarks beach shown in Figure 2.18. Deposits are often limited in thickness existing as a shallow veneer. These materials are predominantly composed of broken shell and coarse sands, the coarse sands of which were shown by Scofield (1970) to have distinct geological origins from sand of the open coast. Schofield (1970) found beach deposits in the vicinity of the Waiuku Inlet to be comparable in mineralogy to those in the current alignment of the lower Waikato River, being mainly feldspar and quartz and consistent with their inferred geological history of the Manukau basin. Their mafic content was also quite low (less than 10%), in contrast to sand sampled from the open coast where mafic content typically exceeded 60% by mass.

New sediments being introduced into the harbour are predominately limited to shoreline erosion, broken shell, and terrigenous runoff from freshwater tributaries. Sediment sourced from shoreline erosion can occur from point sources such as slips, or gradual erosion of the shoreline material by the physical and chemical effects of water currents, waves, salt spray, wind, temperature change, tectonic uplift, biogenic erosion, and manmade effects (Tonkin & Taylor Ltd. 1986). The limited sandy beach deposits along harbour beaches in sheltered areas indicates a generally low supply of sand from eroded terrigenous sediment.

Figure 2.17: Aerial photograph of Pahurehure Inlet, taken in 1964 (J. B. Rowntree Collection, 1964) around low tide showing intertidal areas each side of the inlet channel. Papakura Township shown in background, right side.

Extending further up into the various inlets branches of the harbour leads to comparatively sheltered intertidal areas typically comprising silty sediment, in some areas overlying weathered outcrops of the Tauranga Group, effected by biogenic processes (example shown in Figure 2.18, refer also Section 2.4.2).

Figure 2.18: Stream bank sediment primarily comprising silt, overlying weathered Puketoka Formation adjacent, to Clarkes Creek taken in the vicinity of the Karaka Pressure sensor in TWP02 (Photo: T+T).

Rainfall events transport sediment from surrounding catchments to the streams that discharge into the upper branches of the Manukau Harbour. The mean annual inflow from all freshwater sources into the Manukau Harbour is 30.7 m^3/s, which increases to an estimated 800 m^3/s during a 5-year ARI storm event (Tonkin & Taylor Ltd. 1986). Assuming a 6-hour rainfall, the cumulative water volume from a 5-year ARI rainfall event would only be a small fraction (8%) of the normal tidal exchange or prism of the Manukau Harbour (refer Section 3.1), and it is consequently assumed that sediment input from terrigenous sources is likely less than the fraction from oceanic sources transported into the harbour by tidal currents.

2.5.1.2 Open coast

Sediments on the open coast are derived from a combination of erosion from adjacent cliffs - weakly cemented dune sand on the Āwhitu Peninsula and to a lesser degree volcanic clasts from the Waitākere Ranges, and sediment transported along the open coast from the south, from geologically recent eruptions around Taranaki and from riverine transport via the Waikato River. These sediments move up the coast under the prevailing southwest wave climate and enter the harbour mouth through tidal actions (refer to Section 3.5 Sediment transport). From there the sediments may be moved into the harbour and onto the flood tide delta or offshore on to the ebb tide delta (Manukau Bar).

The construction of dams on the Waikato River has removed a possible sediment source, and it is hypothesised this could have starved the Manukau of sandy sediment, causing increased erosion of the Āwhitu Peninsula (Duder & Senior, 2010). The Āwhitu Peninsula is colloquially termed 'the bad lands' due to its frequent slope instability, visible in Figure 2.19. The sand barrier is eroding rapidly in the northern section (~ 0.77 m/year (Macdonald, 1986)) from the combined effect of slope instability and wave induced erosion of the cliff toe.

Figure 2.19: *The Āwhitu Peninsula (Manukau Barrier) looking south*

2.5.2 Sediment characteristics

2.5.2.1 Previous studies

Location of sediment sampling and inferred distribution throughout the Harbour is shown in Figure 2.20 based on sampling studies up to and including 1986 (Tonkin & Taylor Ltd, 1986). Kelly (2006) produced a more recent spatial distribution as shown in Figure 2.21 which is based on data collection and mapping by (Gregory, Blacksmore, Glasby, & Burrows, 1994).

Maps showing inferred changes in bed sediment across the Manukau Harbour in Figure 2.20 and Figure 2.21 share strong commonalities, with most bed sediments within the Manukau Harbour classified as sand (63 µm – 2 mm in diameter). Coarse sands (1 mm – 0.5 mm) are found in the primary tidal channels south of Cornwallis (Karangāhape Peninsula), medium sands (0.5 mm to 0.25 mm) are found in the Huia Bank, and main channels; Wairopa, Purakau, Papakura, and Waiuku rivers, and fine sands (0.25 mm to 0.125 mm) primarily comprising the sand banks. Very fine sands with a high mud concentration (0.125 mm – 0 mm) is found on the intertidal banks and upper reaches of the estuary. The sand size distribution tends to follow depth contours (likely considered by the cartographer).

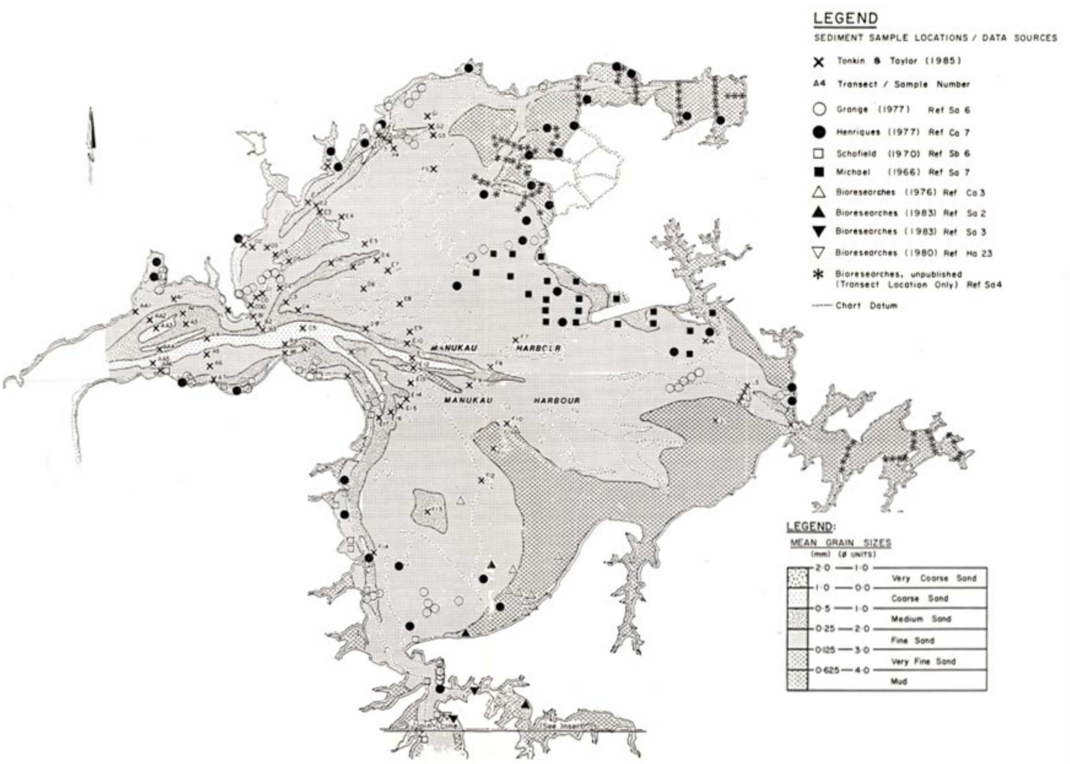

Figure 2.20: Location of sediment sampling locations and inferred distribution of mean grain size distribution (Tonkin & Taylor Ltd, 1986).

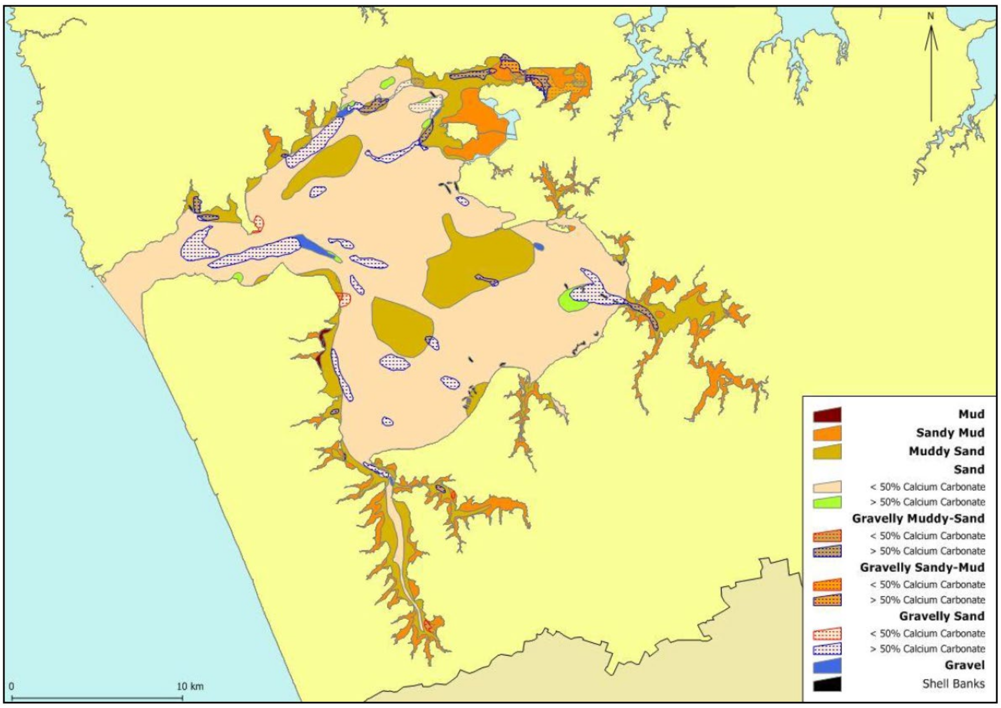

Figure 2.21: Distribution of major sediment types in Manukau Harbour (Kelly, S. 2008)

Previous studies do not extend to the outer harbour or ebb tidal delta. Hicks & Hume (1991) estimate the mean sediment size on the ebb tidal delta as D_{n50} = 0.13 mm (medium sand); however, this was inferred from Schofield's (1970) sampling on the northern beaches of the Āwhitu Peninsula.

2.5.2.2 Sediment characteristics between the open coast and Pāhurehure Inlet

Additional sampling was undertaken in 2023 as part of this study with the locations and sampling and analysis methods set out in *TWP02 Fieldwork.* Results from this field testing in combination with previous studies discussed above have been used to characterise gradational changes in sediment type along the main tidal channel from ebb tidal delta to the Pāhurehure Inlet (Figure 2.22). As a general rule, changes in sediment type correlate strongly with changes in bathymetry, and locations where divergence of tidal channels occurs.

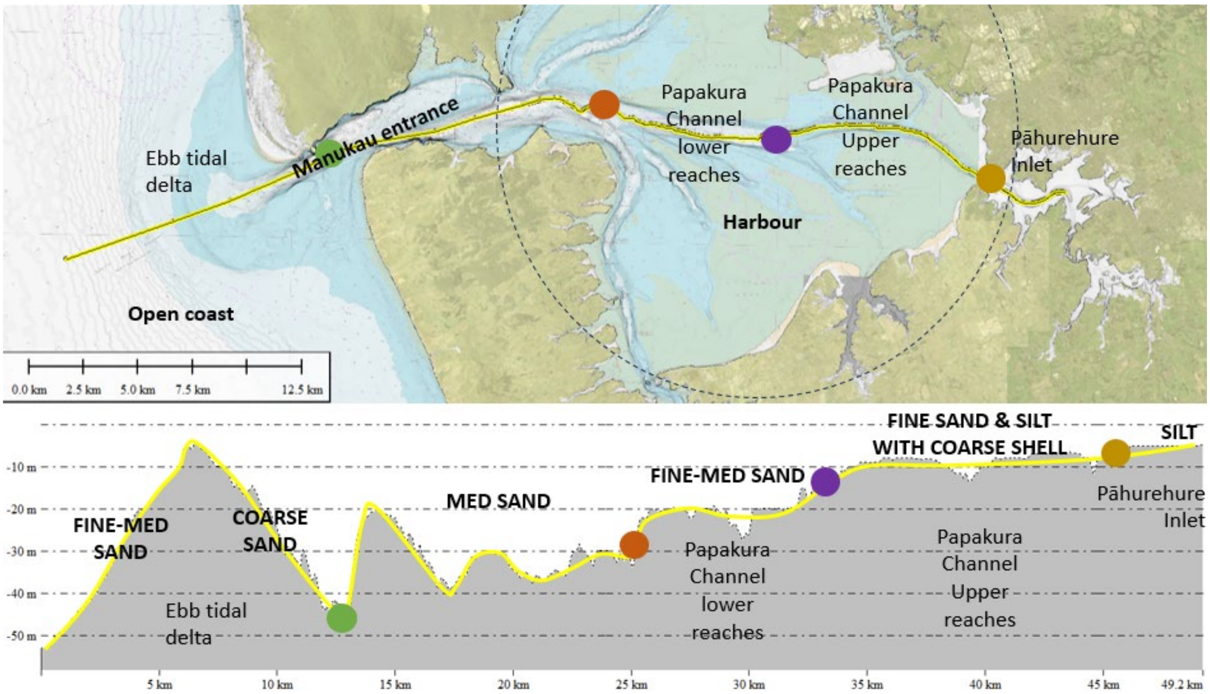

Figure 2.22: Characterisation of gradational changes in sediment type along the main tidal channel from ebb tidal delta to the Pāhurehure Inlet

Ebb tidal delta to flood tidal delta

Starting outside the harbour entrance (Figure 2.23) a large variation in grain size distribution was observed over the ebb tidal delta system. In areas close to the main channels, grain sizes were larger (typically D_{50} = 300 to 500 microns). Further away from these channels grain sizes became smaller (typically D_{50} =150 to 300 microns).

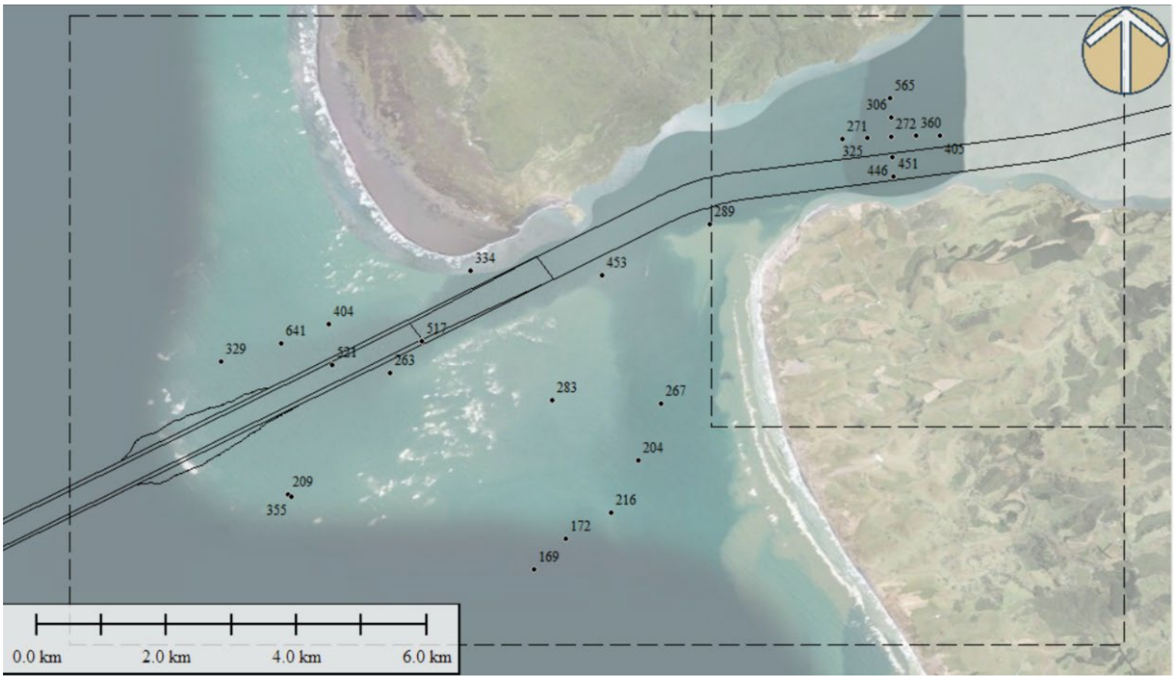

Figure 2.23: Median grain sizes (microns) from T+T (2023) sampling outside the harbour entrance

Analysis of density was undertaken for select sediment samples in the vicinity of the harbour entrance (Figure 2.24). Results indicate density ranged from 2.77 to 3.55 g/cm^3 (2770 to 3500 kg/m^3). It is noted that these densities are considerably lighter than the 4800 to 5300 kg/m^3 assumed for a typical West Coast titanomagnetite sand in previous studies of the Manukau Harbour entrance (i.e. eCoast, 2020).

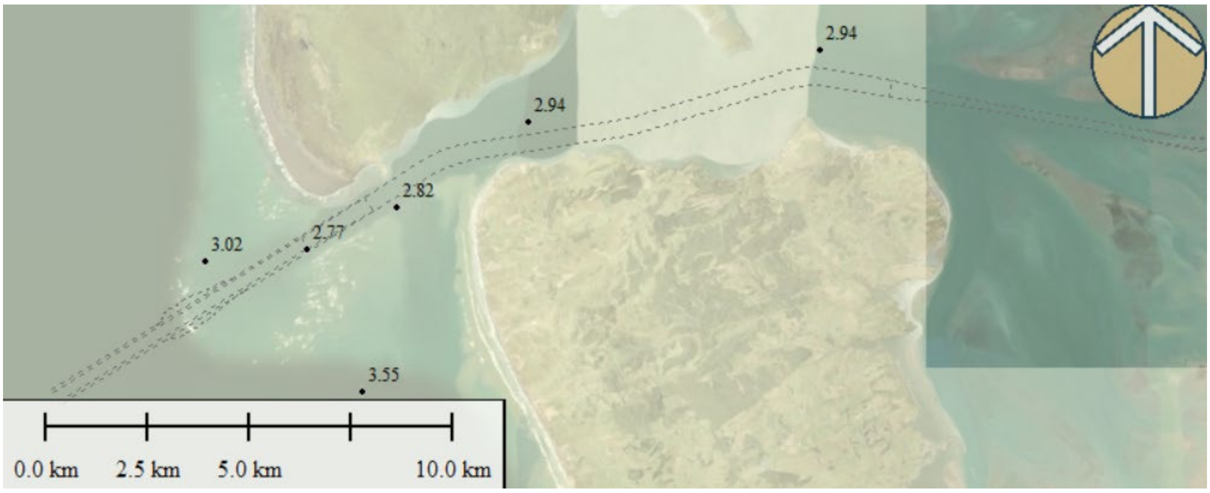

Figure 2.24: Density (g/cm3) results from select sampling locations in the vicinity of the harbour entrance

Papakura Channel to the Pāhurehure Inlet

Inside the harbour (Figure 2.25) median grain sizes reduced, typically becoming less than 200 micron. In the base of channels this material became silty in places (less than 63 micron). Rare coarse loose shell deposits were encountered over some of this material. Outside of the channels in shallower depths, material reverted to a fine sand. These materials are generally more exposed to wind waves, resulting in the remobilisation of fine materials, some of which may contribute to the deposition of finer materials in the base of comparatively more sheltered channels.

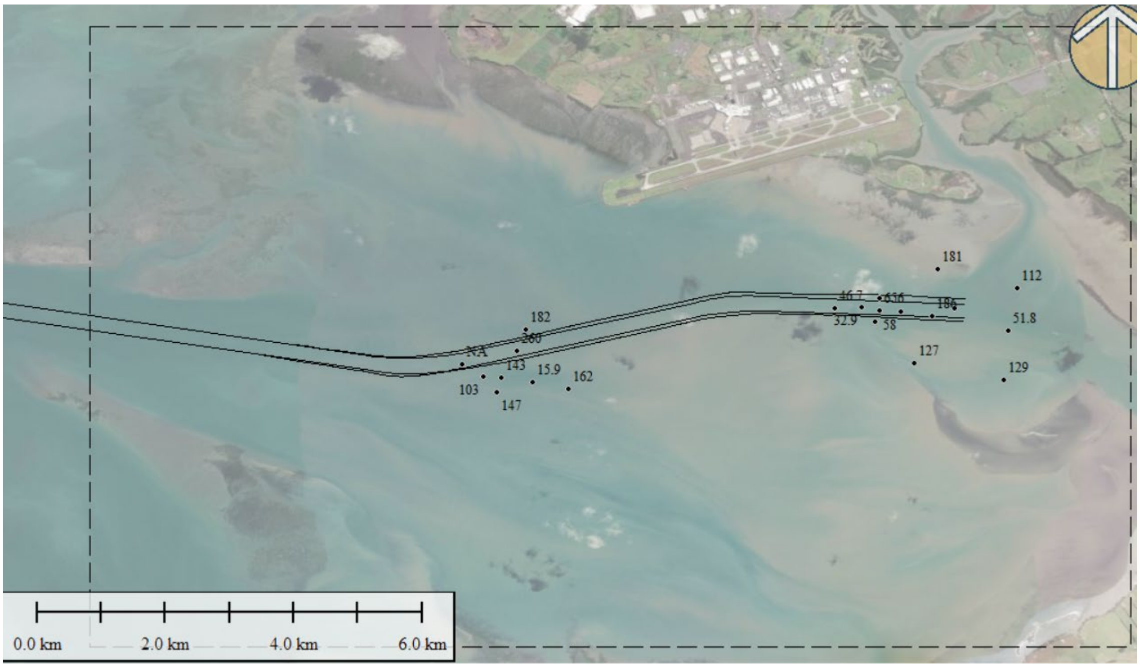

Figure 2.25: Median grain sizes (micron) from T+T (2023) sampling inside the harbour

Figure 2.23 and Figure 2.25 show changes in the median partile diameter, from primarily fine to medium sand in areas close to the harbour entrance to comparitively silty material in the vicinity of harbour inlets and tributaries. This change in silt content is also illustrated in Figure 2.26, comparing channel sediment opposite Cornwallis Wharf, to an inner harbour location south of the airport opposite the Pāhurehure Channel. The sample closer to the harbour entrance (3.01) comprises a clean fine sand with a median particle diameter of approximately 150 micron. Sand of a similar size distribution can be seen in the channel sample in the Pāhurehure Channel, however this is mixed with an approximate equal fraction by mass of silt.

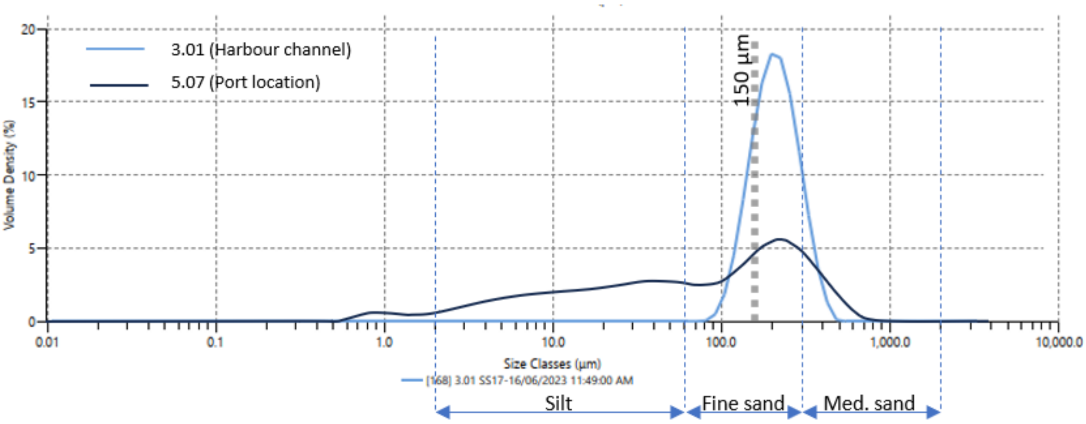

Figure 2.26: Comparison in Particle Size Distribution (PSD) between material located in the Pāhurehure Channel south of the airport (5.07) to a channel sample located some 15 km to west opposite the Cornwallis Peninsula (3.01)

From Figure 2.27, sediment in the base of channels is generally observed to contain higher fractions of silt than material on shallower banks each side of the channel.

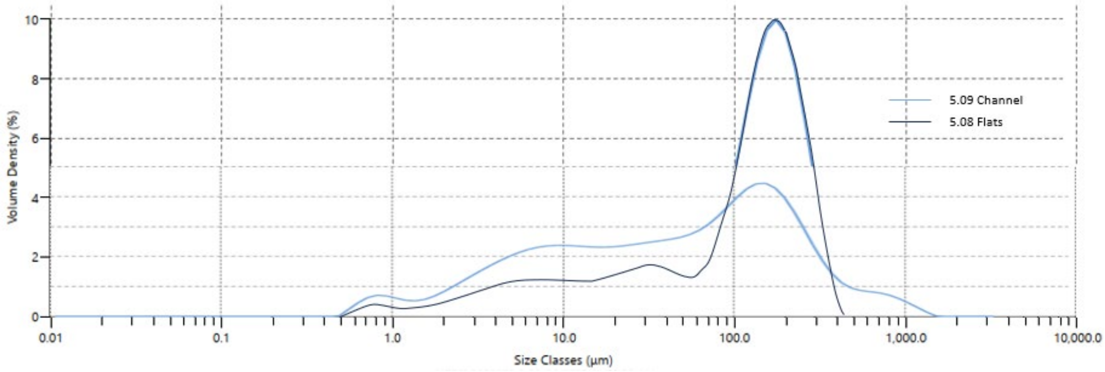

Figure 2.27 Figure comparing PSD results from sampling in tidal channel material with material adjacent to channel in the area of the proposed inner navigation channel.

Extensive sampling undertaken by Reed et. al. (2008) on the banks of the Pāhurehure Inlet towards Papakura Township (pictured in Figure 2.17) show further increasing silt content in stream bank material, becoming more than 90% silt by mass in some locations at the head water of tributary systems.

Analysis of density was undertaken for select sediment samples. Results indicate density ranged from 1.45 to 2.71 g/cm^3 in the upper Papakura Channel (Figure 2.28). Differences in these values to those in the delta systems to the west are likely due to their differing origins with open coast sediment predominantly of volcanic origins and the inner harbour samples predominantly derived from eroded sedimentary material.

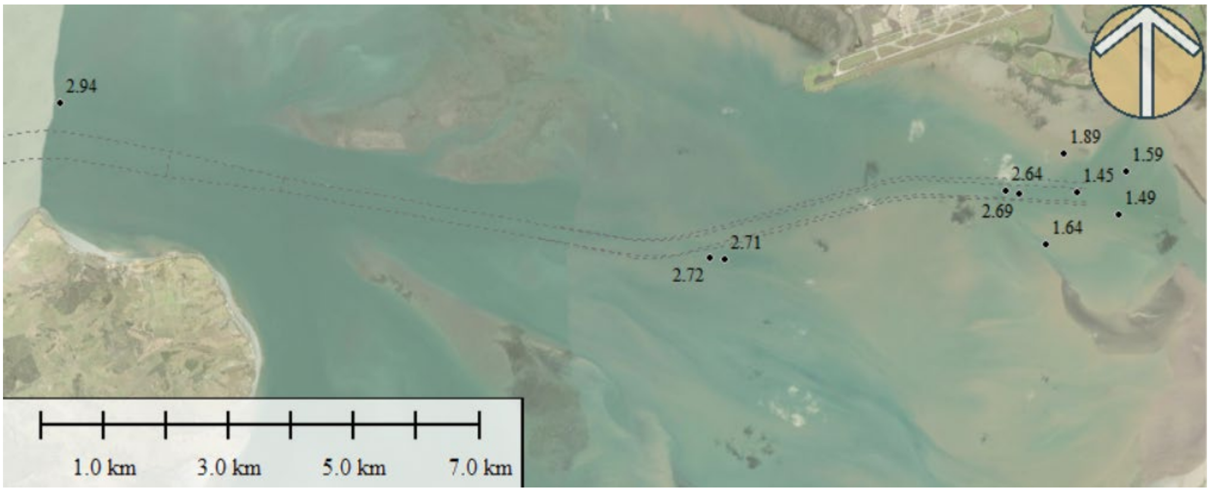

Figure 2.28 Density (g/cm3) results from select sampling locations

2.5.3 Contamination

The Manukau Harbour has a history of poor water quality and sediment contamination through historical pollution sources such as the untreated industrial and domestic wastewater discharge, and untreated stormwater runoff.

Kelly, S. (2008) concluded that the harbour has relatively low concentrations of key stormwater contaminants (copper, lead and zinc), except in Māngere Inlet and Oruarangi Creek. Majority of the contaminants are deposited in the upper reaches of the harbour, with the centre of the harbour being less susceptible to sediment and contaminant accumulation.

Kelly, S. (2008) predicts concentrations of copper and zinc for majority of the harbour to increase above sediment quality guidelines over the remainder of the century, with modelling suggesting that contaminant source control and stormwater treatment only slowing, but not reversing this trend.

Green, M. (2008) created models to analyse catchments for Pāhurehure Inlet for two future scenarios for the remainder of the century: no additional stormwater treatment or increased stormwater treatment. With no additional stormwater treatment, the predicted sediment deposited in the harbour remained constant, with sediment quality Threshold Effects Levels exceeded in the Pāhurehure Inlet upper extremities of the sub-estuaries. Increased stormwater treatment decreased sediment deposited in the harbour by 0 to 9% but had minimal effect on the metal concentrations in the harbour bed sediments.

Additional samples were collected and analysed as part of a 2023 campaign (refer *TWP02 Fieldwork*) with results relevant to contamination presented within *TWP06 Dredging*.

2.6 Coastal geomorphology

2.6.1 Manukau Harbour

The inner harbour (inside of the Cornwallis Peninsula) is generally shallow and sheltered from the oceanic swell, although is subject to moderate wind-generated waves generated across the harbour and tidal currents due to the high tidal range (refer Section 3.4). The drowned river valley acts as a sediment sink, accumulating both open coast sands and freshwater silts. As a result, the harbour is shallow; approximately one third of the harbour area is exposed at low tide (Tonkin & Taylor Ltd, 1986). The intertidal mud flats and sand banks make up a large portion of its area and consist of fine sands, silts and vegetation. Mangroves line the sheltered shorelines, and exposed shorelines are generally sandy in composition. Channels cut through the mudflats and sand banks, with the deepest channels formed over remnant valley floors that have infilled with sediment. These deep channels range between 20 – 30 m deep (CD) in the primary channels, with a maximum of 50 m depth between the two heads.

The outer harbour, between the Cornwallis Peninsula and open coast beaches at Whatipū and Āwhitu, comprises the flood tide delta which is a shallow feature comprised of sands and the deeper inlet channel at the entrance between the two heads. This delta is geomorphologically linked to the open coast and ebb tidal delta, exchanging sediment under tidal processes. The delta appears to be more stable than the ebb tidal delta (refer Section 2.6.3), with less observed movement over time.

2.6.2 Open coast

The Āwhitu Peninsula, is a sand barrier extending between the Waikato River mouth and South Head at the entrance to Manukau Harbour. It is currently eroding rapidly with estimates of around 0.77 m/year. In contrast, the North Head, Whatipū (Figure 2.3), is a prograding sand flat that expanded rapidly at a rate of 25.9 m per year between 1940 to 1960, slowing to 3.0 m /year between 1987 and 2003 (prograding only at the north end, seemingly eroding at the south end), and 4.6 m per year from 2003 to 2010 (Blue & Kench, 2016). Figure 2.29 shows the Whatipū shoreline from years 1853 to 2000, showing over 900 m of progradation over a multi-decadal time frame.

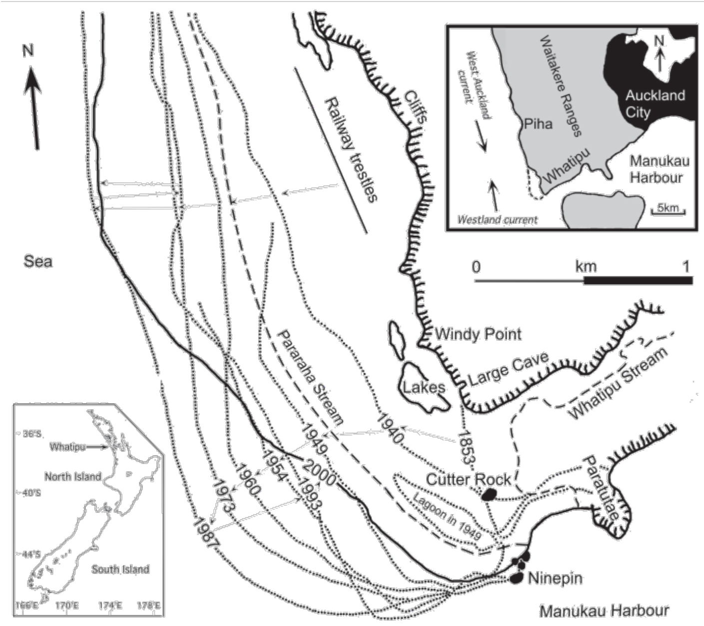

Figure 2.29: Excerpt from (Pegman, 2005) showing Whatipū shoreline changes from 1853 to 2000

Historical accounts from local Māori circa 1878 describe the Āwhitu Peninsula as having a large sand flat and dune system fronting its northern cliff edge 'many generations' ago (prior to 1865). This area is coined 'the lost land of Paorae' and was described to have been scattered with lakes and 'clumps of tall Manuka' similar in geology to the prograded portion of the South Kaipara Barrier (Schofield, 1979). Schofield (1979) estimates this land was present around 1700 AD, until longshore drift, sea level rise, and increased storminess led to the movement of this sandy flat northwards, possibly helping form the prograded Whatipū area, and causing dry patches of sand banks on the ebb tidal delta - as noted in historic charts (refer Section 2.2).

It is presumed that this large 'sediment lug' was historically sourced from the Waikato and will continue to move northwards up the west coast from prevailing southwest wave actions and associated longshore drift. The slowing progradation of the Whatipū Peninsula could be evidence that the bulk of the 'sand lug' shifted prior to 1960.

2.6.3 Tidal delta system

Tidal inlets systems, regardless of size, tend to have similar general morphology (Davis, 2013) comprising an accumulation of sediment at the landward end of the inlet channel known as a flood-tidal delta, and an accumulation of sediment at the open water end termed an ebb tidal delta (ETD; Figure 2.30). These features are shaped by tidal flows and, in the case of the ebb tide delta, waves. Hicks & Hume (1996) found a relationship between the volume of the tidal exchange, or tidal prism of an estuary and the size of the ebb tide delta, with larger estuary systems having larger deltas. Deltas act as sediment sinks along sandy coastal systems (Davis, 2013), with the sediment that comprises them potentially having a long residence time before continuing along the coast.

The ETD at the mouth of the Manukau Harbour (METD) is the second largest in New Zealand, second only in size to the ETD at the entrance to the Kaipara Harbour. Hicks & Hume (1991) estimate the sand storage volume within the METD at 1250M m^3. Hicks & Hume (1991) also classify the METD as 'free-form' rather than 'constricted by headland' because although the rock headland (Waitākere Ranges) acts as a jetty and constricts the throat of the estuary, it does not constrict the lateral extent and thus the ETD forms freely.

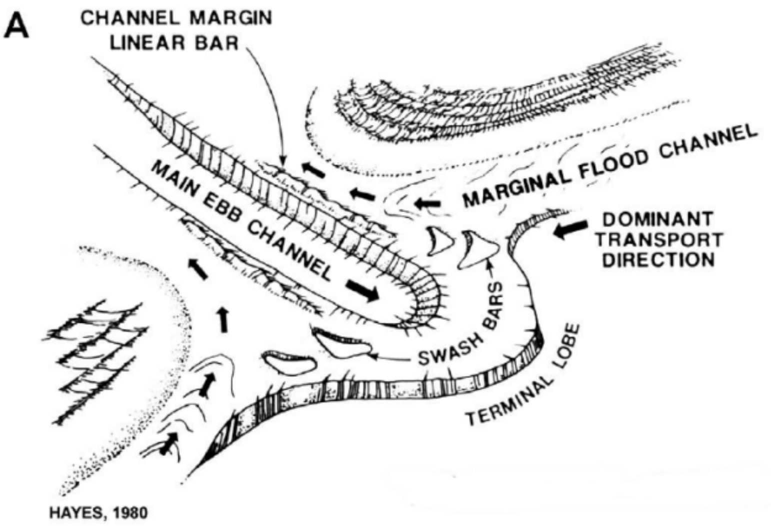

Figure 2.30: General morphology of ebb tidal deltas in mesotidal settings (Hayes and FitzGerald, 2013, after Hayes, 1980)

The complex array of channels and bars and their ever-changing movement makes the METD both a challenge for safe vessel navigation and a difficult system to understand from a geomorphic perspective. The dynamic nature of the channels and bars are frequently noted but have rarely been described within scientific studies. The form of the bar and location of the main South-West Channel is known to change over time, with a hypothesised cyclic rotation of the main channel from southeast to northwest over a 30–40 year timeframe (Tonkin & Taylor Ltd, 1986, Duder & Senior, 2010) based on historic bar surveys between 1863 and 1982.

Ford (2023) has updated this analysis using a combination of historic navigation charts, hydrographic survey data from 1862-2018, and optical satellite imagery from 1999-2022 (Refer *TWP 03a*). Results reveal the behaviour of the METD closely conforms to the model of ETD breaching and outer delta breaching processes as suggested in a widely used conceptual model produced by FitzGerald et al. (2000) and shown in Figure 2.31. This process involves a cycle of channel migration, abandonment and new channel formation that has been observed in the satellite record and demonstrated in similar settings using numerical models, i.e. Dastgheib (2012) and Lenstra et al. (2019). Of note, the inner section of the channel, the first ~2.5 km seaward of Paratutae Island, shows relative stability as observed in numerical models, while the outer section of the channel is highly dynamic. This cycle of morphological adjustment of the channels and bars at the entrance to the Manukau Harbour appears to have taken place several times since 1862 (Figure 2.32) with the sequence of satellite images since 1999 clearly showing a near-complete phase of this cycle (Figure 2.33).

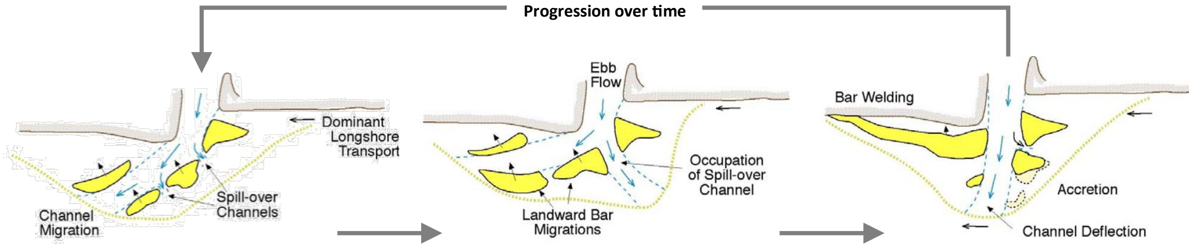

Figure 2.31: Ebb tidal delta breaching conceptual model, adapted from (FitzGerald, Shoreline erosional-depsitional processes associated with tidal inlets, 1988)

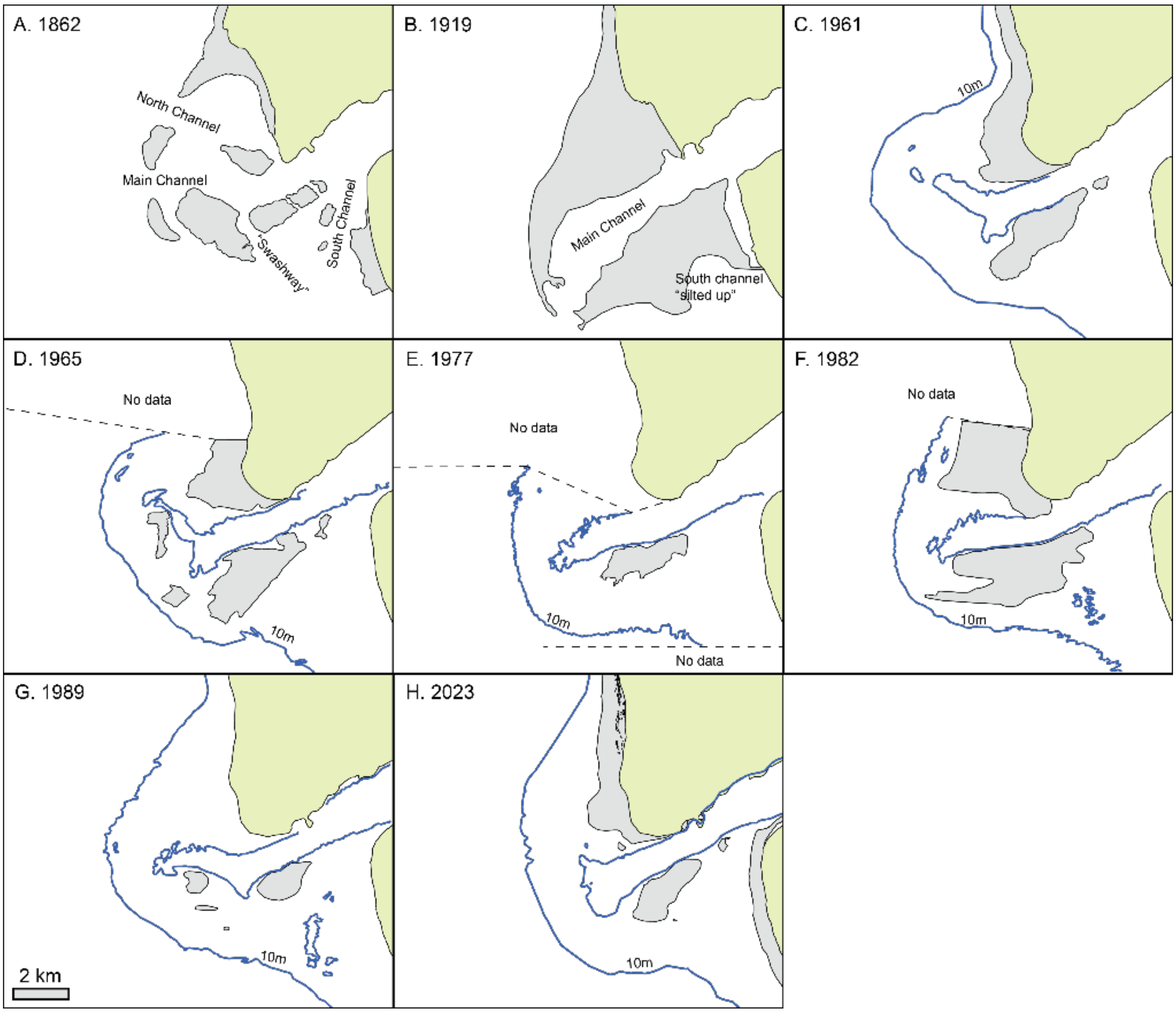

Figure 2.32: Channel and bar positions on the Manukau ebb tidal delta interpreted from historic charts and recent survey (refer TWP03a for detail)

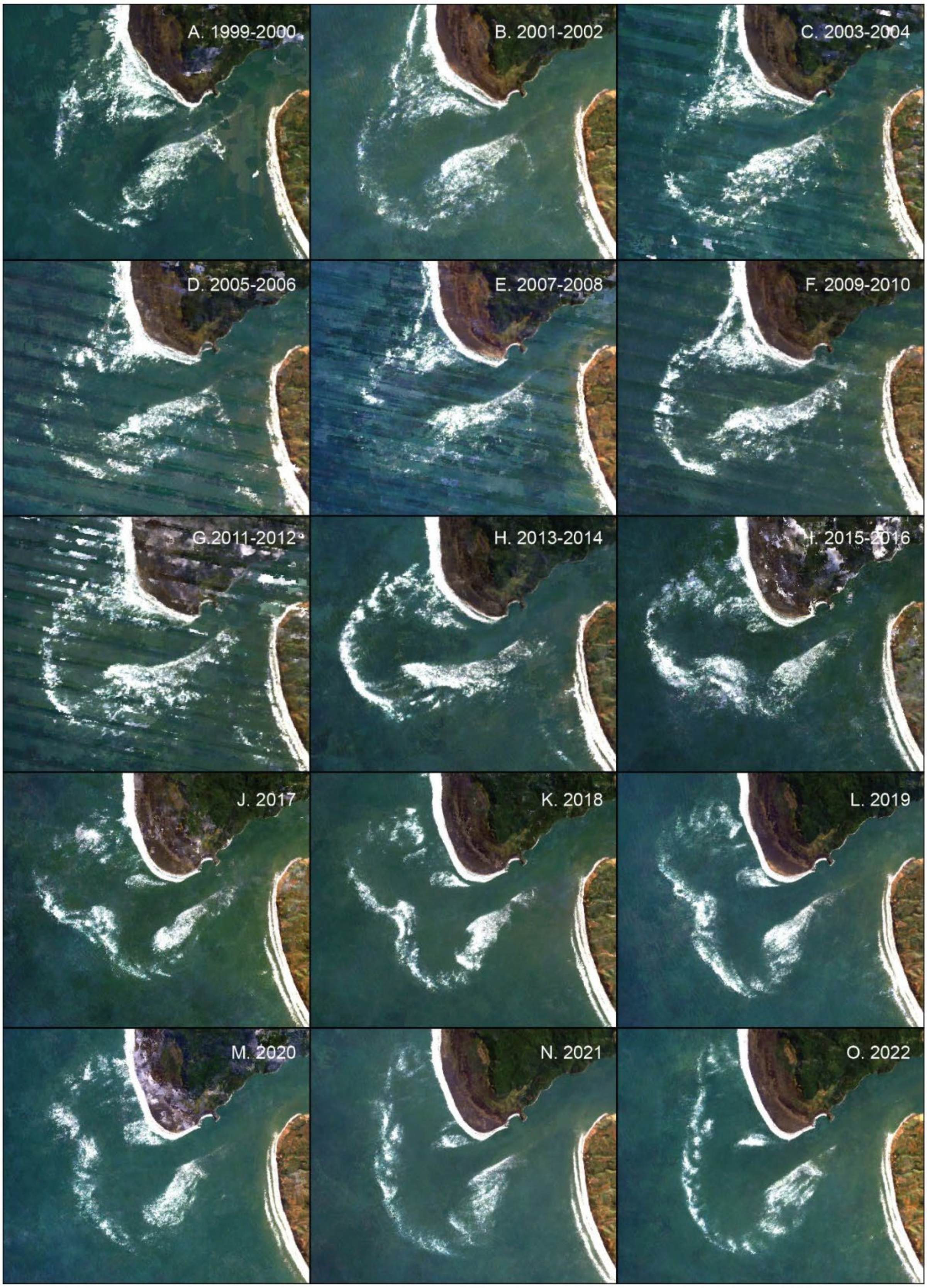

Figure 2.33: *Averaged Landsat and Sentinel 2 imagery of the Manukau ETD over time indicating a gradual migration of the main (SW) channel to the north (2009 to 2015) before a channel bifurcation starting in 2015 and re-establishment of a main SW channel to the SW in around 2019-2020.*

The last comprehensive survey undertaken in 1989 appears to align with a state of NW channel migration with a substantial bar across the proposed navigation channel. The present survey appears to show a SW channel alignment with a bifurcation starting in around 2015 resulting in the re-establishment of a main SW channel in around 2019-2020 (Figure 2.33). Further analysis of discrete surveys collected by POAL between 2005 and 2016 illustrate the rate of channel migration with rates of movement in the order of 115 m/year, in general agreement with rates from satellite imagery. Average cross-sectional change was found to be in the order of 530 m^3/year per linear metre of channel. With an assumed 4 km long channel, this may be in the order of 2 million m^3/year.

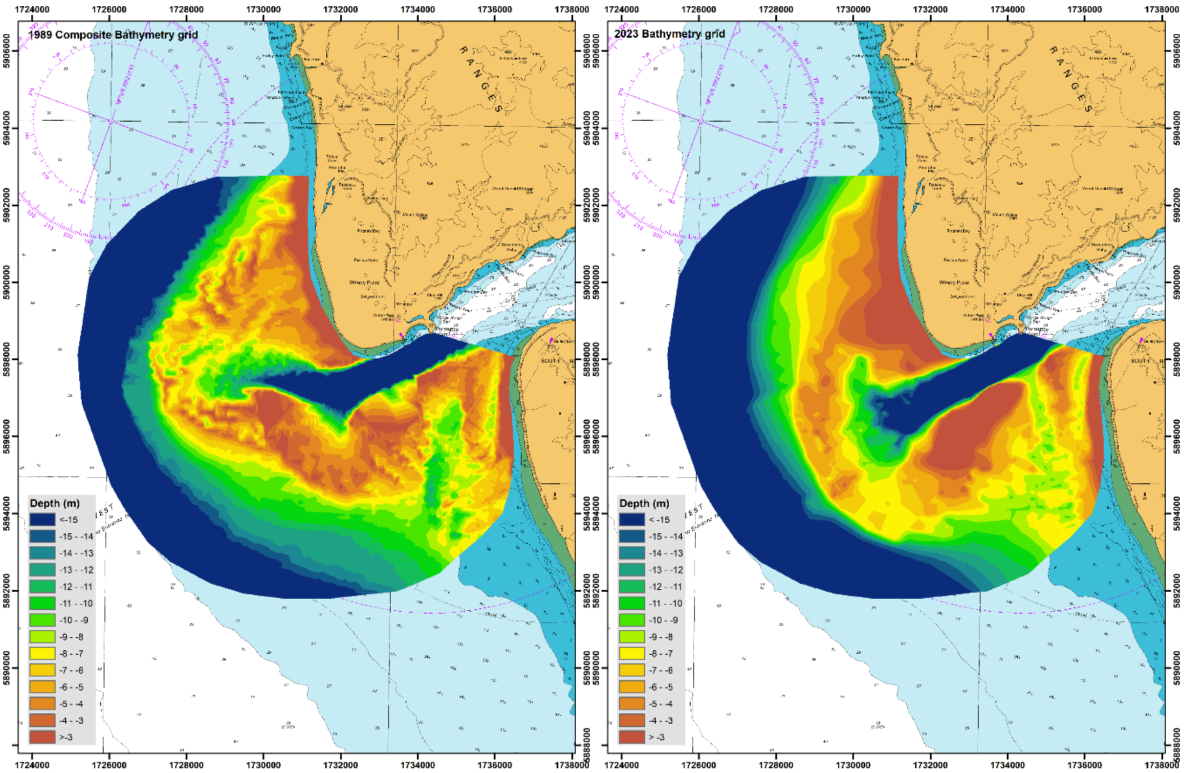

Figure 2.34: 1989 (left) and 2023 (right) surveys illustrating two different bar configurations.

Based on the high temporal resolution of channel alignment information over the last 25 to 35 years a conceptual model for the change in channel position can be developed (Figure 2.35, lower) and then using this model, hindcast back in time to match previous records (Figure 2.35, upper). While these cycles are not likely to be exactly uniform, and it is still unclear the precise mechanism for initiating a breach to the south, the model provides reasonable agreement with previous surveys and indicates there is likely to have been around six cycles since the first survey in 1836, with an average rate of 31 years, in keeping with estimates by Tonkin & Taylor Ltd (1986) and Duder & Senior (2010).

The implications of this cyclic bar process on the development and maintenance of a navigation channel into the Manukau Harbour are:

1 The configuration of the channel makes a considerable difference to the position and depth of the shallow bars (or vice versa) which in turn affects the dredge volumes and plant requirements (refer TWP06). The present channel configuration represents a ‘low volume’ state in the bars along the proposed alignment, with future movement towards the northwest likely to increase the volume of bars along the alignment. Timing of this is uncertain but could occur in the next 10 to 15 years.

2 Large scale morphological evolution has the potential to, at times, result in very large volumes of sediment migrating into the navigation channel. This is evident in Figure 2.33 where between 2009 and 2015 the inner bar (shown by the white signature of wave breaking on shallow bathymetry) extends north, pushing several M m^3 of sediment across the proposed alignment. The results of this can be seen in Figure 2.7 where the depth increased by >10 m over a length of some 2 km. It is unclear whether accumulation of sediment on the south bank initiates this movement, but the placement of maintenance dredge material will be important in managing this process.

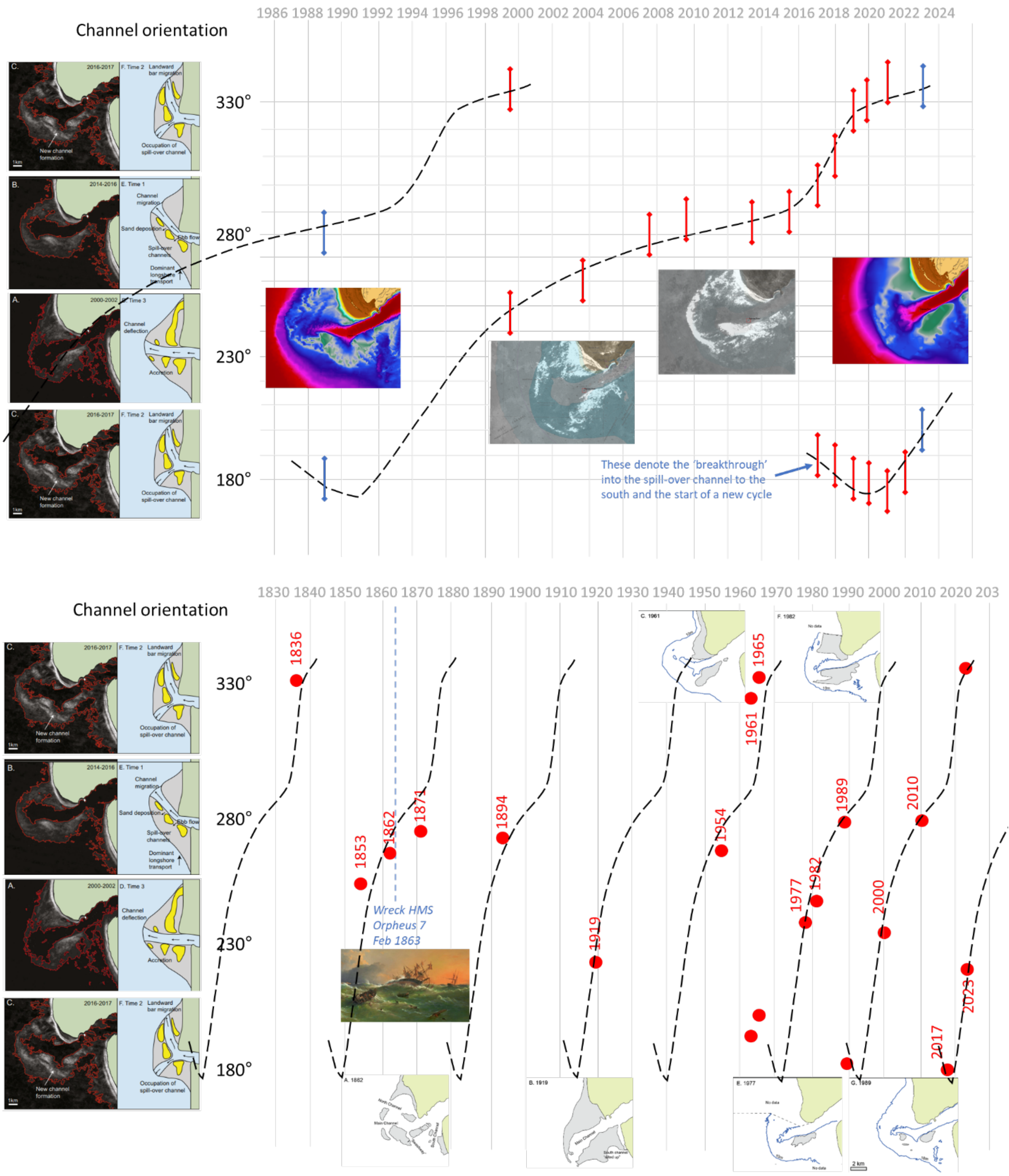

Figure 2.35: Conceptual model of channel configuration during the past 35 years (top) and 200 years (lower)

3 Coastal processes

This section presents a summary of coastal processes occurring within the Manukau Harbour and entrance. The summary includes recent findings and results of fieldwork (refer *TWP02 Fieldwork*), numerical modelling (*TWP03b Metocean Study* and *TWP03c Sediment Transport*), and analysis of historic bathymetry and imagery (*TWP03a Historic Bar and Channel Dynamics*) and readers are referred to those papers for technical working paper for detail.

3.1 Water levels

Manukau Harbour is a large body with tidal levels and timing varying across the harbour. Tides are semi-diurnal (twice daily) with a monthly spring-neap cycle. Tidal information is available for several locations, reproduced in Table 3.1.

Table 3.1: Manukau Harbour tidal levels (sourced form LINZ)

Tidal levels (m CD)	Locations				
	Paratutae Island	Cornwallis	Papakura Channel - LPG Terminal	Onehunga	Clarks Beach
Highest Astronomical Tide (HAT)	-	-	-	4.54	-
Mean High Water Springs (MHWS)	3.3	3.7	3.9	4.17	4.4
Mean High Water Neaps (MHWN)	2.6	3.1	3.2	3.34	3.5
Mean Sea Level (MSL)	1.9	2.2	2.1	2.43	2.6
Mean Low Water Neaps (MLWN)	1.1	1.2	1.1	1.44	1.6
Mean Low Water Springs (MLWS)	0.4	0.6	0.4	0.56	0.6
Lowest Astronomical Tide (LAT)	-	-	-	0.12	-

Paratutae Island is located within the channel entrance, while the others are located within the inner harbour. The difference between tidal levels shows that the tides are generally amplified within Manukau Harbour with spring tidal range at Paratutae Island and Cornwallis being 2.9 and 3.1 m respectively and at Onehunga being 3.6 m. The spring tidal prism within Manukau Harbour is reported at 918M m^3 (Hicks and Hume, 1996)

Water level data was collected at several locations within the Manukau Harbour during the fieldwork campaign (refer *TWP02 Fieldwork*) and used together with current data to calibrate a hydrodynamic model (refer *TWP03a Manukau Harbour Numerical Modelling - Metocean Study*). Results of calibration indicates a slight (7-14%) over-prediction in tidal prism compared to measurements with water levels having good agreement over high tide but the model tending to slightly overpredict the low tide amplitude.

Measurements indicate a spring tidal prism in the order of 1,040M m^3 during flood tide and 992M m^3 during ebb tides, slightly higher than Hicks and Hume (1996), with modelled levels slightly higher than measured at 1,160M m^3 and 1,140M m^3. Modelled neap tidal prism was in order of 600M m^3.

Figure 3.1 shows water level corresponding to a peak high tide at the harbour entrance (top), Cornwallis Peninsula (centre) and in the mid harbour (lower). The amplification of tidal level and time delay of the tidal wave with distance into the harbour is evident in the plots.

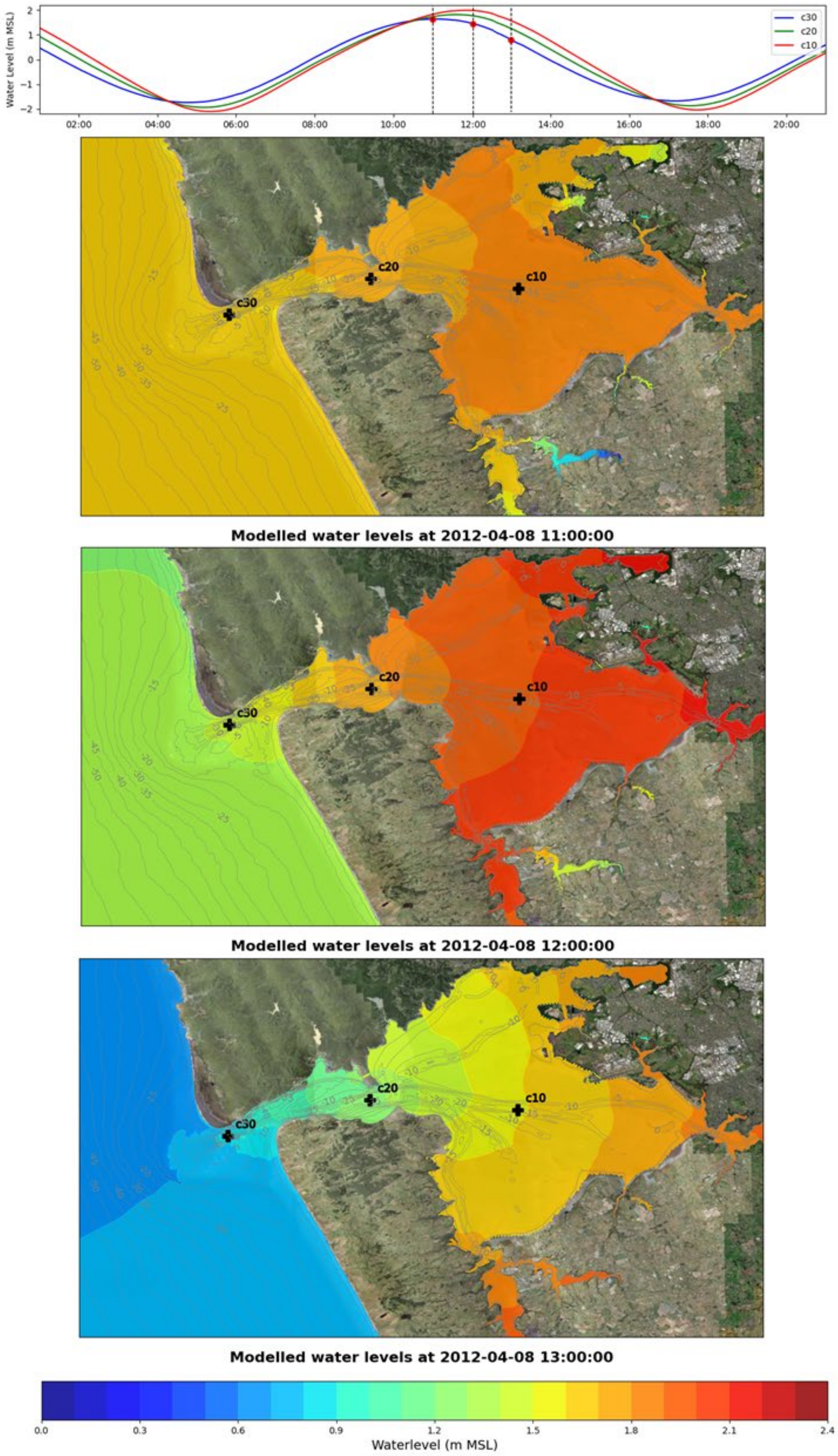

Figure 3.1: Water level corresponding to a peak high tide at the entrance (top), Cornwallis Peninsula (centre) and in the mid harbour (lower)

3.1.1 Extreme water levels

Extreme water levels are largely influenced by storm surge occurring concurrently to a high tide, a term coined 'storm-tide'. Extreme water levels for the Manukau Harbour are provided by Stephens et al. (2016). This study used a joint probability method and a calibrated numerical model to predict extreme water levels around the harbour (Table 3.2).

Table 3.2: Extreme water levels (m CD) (Stephens, et al., 2016)[1]

	Annual Exceedance Probability (AEP)	39%	18%	10%	5%	2%	1%	0.50%
	Average Recurrence Interval (ARI)	**2yr.**	**5yr.**	**10yr.**	**20yr.**	**50yr.**	**100yr.**	**200yr.**
Locations	Paratutae Island	4.39	4.42	4.45	4.49	4.55	4.63	4.72
	Cornwallis	4.58	4.63	4.66	4.70	4.76	4.81	4.88
	Papakura Channel - LPG Terminal	4.80	4.86	4.93	5.01	5.14	5.25	5.36
	Onehunga	4.78	4.86	4.92	5.00	5.12	5.21	5.32
	Clarks Beach	4.73	4.78	4.83	4.91	5.08	5.21	5.35

[1] Note that an additional allowance for mean sea level rise since the study has been incorporated (+0.04 m).

3.2 Wind

Winds within Manukau Harbour are predominantly from the south-west quarter with less frequent winds from the north to north-east. Figure 3.2 presents a wind rose for Auckland Airport (1965 to 2012) and indicates that 10 min average wind speeds are typically 3 to 9 m/s (6 to 18 knots) with winds up to 23 m/s (45 knots) observed.

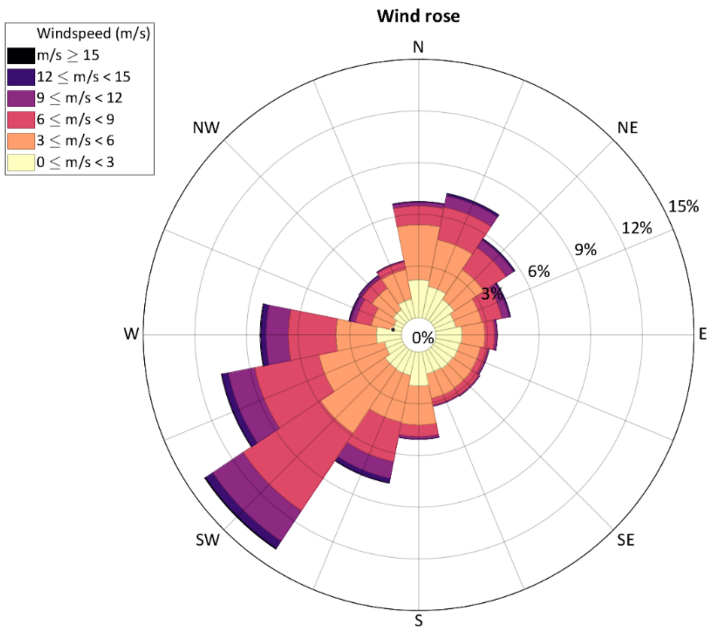

Figure 3.2: Wind rose for Auckland Airport 1965 to 2012 (10 min average speed).

A 41 year wind-wave hindcast (1980 – 2020 inclusive) was undertaken by MetOcean Solutions Ltd. as part of this study (refer *TWP03a Manukau Harbour Numerical Modelling - Metocean Study* for set up and calibration detail). A wind rose for a location offshore of the Manukau Bar is presented in Figure 3.3 indicating a dominance of wind from the SW quadrant, although strong winds (>14 m/s) did occur from all directions. High winds occurred more often in winter and spring than summer and autumn. Climate change projections for New Zealand (Mullan et al., 2011) suggest that westerly flow will increase in frequency in spring (up to 20%) and winter (up to 70%) and to decrease in summer and autumn (up to 20%). Mullan et al. (2011) suggest a 2.4% averaged increase in the maximum wind speed, in the period 1961-2100 relative to 1961-2000 (refer *TWP 03b*).

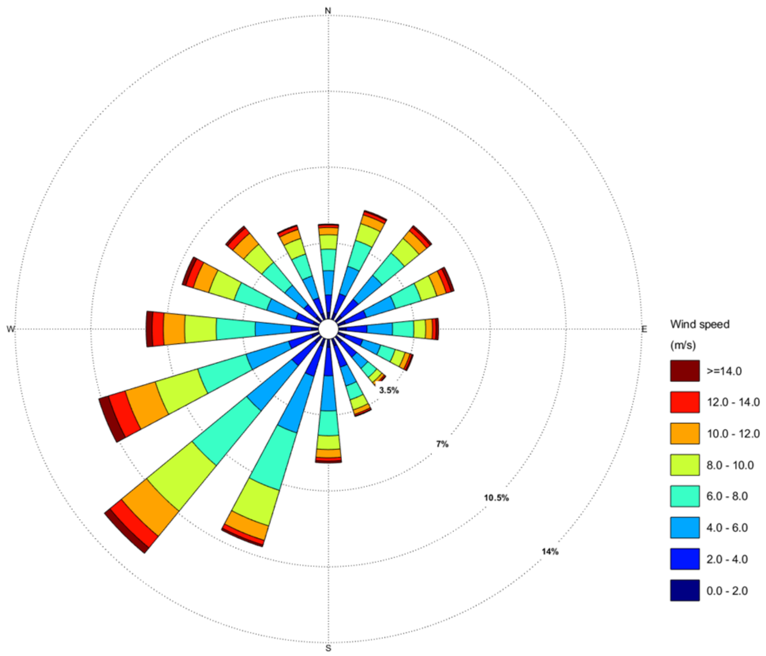

Figure 3.3: Annual wind rose offshore of the Manukau Bar (refer TWP03a Manukau Harbour Numerical Modelling - Metocean Study)

3.3 Wave climate

Manukau Harbour's wave climate can be considered separately between the open coast and within the harbour.

3.3.1 Open coast

The open coast outside of the Manukau Harbour is a highly energetic environment, exposed to swell and sea generated within the Tasman Sea and Southern Ocean. Weather systems responsible for generating waves on the open coast include: low pressure systems tracking south of New Zealand or up into the southern Tasman Sea; Tasman lows, often generated off the east coast of Australia moving east, and ex-tropical cyclones or storms generated in the SW Pacific or Coral Sea tracking south into the Tasman.

A 41-year (1980-2020) wave hindcast has been developed by MetOcean Solutions Ltd (refer *TWP03a*) for the area offshore of the Manukau Harbour entrance, within the entrance and inside the harbour (Figure 3.4). Offshore of the harbour entrance (Figure 3.5 and Figure 3.6), waves predominantly occur from the south-west, but can occur from the SSW through to NW. The annual median (50% exceedance) significant wave height is 2.23 m, and 10% exceedance is 3.64 m. Larger waves tend to occur over winter months (May to Oct) than summer (Sept to April) with waves over 4 m occurring 8-11% of the time over winter and 2-5% over summer. Peak wave period of 12-16 s is most common with large waves (>6 m) having peak periods of between 10 and 18 s. Extreme wave heights reach around Hs = 7 m during an annual event and over 10 m during a 50-year ARI event. While the largest events tend to occur from the SW, large waves can occur from the NW with generally slightly shorter periods.

Climate change is expected to change wave height. Albuquerque et al. (2022) predicts wave height and peak period to increase along the west coast of New Zealand throughout this century with Hemer et al. (2013) and Rouse et al. (2017) suggesting wave height increases in the order of 5% for 2070–2099 for parts of New Zealand exposed to Southern Ocean swell. Extreme values including these increases are presented in Table 3.3. Refer to *TWP03b Manukau Harbour Numerical Modelling - Metocean Study Report* for further detail.

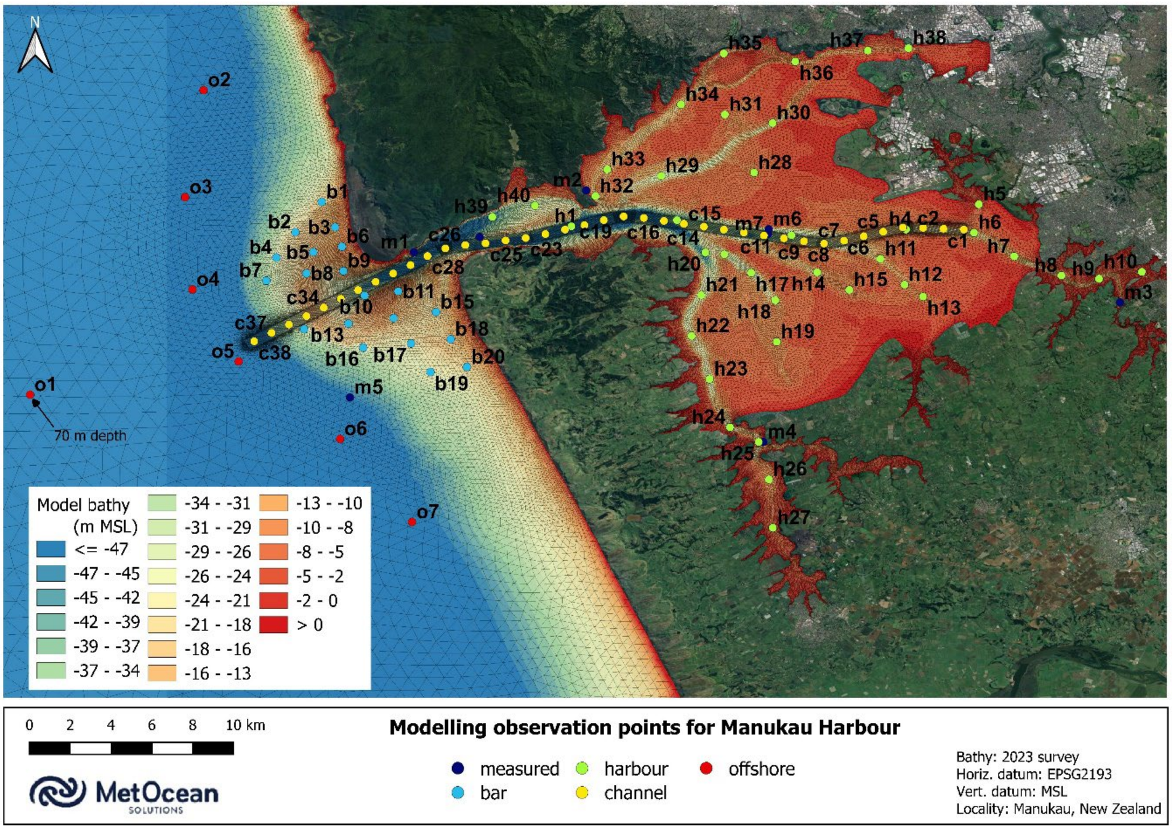

Figure 3.4: Wave hindcast output locations

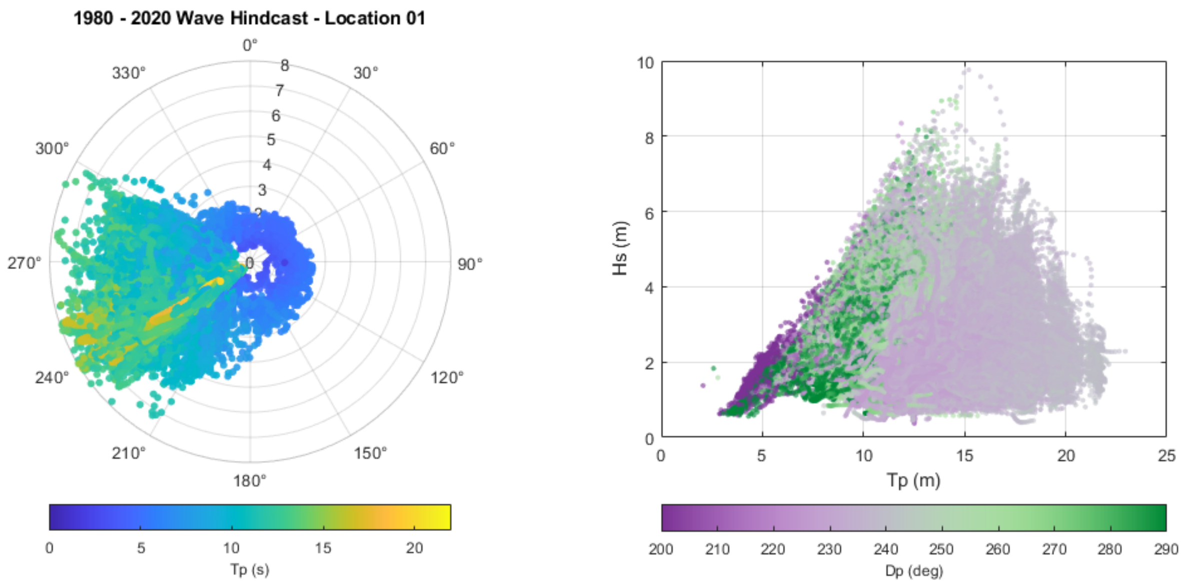

Figure 3.5: Polar plot (left) and scatter plot (right) showing wave height, direction, and peak period for location O1 offshore of the harbour entrance

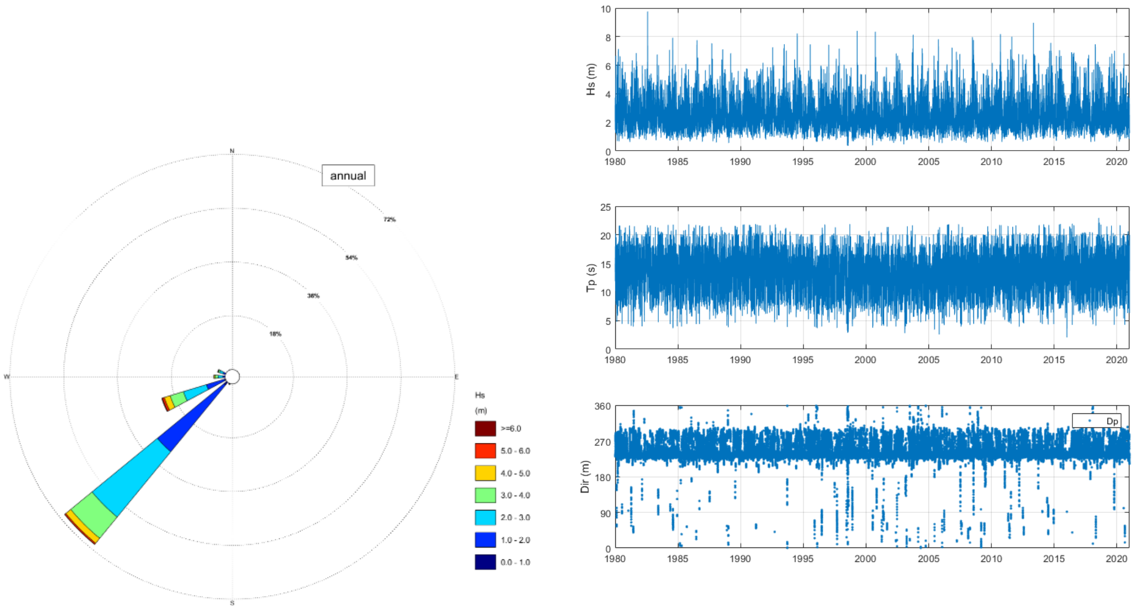

Figure 3.6: Wave rose for the 1980- 2020 hindcast (left) and time series of the hindcast (significant wave height (m) - top, peak period (s) - middle, direction of swell (s) – bottom) for location O1 offshore of the harbour entrance

Table 3.3 Extreme values for wave output location o1 offshore of the harbour entrance

ARI	Hs (m) – All directions	Peak period (s) – all directions	Hs (m) – All directions +5% (climate change projection)
1 yr	6.9	13.7	7.3
10 yr	8.8	14.4	9.2
25 yr	9.5	14.6	10.0
50 yr	10.1	14.7	10.6
100 yr	10.6	14.9	11.1

3.3.2 Manukau Harbour

Manukau Harbour consists of large intertidal flats and sand banks, which are separated by channels. The fetch across the harbour is greatly reduced as the tide falls and the sand banks and mud flats are exposed. During low tide, large fetches are restricted to the channels. Fetch distances are therefore duration limited, in correlation with the tidal cycle. Smith et al. (2001) noted that the fastest wave takes approximately two hours to propagate across the harbour.

The sand banks and intertidal areas are likely to create depth limiting conditions during high tide. Therefore, waves propagating across the harbour are likely to encounter multiple variations in water depth and depth limiting conditions.

The largest waves will coincide with the largest fetch, during the highest tide, and the strongest winds. At high tide, fetches can exceed 25 km for south-west and northeast winds, creating waves larger than 1 to 1.5 m with short periods of 1 to 4 seconds (Green et al., 2000). Wave data collected during the field campaign (*TWP02*) confirms this with waves in excess of 1 m being recorded (Figure 3.7).

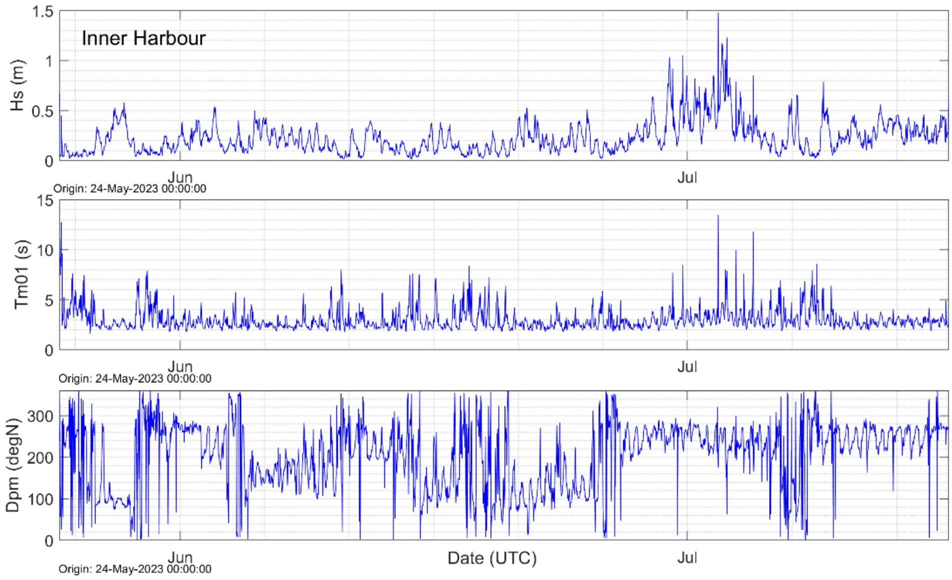

Figure 3.7: Measured wave parameters at the inner harbour wave buoy

3.4 Currents

Currents in the Manukau Harbour are predominantly tidal driven. Inside the harbour, tidal currents are relatively low (<0.5 m/s) on the shallow banks, increasing in the deeper channels (Figure 3.8). The currents are strongest and most complex in the harbour entrance. The entrance converges at the 2.2 km gap between Puponga Point and Mako Point, with Huia Bank creating an obstruction in the channel. Huia Bank directs the current into the western edge of Puponga Point during the incoming tide, creating strong peak tidal speeds that reach 2.25 m/s at the surface and 0.6 m/s near the seabed (Heath, R. A. et al., 1977). This was confirmed by ADCP current measurements with surface velocities during ebb tides reaching 3 m/s (Figure 3.9).

Verbal accounts by local kayakers indicate that a large gyre forms around the Huia Bank on the ebbing and flooding tide. Flow is observed to move eastwards on both ebbing and flood tides on the northern side closest to Huia town. This rotational flow has not been included in previous assessments, with current published knowledge indicating that there are ‘no large-scale eddies’ within the harbour (Bell, Hume, Dolphin, Green, & Walters, 1997).

On the Manukau Bar, flow velocities during flood tides tends to be more evenly distributed around the feature with relatively high flows in the southern ‘flood channel’. During ebb tides, high flow velocities are focussed in the main channel and across the bar to the south-west with much lower velocities being reached in the southern flood channel.

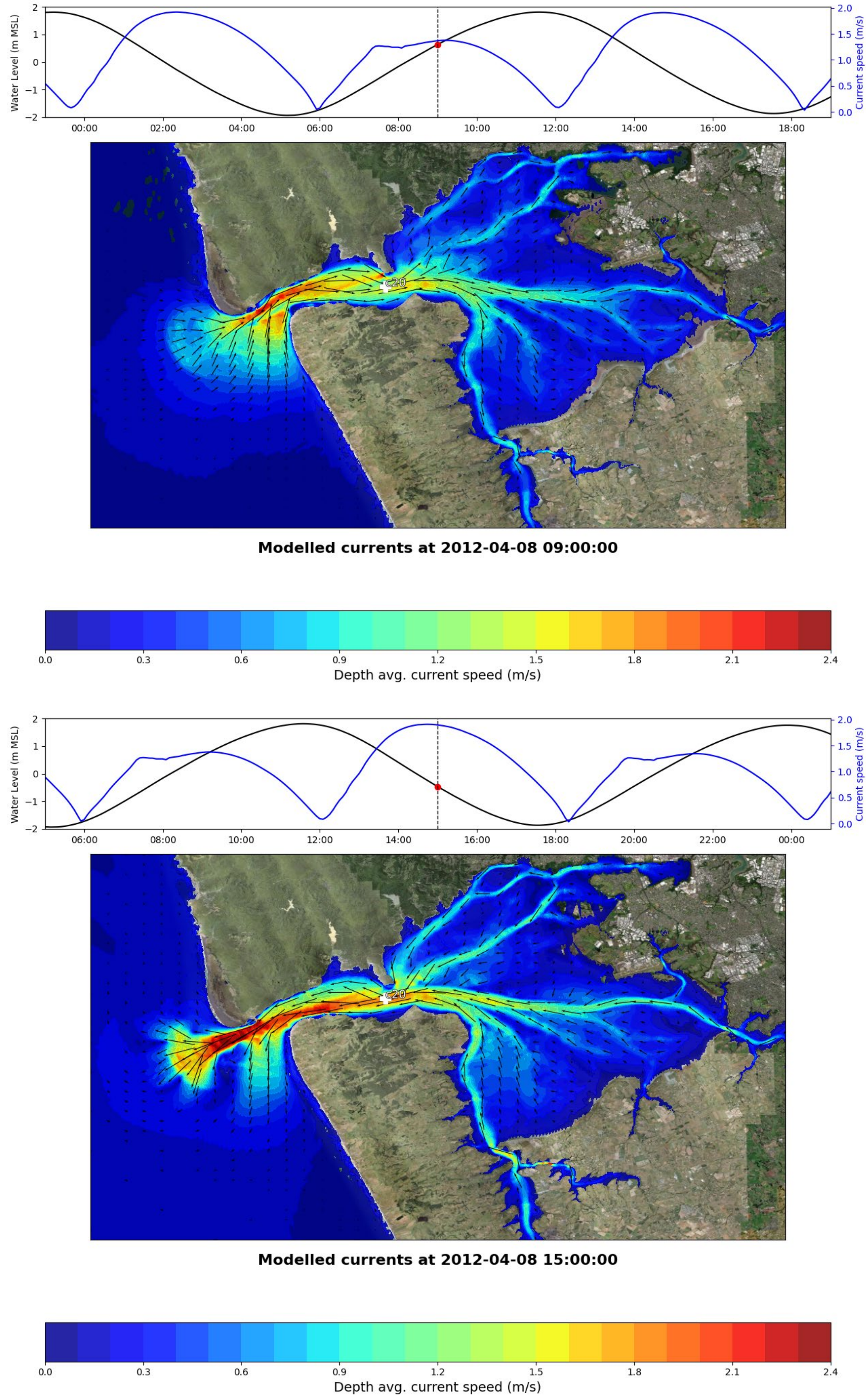

Figure 3.8: Modelled velocities during a spring flood tide (top) and ebb tide (bottom)

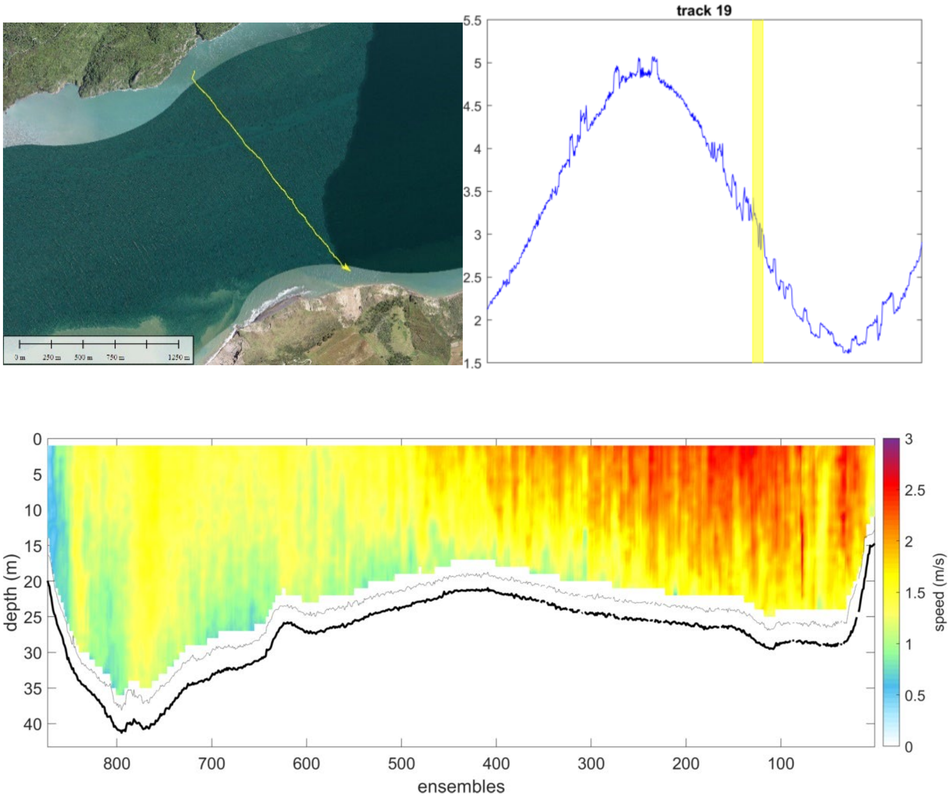

Figure 3.9: ADCP transect of flow velocity during a spring ebb tide at the Manukau entrance

3.5 Sediment transport

3.5.1 Manukau Harbour

Sediment transport within the harbour includes both sand and silt, which are transported by different processes. This section discusses sediment transport processes within the inner harbour of both these sediment types. Green et al. (2000) sheds light on different processes by which sand and silt are transported at different tidal stages, through different pathways, influenced by different weather conditions, and accordingly their estimation requires independent consideration.

3.5.1.1 Terrigenous silt

Section 2.5 discusses the sources of terrigenous silty sediments located within the upper reaches of the harbour. Reed (2008) found that the majority of sediment sourced from the Pāhurehure inlet remains trapped in tidal creeks with any fine sediment entering tidal channels dispersing throughout. (Anderson, 2006) indicates that harbour creeks and bays supported by mangroves are becoming shallower.

Reed et. al. (2008) undertook vibrocores within the banks of the Pāhurehure inlet that were used to derive Sedimentation Accumulation Rates (SAR) over the last 150 years, estimated from radioisotope profiling. Vibrocores were only undertaken in shallow intertidal areas (not in tidal channels) and SAR results were variable ranging from no accumulation (0 mm/y) over coarse sand deposits in an exposed area, to 13 mm/year in sheltered confines of the Pāhurehure inlet. Over the long term, sedimentation rates derived from cores represent net or cumulative effect of potentially many cycles of sediment deposition and re-suspension. At short time scales (i.e., seconds–months), sediment may be deposited and then subsequently re-suspended by tidal currents and/or waves. Net sedimentation rates statistics also mask the fact that estuary sedimentation is an episodic process, which largely occurs during catchment floods, rather than the continuous gradual process that is implied.

Fine suspended sediment in the vicinity of tidal channels generally enters the tidal streams via streams and edge erosion and flows out to depths offshore where wave induced stresses and tidal currents are low - this being the edge of the Manukau ebb tidal delta lobe. Alternatively, on the flooding tides, fine suspended sediment will be pushed up onto the intertidal flats where the tidal velocities will reduce, and the sediment will fall out of suspension. Fine sediment in these areas may be subsequently remobilised by wind due to drag on the water surface, and by wind waves (Green & Coco, 2013). Green (2001) determined that wave activity on surrounding intertidal flats was the primary determinant of suspended silt load in the channel and approaches. Wave generation and propagation models must therefore be considered within sediment transport models.

Wind waves break on these intertidal flats uplifting deposited fine sediments and increasing the silt concentration within the tidal channels. Exposure to wind waves varies across the Manukau Harbour, with more exposed areas such as the Papakura channel having fetch distances from prevailing south-west conditions in excess of 10 km at high tide, reducing to as little as several hundred metres at low tide. Deployment of an optical back scatter sensor by Green et.al., (2000) within the Manukau indicated semi-diurnal spikes in suspended silt approaching low tide when water depths reduced. Suspended sediment at this time was described as a ‘Turbid fringe’. Aerial imagery taken at such a time in the Wairoa channel north of the proposed navigation channel demonstrates this process (Figure 3.10).

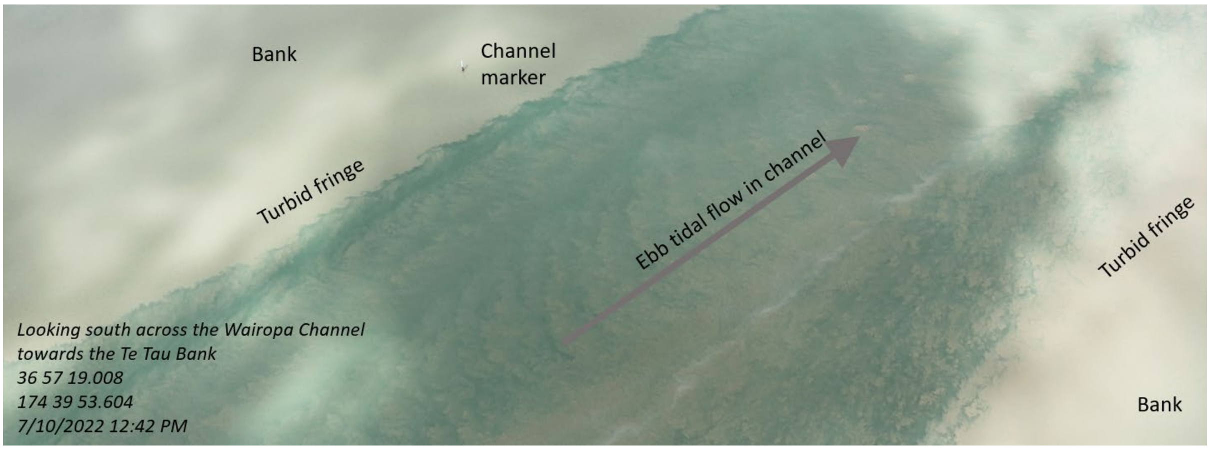

Figure 3.10: Figure showing silt suspended

Hydrodynamic model outputs presented in associated numerical modelling report *TWP03b* are reproduced in Figure 3.8 and indicate strong ebb-dominant tidal asymmetry. Green (2000) measured similar asymmetry using bed mounted electromagnetic current meters in the Poutawa Channel (approximately 2 km south of the Papakura channel) and related this ebb-tidal dominance to likely net transport of fine material out of the harbour via tidal channels. Ebb-dominant transport is consistent with gradational changes in sediment type and comparatively limited supply of sand approaching the Pāhurehure Inlet.

3.5.1.2 Sand

Existing sand deposits dating back to early origins (infilling) of the Manukau Basin are the primary source of sandy sediment, with the majority of this material transported along open reaches of channels that serve as conduits and temporary repositories. Tidal currents are primarily responsible for sand transport, which are ebb-dominant thus favouring net-transport from upper extents of the harbour towards the flood delta system (Figure 3.11).

Sand from the open coast also enters the harbour on flooding tides and transported along main tidal channels to distribute throughout the estuary, and deposit where tidal currents diverge and decrease. Shoals and sand banks within the harbour are largely fed by these marine sands, notable examples within the Manukau Harbour include the flood tidal delta – Huia Bank, the Karore Bank, Te Tau Bank, and Hangore Bank. Wind-wave processes within the harbour can push sand and shell sourced from intertidal material up onto the shoreline forming beaches that fringe much of the harbour environment.

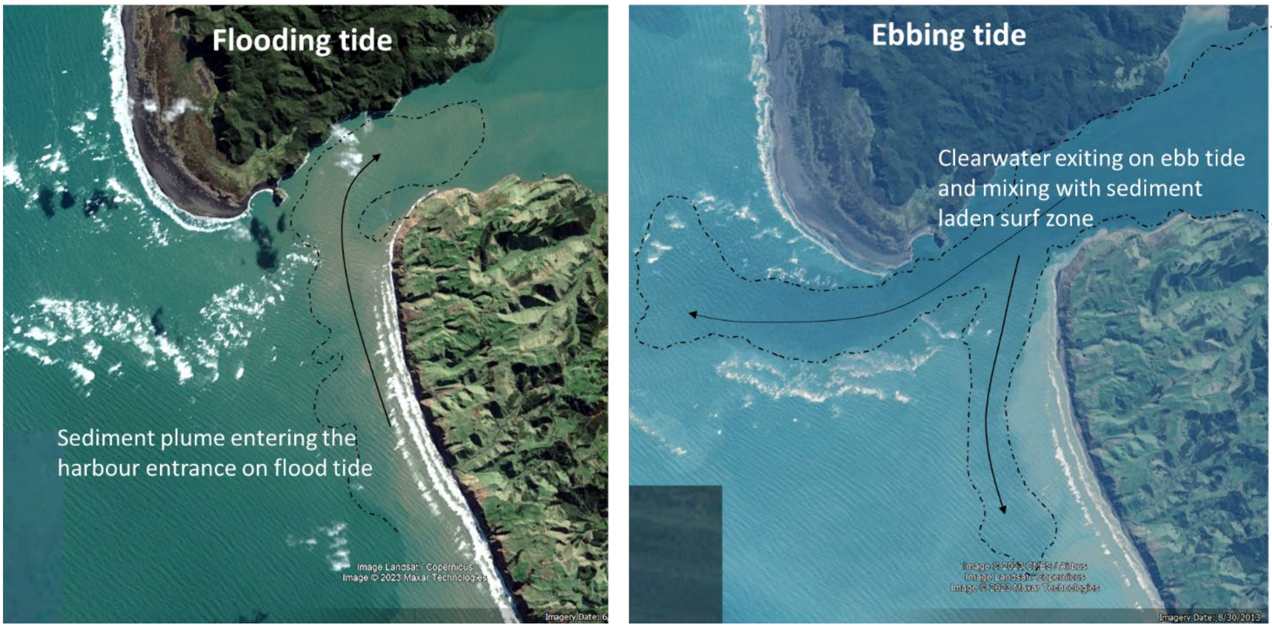

Figure 3.11: Sediment source from Āwhitu Peninsula entering the Manukau Harbour on a flooding tide (left), and an alternative aerial showing clearwater exiting the harbour and mixing with surf zone sediments (right)

Green et. al., (2000) describes sand suspension in channels as a "local process" due to the channel bed being both the source and the pathway for the suspended load. This study assembled bed mounted optical back scatter device in the Poutawa channel and measured spikes in suspended sand at times coinciding with peak ebb and flood currents. Figure 3.12 shows erosion deposition thickness associated with the flood and ebb stages of a spring tidal cycle. This shows sand transport primarily occurring within tidal channels and distinctive ebb-dominance. Differences are particularly noticeable in the upper reaches of the Papakura channel, upstream of the divergence of Clarks Creek, coinciding with a step change in bathymetry and approximate halving in water depth from 15 m to 7 m CD as shown in Figure 2.22.

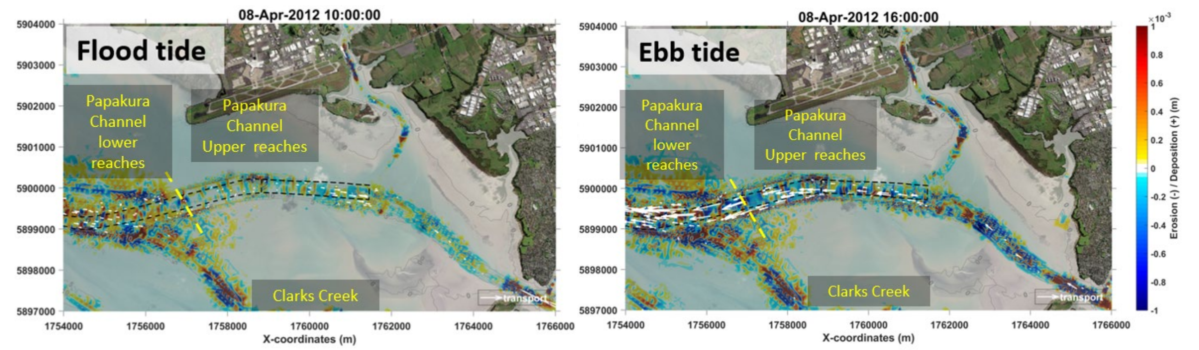

Figure 3.12: Figure showing erosion (blue) and deposition (red) of 150 micron sand within the existing Papakura channel for flood and ebb tide, over a spring tide.

3.5.2 Open coast

Sediment transport on the open coast is driven by the wave climate, with predominant waves from the south-west arriving slightly oblique to the coastline, driving sediment to the north. Less frequent, but at times highly energetic and highly oblique waves from the northwest can drive sediment in a southerly direction.

Potential longshore transport or *littoral drift* rates on the open coast south of the Manukau Harbour entrance and bar have been calculated using an empirical longshore transport formula described in Kamphuis (2000) with the parameters used in the calculation listed in Table 3.4. Waves at the hindcast location o1 (refer 3.3.1) were transformed from 70 m depth to break point using the methodology presented in van Rijn (2014) including the wave refraction and shoaling. Longshore transport rates were then computed for each time step in the 41 year hindcast (Figure 3.13) with results summarised in Figure 3.14 and Figure 3.15.

Table 3.4: Sediment transport parameters used in the empirical formula calculations.

Parameter	Adopted value	Notes
Shoreline orientation	245 degrees	Based on average shoreline orientation 5-20 km south of the Manukau entrance
Grain size	250 microns	Based on average sample D_{50} of samples taken on the Manukau Bar (refer 2.5.2)
Porosity	0.4	Typical value
Gamma	0.6	Typical H_s/d breaker index
Density of particle	3000 kg/m^3	Based on average particle density of samples taken on the Manukau Bar (refer 2.5.2)
Surf-zone slope	0.007 (1V:140H)	Average slope between the beach and -10 m depth

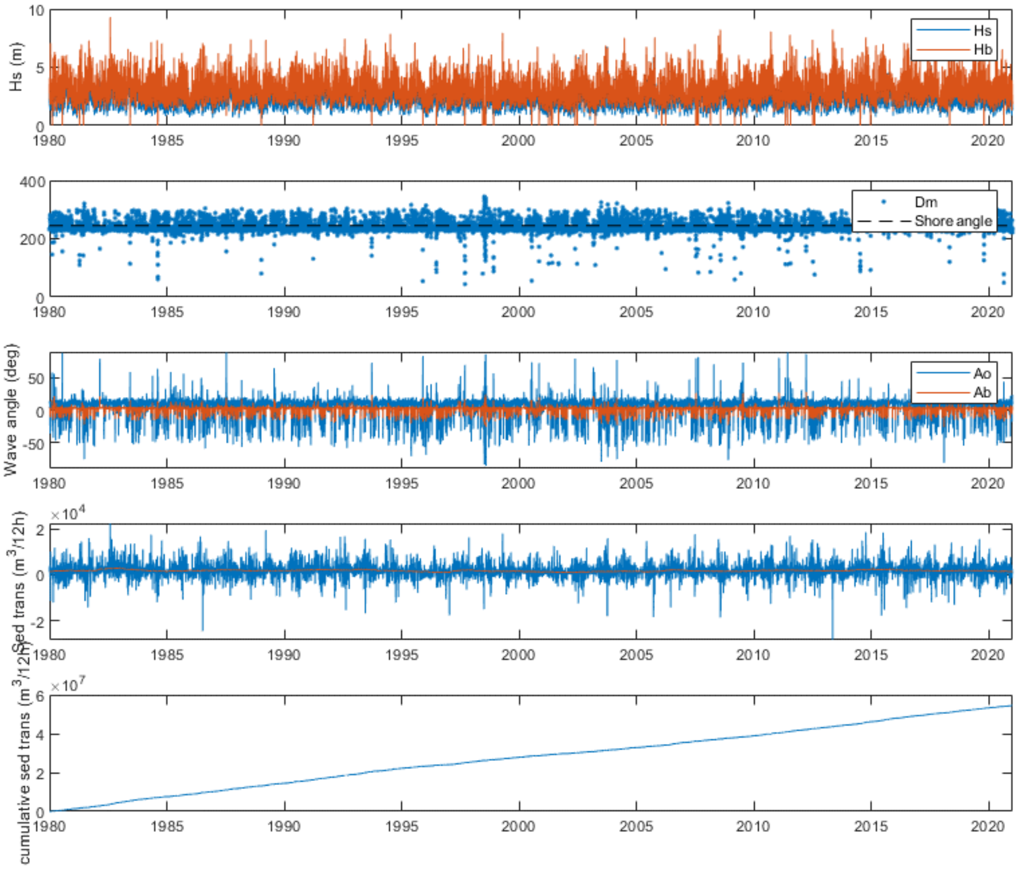

Figure 3.13: Nearshore wave characteristics and longshore sediment transport rates south of the Manukau Harbour entrance. Note positive transport is south to north.

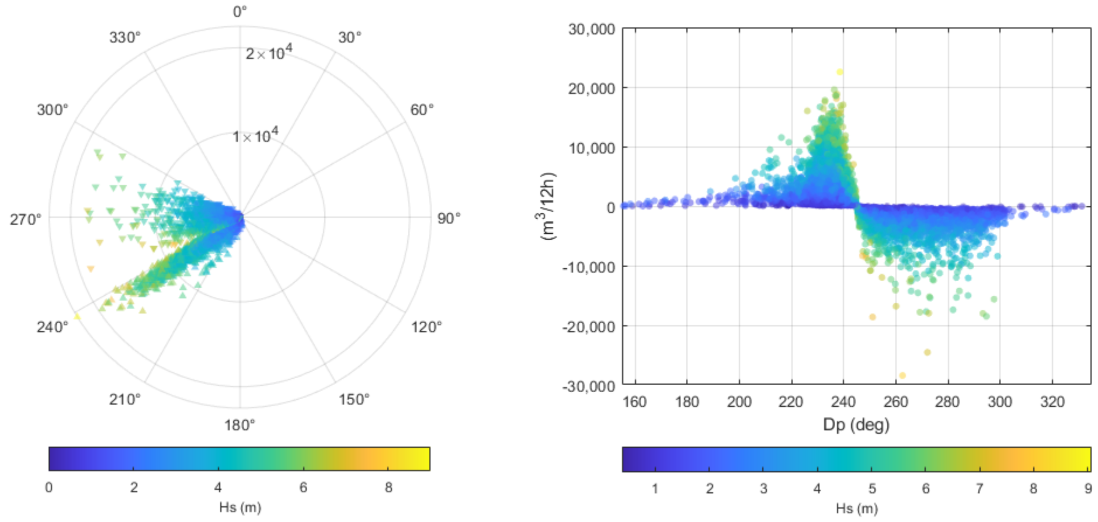

Figure 3.14: Longshore sediment transport rates (m^3/12hr) as a function of wave direction and height south of the Manukau Harbour entrance

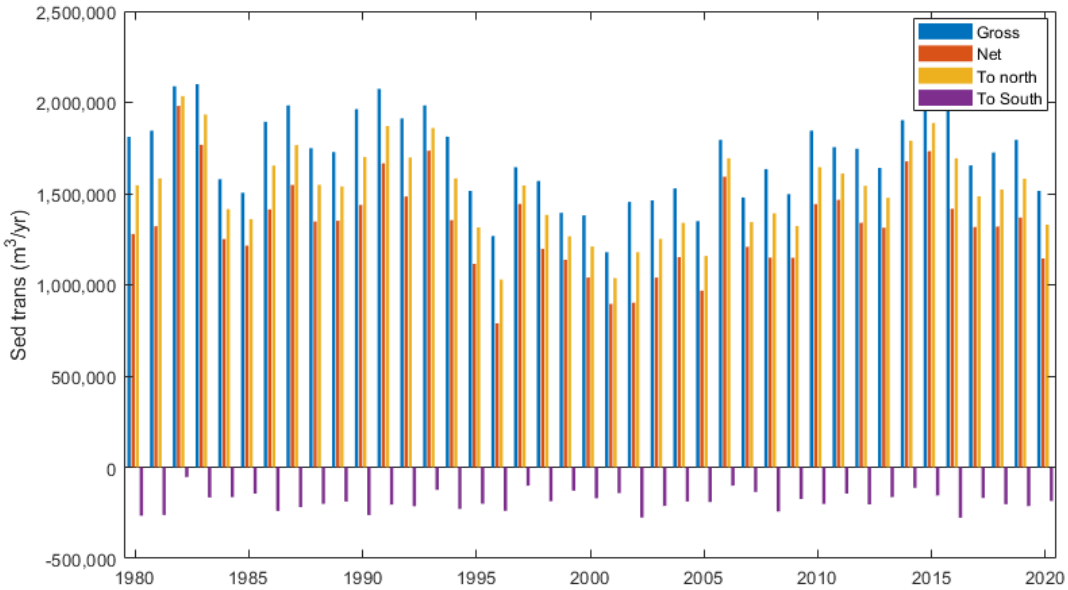

Figure 3.15: Cumulative longshore sediment transport and annual longshore transport rates south of the Manukau Harbour entrance

Results indicate that longshore transport is predominantly from south to north, under the predominant south-west wave climate, but episodic events from the NW can generate large transport rates to the south. Gross transport (combined directions) ranged from 1.2 to 2.1M m^3/year with an average rate of 1.7M m^3/year. Net transport ranged from 0.8 to 2.0M m^3/year to the north with an average rate of 1.3M m^3/year. These rates are substantially higher than identified previously, i.e. eCoast (2020) report longshore transport rates of 375,000 m^3/year for this coast and Hicks and Hume (1996) reported 175,000 m^3/year. However, the assumptions made in these previous studies are not clear. Assumed beach slope and shoreline orientation can make a substantial difference to estimated rates. The updated values are in keeping with longshore transport rates found in other locations with similar wave climates, i.e. longshore transport of 1M m^3/year reported at Figueira da Foz, Portugal with a mean significant wave height of 2 – 2.5 m (Fernández-Fernández et al., 2019) and 500,000 m^3/year on the Gold Coast (Castelle et al., 2007) with a mean significant wave height of approximately 1.5m.

Sediment transport rates were also extracted from the coupled wave-sediment transport model Delft-3D (refer *TWP03c*) for the same conditions at approximately the same location. Results (Figure 3.16) indicate the empirical model to predict roughly twice the transport of the Delft-3D model. This does not provide guidance as to which (if either) model is correct, as calibration data to confirm the accuracy of either model is not available, but this can provide an indication of the magnitude and potential range of prediction.

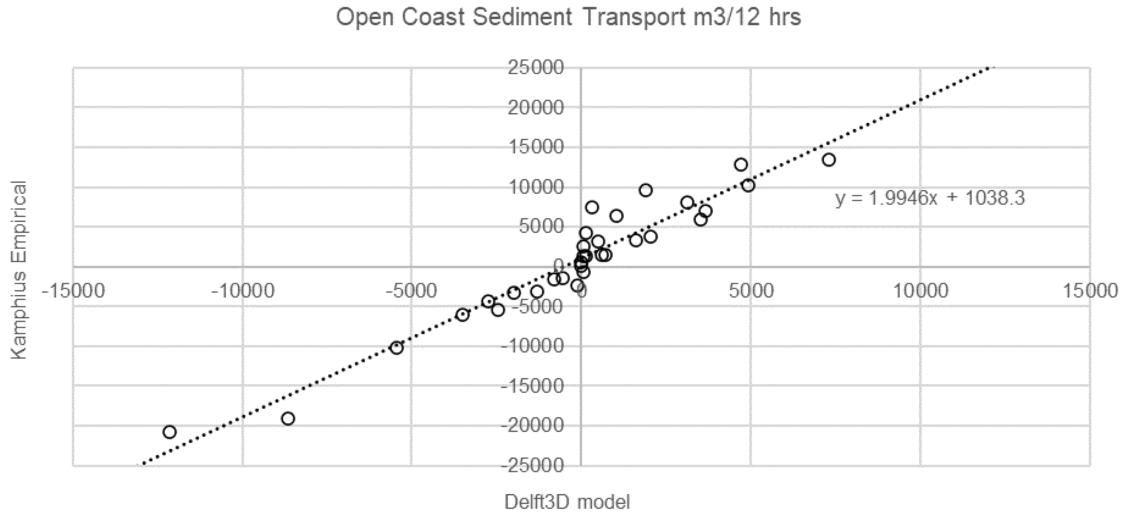

Figure 3.16: Comparison of longshore transport (m^3/12 hour) south of the Manukau Harbour Entrance predicted using the Kamphius (2000) empirical formula compared to the coupled wave-sediment transport model, Delft-3D

3.5.3 Ebb tidal delta

Sediment transport patterns on the Manukau Bar are influenced by the strong tidal currents as well as waves. Sediment is transported along the coast from the south under wave action and then carried by flood tides flowing into the harbour through the South Channel and into the main channel. Sediment may then be transported into the harbour and onto the flood tide delta or transported offshore during the stronger ebb tide being deposited onto the shallower ebb tide delta (Manukau Bar) as tidal currents dissipate.

During wave events, sediment is transported north and south onto the adjacent shallow bars due to radiation stresses before being moved onshore over the bars and eventually back into the main channel forming a semi-closed system (Figure 3.17). Some material is likely lost from this system to the open coast to the north. Material also moves onshore, accumulating a shallower bar with tides during low wave conditions then reducing the bar height.

A range of scenarios were modelled (refer *TWP03c*) for the existing Manukau Bar, with transport observed across several transects and changes in bed level on the bar and in volume within the proposed channel alignment noted (Figure 3.18).

The volume of sediments being transported on the Manukau Bar was found to be considerably higher than on the open coast with modelling showing volumetric transport on the bar during high energy events an order of magnitude greater than occurring on the open coast (refer Section 4.3 of TWP03c). This is likely due to a combination of waves mobilising sediment over large areas and strong radiation-stress driven and tidal currents able to transport this material. As described above, the semi-closed nature of the system means that much larger volumes can be moving around the ebb tidal delta system while lower volumes move along the open coast to the north and south. Pearson (2022) noted similar on the Ameland ebb tidal delta with net transport being relatively stable but gross transport being more variable. Ford (2023 – TWP03a) noted during his analysis of recent Port of Auckland surveys that the net volumetric change between surveys (~100 to 400 days) ranged from 2 to 3M m^3 (refer *TWP03a*) with an average net volume change of -0.5M m^3. This demonstrates the very large volumes being moved and the large changes in bedforms occurring on the Manukau Bar.

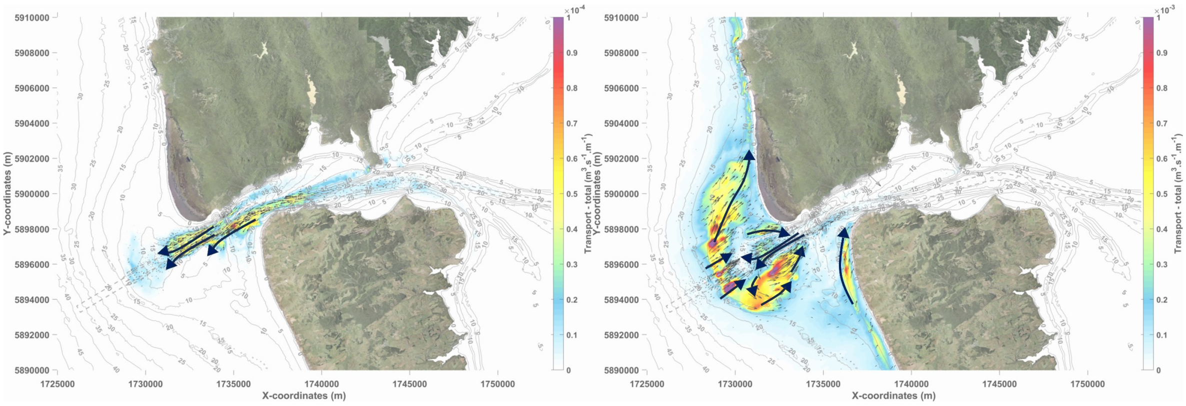

Figure 3.17: Figures of mean sediment transport during tide only (left) and large wave conditions (right) with conceptual sediment transport pathways overlaid in blue arrows (source TWP 03c)

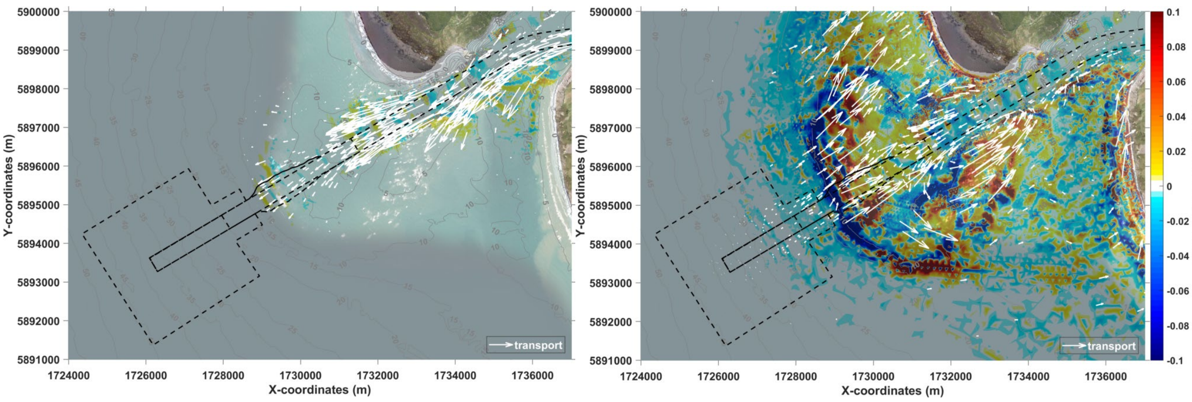

Figure 3.18: Figures indicating the changes in bed level (erosion = blue, accretion = red) during tide only (left) and large wave conditions (right) (source TWP 03c)

Part II – Impacts of proposed works

4 Proposed works

4.1 Summary of proposed works

As set out in Section 1.3, a navigation channel is proposed to be dredged through the Manukau Bar (ebb tide delta, or entrance bar), to a port located in the inner harbour. Channel design (refer *TWP04 Navigation and Channel Design*) indicates the navigation channel would be dredged to a maximum depth of around -19 m CD across the Manukau Bar (plus 1 m for over-dredge allowance), with a channel width of some 295 m and side batter slopes of 1(V):7.5(H) below -12 m CD and 1(V):25(H) above -12 m CD. Dredging would be undertaken between the deeper offshore areas and the deeper channel between the heads, a distance of some 4 km for the South-West Channel option and 9 km for the South Channel option (refer Figure 4.1). Note that cross-sections show the initial channel design used for hydrodynamic and sediment transport modelling rather than the refined channel design. The navigation channel then extends another 25 to 30 km to reach a potential port location within the Manukau Harbour with dredging occurring within the inner 10 to 15 km to a depth of -16 m CD, with side slopes of between 1(V):3(H) and 1(V):5(H).

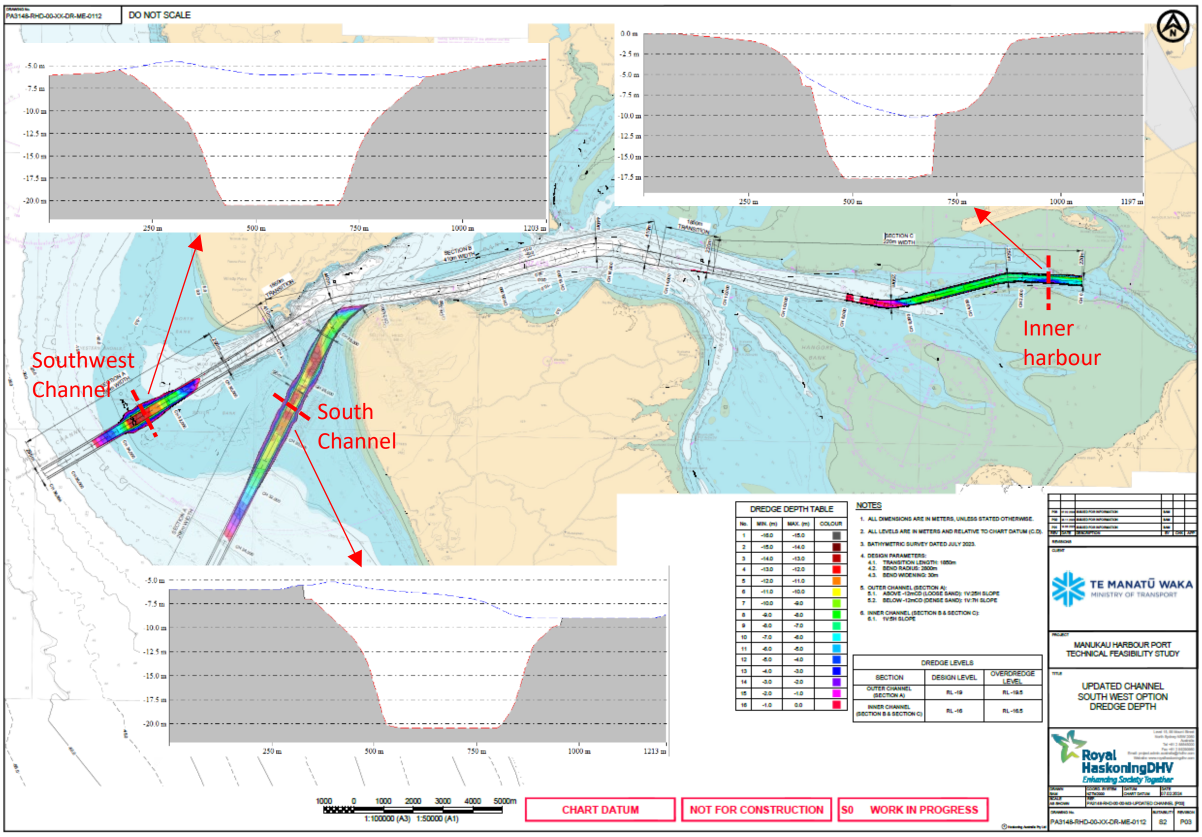

Figure 4.1: Concept Design for South-West and South Channel options including plan and cross-sections (source: TWP04)

Maintenance dredging is then proposed to maintain a navigable channel. Infill volumes required to be dredged are described in Section 6 below. Detail on the dredging is set out in *TWP06 Dredging,* but has assumed that material dredged from the Manukau Bar is deposited within 5 nautical miles of the dredge location, within the active littoral system. Surplus material dredged from the inner harbour including the port area would be placed in an offshore dredge material ground (DMG) outside of the active littoral system.

The working conditions of the proposed dredging equipment and the placement depth is dependent on the selected size of the dredger. However, an assumed medium sized TSHD with 10,000 m^3 hopper capacity (refer TWP06), has a threshold working condition of significant wave height (H_s) = 3 m, daily production rate of 50,000 m^3 and can place dredged material in a minimum depth of around 17 m (15.1 to 16.6 m CD depending on tidal range). A smaller dredger may deposit dredged material in shallower water but will be limited to operating in lower wave conditions (refer to TWP06 for further details).

4.2 Geotechnical considerations

Geotechnical considerations for the channel design and preliminary static and seismic slope stability analysis are presented below.

4.2.1 Inferred subsurface conditions

Section A – Manukau Bar

The upper part of the entrance bar is highly active with recorded movement of seabed above -10 m CD and deeper at the front and rear of the bar (Figure 4.2). This indicates that this material is active marine sediments that could be characterised by surface samples. The centre of the bar does not have recorded movement (though the records only extend over a 20 year period) and no additional sub-surface information is available in the immediate area. The closest borehole is at Hamilton’s Gap some 10 km to the south, however, that is located at the base of the Āwhitu Peninsula and is likely to include Pleistocene aged materials of the Kariotahi Group.

Given the evolution of the Manukau Harbour over the last 20,000 years with an increase in sea levels from approximately 120 m below present sea levels, it is likely that the bar has been re-worked by wave and tidal flows over this time therefore limiting the potential for silts to be present (the silt would be mobilised by waves and transported by tidal flows either into the harbour or offshore). Therefore, it is reasonable to assume that the lower parts of the bar generally comprise the same sediment, although may be denser.

Based on available sediment and bathymetric information (Figure 4.2), the following is inferred:

- Above -10 to -12m CD (depending on position across bar), fluctuations in seabed level indicate that this material is active and can most likely be characterised as loose, fine to medium sands (D_{50} between 200 and 350 micron) with pockets and lenses (could assume 20%) of medium to coarse sands (D_{50} 350 to 500 micron).
- Below -10 to -12m CD (depending on position across bar), the material is less active but is most likely medium-dense, fine to medium sands.
- There is a very low probability of encountering strong andesitic breccia-conglomerate of the Piha Formation at depth, but we suggest this is allowed for as a low likelihood risk (<5%) within the fatal flaws assessment.

Section C – Inside the harbour

Based on available sediment and bathymetric information inside the harbour the following is inferred:

- Interbedded loose to medium-dense sands and silts, whose respective depths and thicknesses are shown to vary over relatively short distances, extending to depths that typically exceed 20 m in depth.
- Potential for rare gravels and/or shell lenses.
- There is a very low probability of encountering very dense weathered ECBF rock towards the very base of the proposed channel excavation. Very dense material was encountered as shallow

as -8 m CD in areas situated well away from natural harbour channels, in contrast to boreholes located closer to these channels that did not encounter this material at any depth (extending to between 20 and 30 m depths). We suggest this is allowed for as a low likelihood (<5%) risk within the risk assessment.

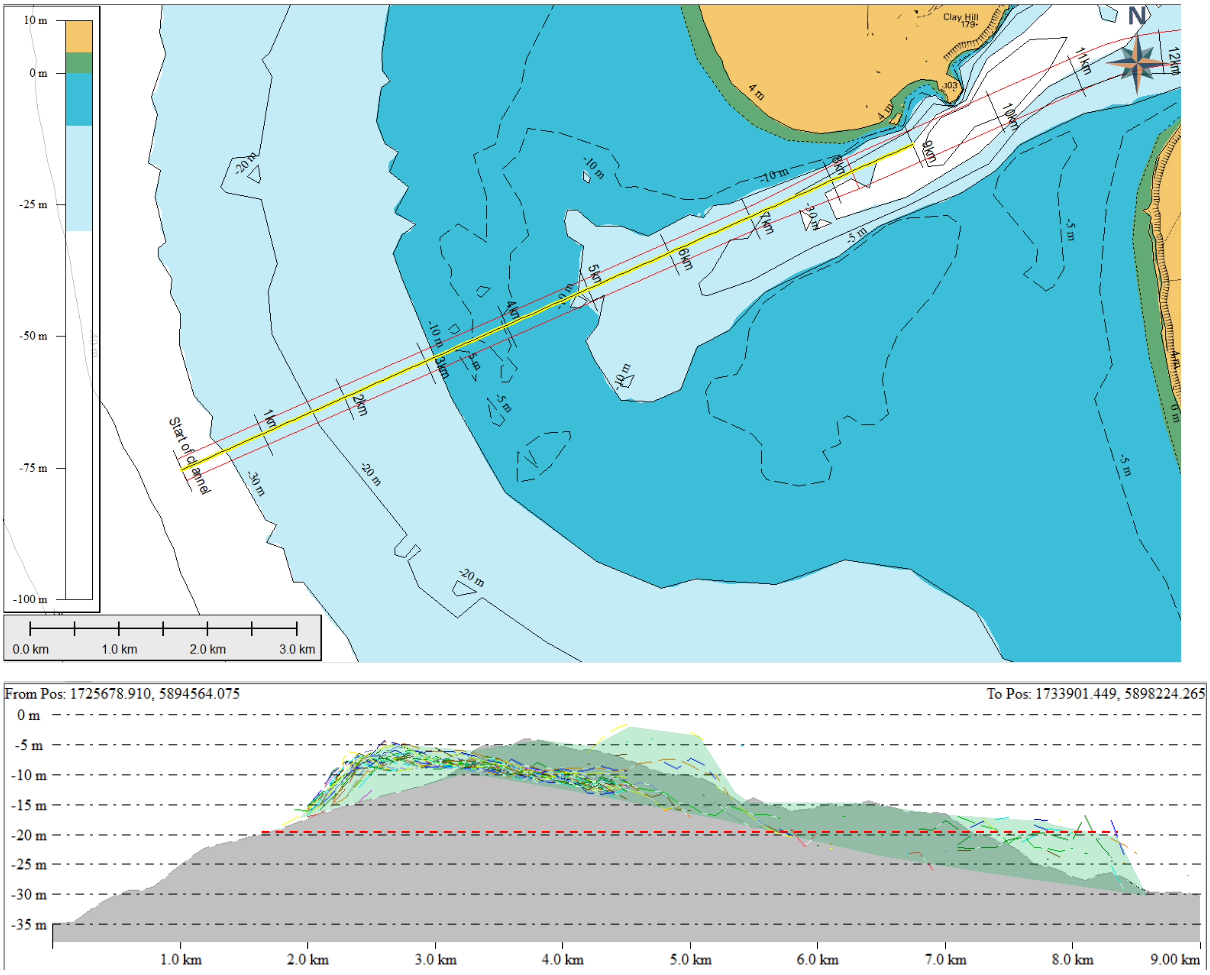

Figure 4.2: Plan (top) and cross-section (lower) of the previous POA surveys (coloured lines) overlain on 2023 bathymetry (grey) with area of fluctuating levels seabed indicated by green hatch and proposed dredge depth indicated by red dashed line

Table 4.1: Summary of inferred subsurface conditions

Location	Unit depth (m RL)	Unit description
Section A (Manukau Bar)	> -12 m CD	Loose, fine to medium sized sand (80%) and medium to coarse sand (20%)
	< -12 m CD	Medium dense, fine to medium sized sand
	< -12 m CD (<5% likelihood)	Outcrop strong andesitic breccia-conglomerate (say 5% total volume)
Section C (Manukau Harbour channels)	Above -20 m CD	Medium dense interbedded fine sized sands and silts
	Above -20 m CD	High likelihood (> 50%) of encountering localised gravels and/or shell lenses (<5% total volume)
	Below -15 m CD	Very low Likelihood (<5%) of encountering very dense weathered ECBF rock

4.2.2 Existing side slopes

Side slopes along the existing channel alignment have been extracted from the composite bathymetry. Chainages are defined from the seaward end of the indicative channel and the side slope is given for the closest natural channel to the proposed navigation channel (refer Appendix B1). Results are summarised below:

Section A – Manukau Bar

- At chainages 1 to 5 km, the seabed slopes offshore are less than 1°. This area is controlled predominantly by wave processes and not likely indicative of dredge channel side slopes.
- Along chainages 6-7 km the side slopes are relatively flat, 1 to 2°, as tidal currents reduce, and waves may also be flattening the slope.
- Along chainages 8 to 10 km the existing slopes are steep (3 to 8°) as the channel constricts between Whatipū and the inshore bar on the south side of the channel. High tidal currents are likely maintaining a steep slope by removing materials from the toe as they are pushed into the main channel from the shallow areas above.
- Figure 4.3 provides an example of this with a relatively consistent side **slope of 4° (1V:15H)** adjacent to the shallow southern bank maintained by high tidal currents.

Section B – Harbour Entrance

- Side slopes between chainages 13 and 15 km are likewise steep (7 to 15°) as the existing channel runs adjacent south head with similar tidal processes likely maintaining this channel near its stable limit.
- Further into the harbour (chainages 16 to 20 km), side slopes flatten to 1.5 to 3.5° above -10 m CD and 2.5 to 4° below -10 m CD.

Section C – Inner Harbour

- Chainages 20 to 28 km (within the harbour but seaward of where inner harbour dredging is likely required), side slopes range from 1.5 to 3° with some sections exhibiting steeper slopes in the upper portion and some steeper in the lower portion.
- From chainages 29 to 37 km (area where inner harbour dredging is likely required), side slopes steepen slightly to 2 to 4°. However, these are average slopes above -10 to 12 m CD (as deeper sections do not existing) with locally steeper sections in the upper parts of the slope (refer Figure 4.4) particularly where higher tidal flows have maintained steeper sides, and evidence of sediment accumulation at the base of the slope. These **upper slopes can reach up to 10° (1V:6H)** but unless maintained by a tidal flow, some flattening is likely to occur.

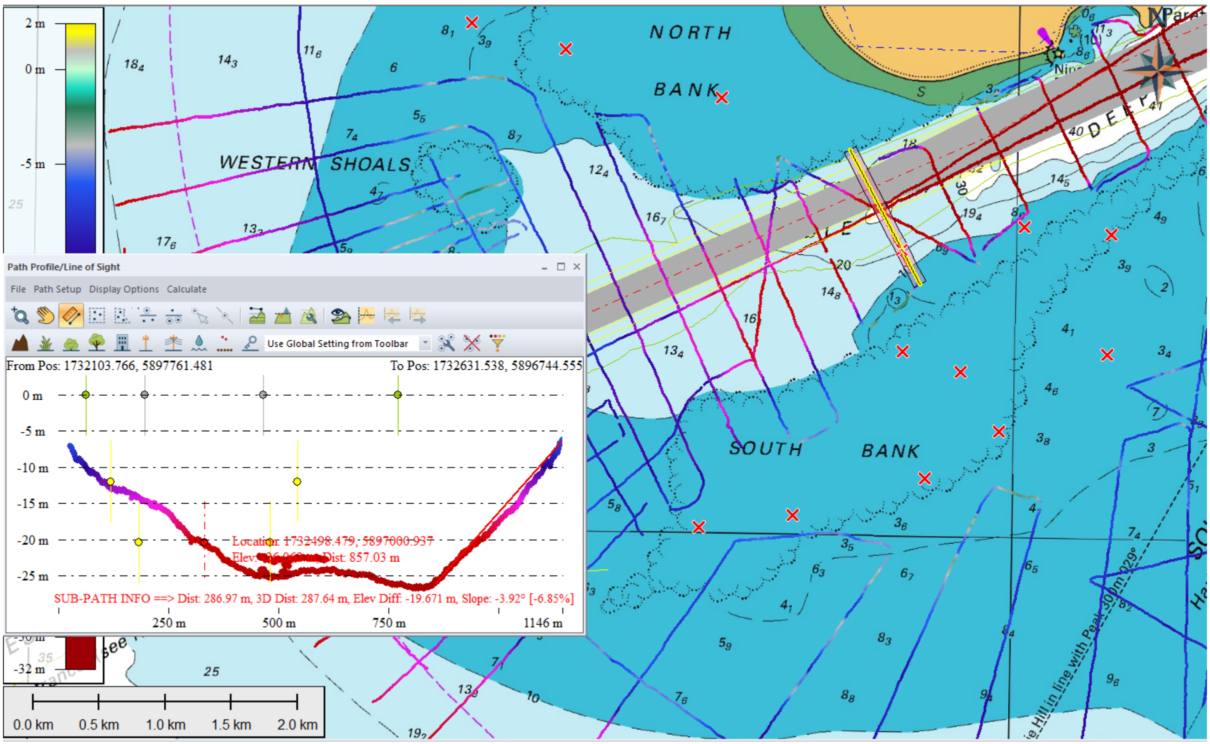

Figure 4.3: Example of side slope of approximately 4° (1V:15H) at approximately Chainage 8 km

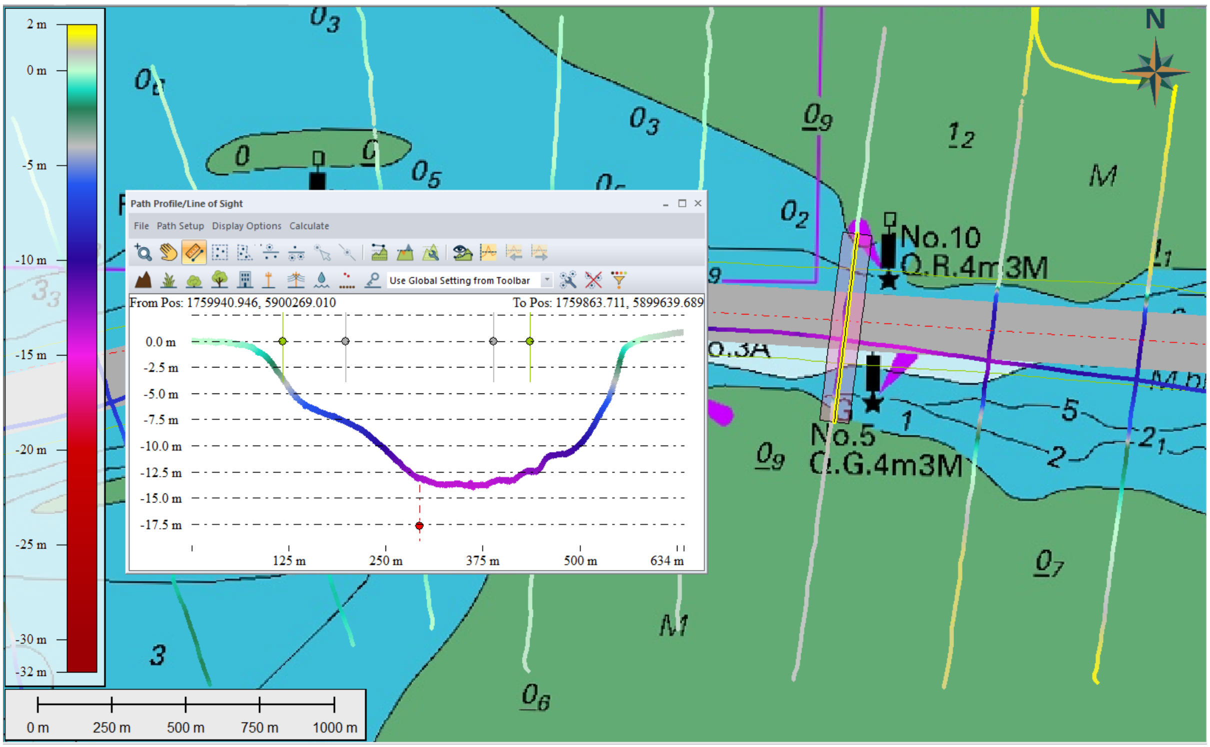

Figure 4.4: Example of side slope at approximately Chainage 36 km with the upper parts of the channel reaching up to 10° (1V:6H)

4.2.3 Side slope modelling

Preliminary side slope modelling was undertaken using the model SlopeW and the following channel design parameters:

Manukau Bar

- Seabed at -5 m CD, channel base at -20.5 m CD (channel depth prior to optimisation)
- Above -12 m CD - slopes were modelled at 1(V):25(H) with loose sand
- Below -12 m CD slopes were modelled at 1(V):7.5(H) with dense sand
- FoS found >1.5 (static).
- And Seismic >1.0

Inner harbour

- Seabed was modelled at 0 m with channel base at -17.5m CD (channel depth prior to optimisation)
- Slopes at 1(V):5(H)
- Materials as per Beca borehole BH7 (Loose sand overlaying silts, over dense sand) and Beca borehole BH8 (soft silt over very still clay over dense sand) – refer Appendix A
- FoS found > 1.5 (static)
- Seismic – yield at 0.068g (about 1 in 60 year event)
- About 10 mm to 50 mm seismic displacement

Results are presented in Appendix B2 but indicate general stability with a factor of safety above 1.5 for static conditions. Seismic conditions may lead to displacement in the inner harbour during an event greater than 60 year average recurrence interval.

5 Changes to coastal processes

The effects of the proposed works on coastal processes were assessed primarily using the coupled wave-hydro-sediment transport model Delft-3D as set out in *TWP03b Metocean Study* and *TWP03c Sediment Transport.* Assessment has focussed on the South-West Channel alignment being the more likely scenario, with limited sensitivity testing on sediment transport and infill being undertaken for the South Channel.

5.1 Water levels

The effect of the proposed (South-West) navigation channel has been assessed by comparing flow characteristics under the existing bathymetry and with the proposed channel. Results indicate that flow more effectively enters the Manukau with the spring tidal prism (the amount of water exchanged each tidal cycle) increasing by around 6M m^3, or around 0.5%. The neap tidal prism remains generally unchanged (<0.5M m^3 or <1% difference) indicating a lessor increase in efficiency at lower tides.

The effect on water levels is shown in Figure 5.1. These plots present changes during particular tidal phases during a spring tide rather than comparison of maximum levels. Results indicate the addition of the navigation channel increases water levels in the upper harbour during the ebb tide, although the difference in level at high tide is small (generally < 25 mm with a maximum of 50 mm compared to a difference between neap and spring high tide of 800 mm). Likewise on the outgoing tide, levels drop more quickly with lower levels reached earlier particularly in the upper harbour.

This change in tidal prism and symmetry is relatively small, but effects the entire harbour and, being a permanent modification, could result in changes (albeit relatively small) to harbour-wide sediment transport patterns, potentially erosion and accretion at the coastal edge, and bedform locations.

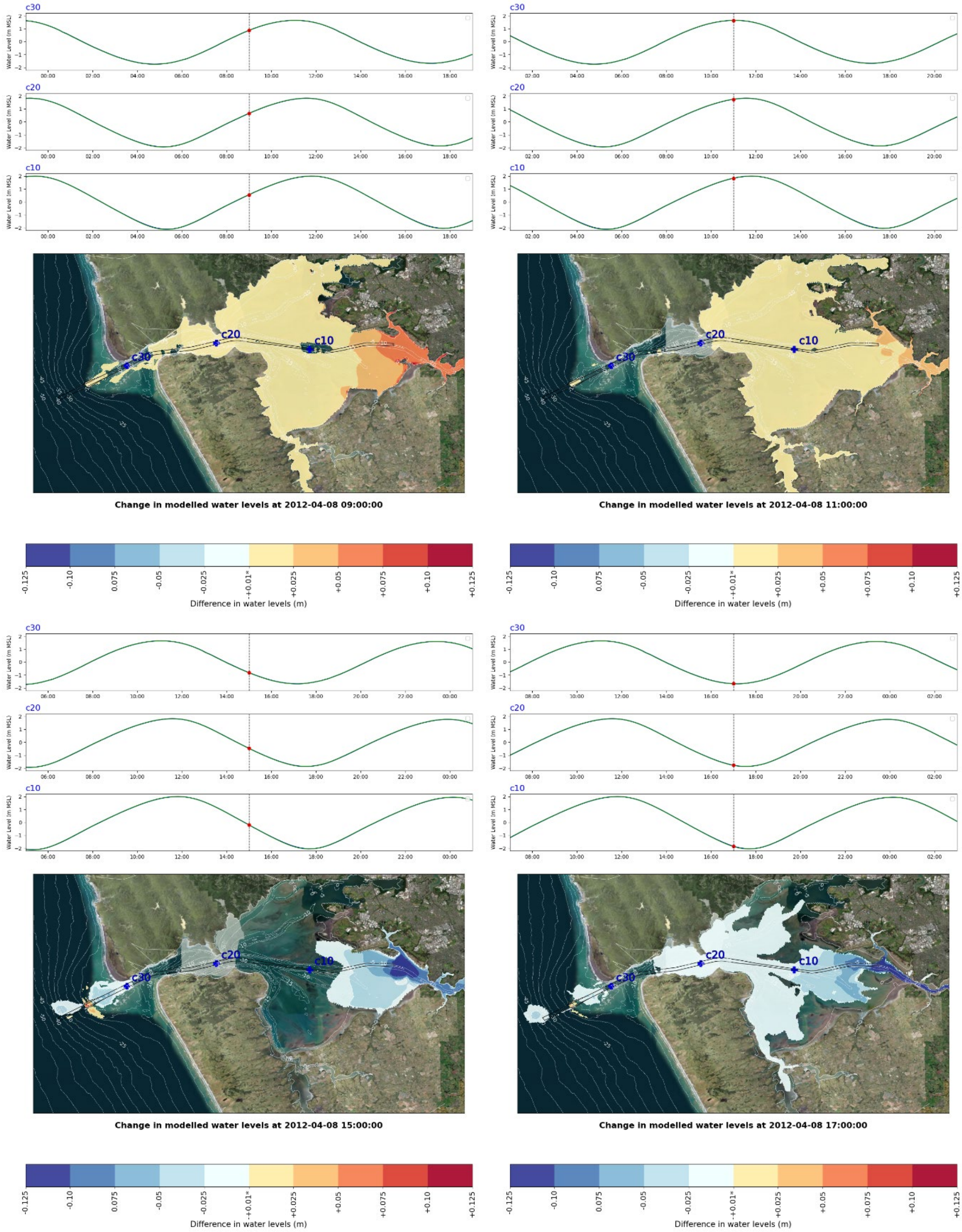

Figure 5.1: Example of changes in water level with the proposed dredged navigation channel for a flood (top left), high (top right), ebb (lower left) and low (lower right) period during spring tide.

5.2 Currents

The effect of the proposed (South-West) navigation channel on currents within the harbour is shown in Figure 5.2 as a difference from the existing situation. During a flood tide, currents tend to be slightly lower around the bar (up to 0.2 m/s or 10 to 20%), except for immediately offshore of the dredged channel where currents are slightly increased (up to 0.2 m/s or 20%). This will be due to the increased efficiency of the dredged channel with more of the flood tide now flowing through this deeper channel. Similarly, within the harbour, currents are decreased on the intertidal banks (up to 0.2 m/s) alongside the dredged Papakura channel with increased velocities (up to 0.2 m/s) in the upper reaches of the harbour where the tidal wave is propagating more efficiently.

Similar changes are noted during ebb flows with higher velocity flows in the dredged channel and lower flows on adjacent areas. This particularly notable over the Manukau Bar where the flows are increased by over 1 m/s (or around 50%) higher owing the greater flow efficiency of the deeper channel.

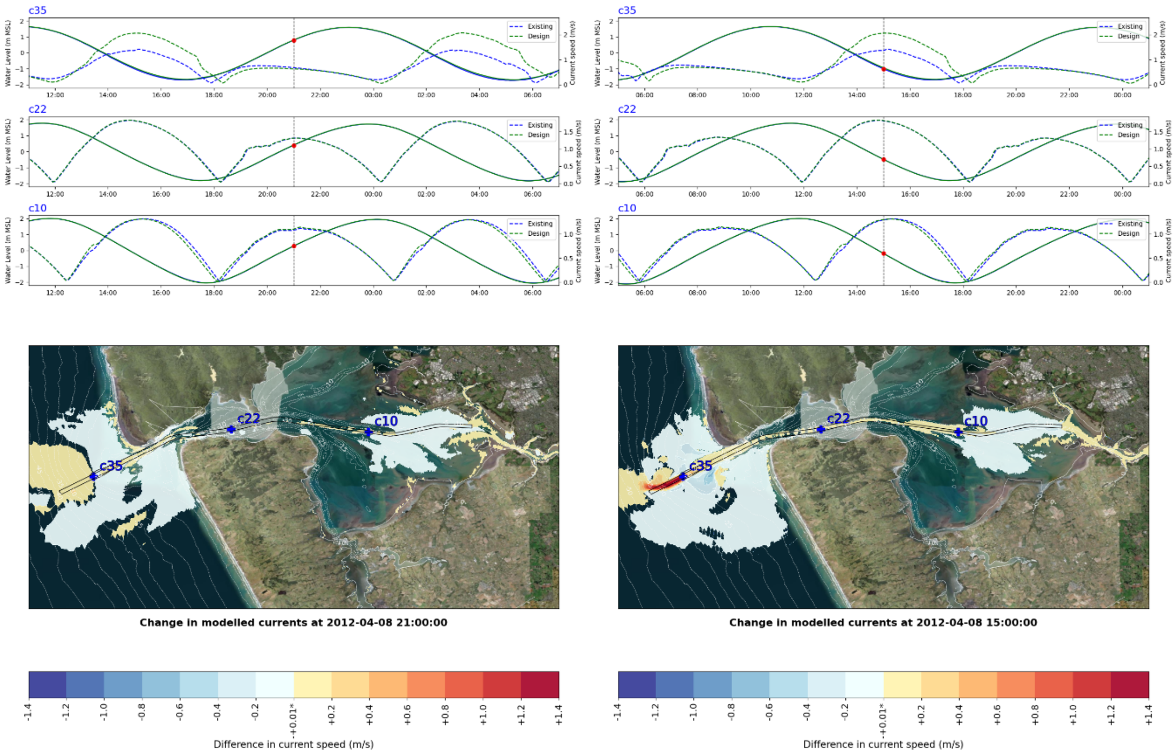

Figure 5.2: Change in current during a flood (left) and ebb (right) tide.

5.3 Waves

Prior to the navigation channel waves tend to exhibit a slight focussing onto the outer portion of the Manukau Bar. The exact position of this focussing will depend on the specific bar configuration at the time, wave direction and tidal stage. Waves are then slowly dissipated on the shallow sand banks. The effect of the proposed navigation channel is to focus waves along the side of the channel on the outer portion of the bar (Figure 5.3). This is expected to be due to a combination of the increased currents exiting the navigation channel (refer Section 5.2) turning the oblique waves during low and outgoing tides and, closer to the bar and during flood and high tides, due to the deeper channel causing waves to refract towards the edges. This focussing is expected to occur on the southern side of the channel during south-west waves (i.e. Figure 5.3), and to the northern side of the channel during northwest waves. No change in wave climate inside the bar or another open coast is evident.

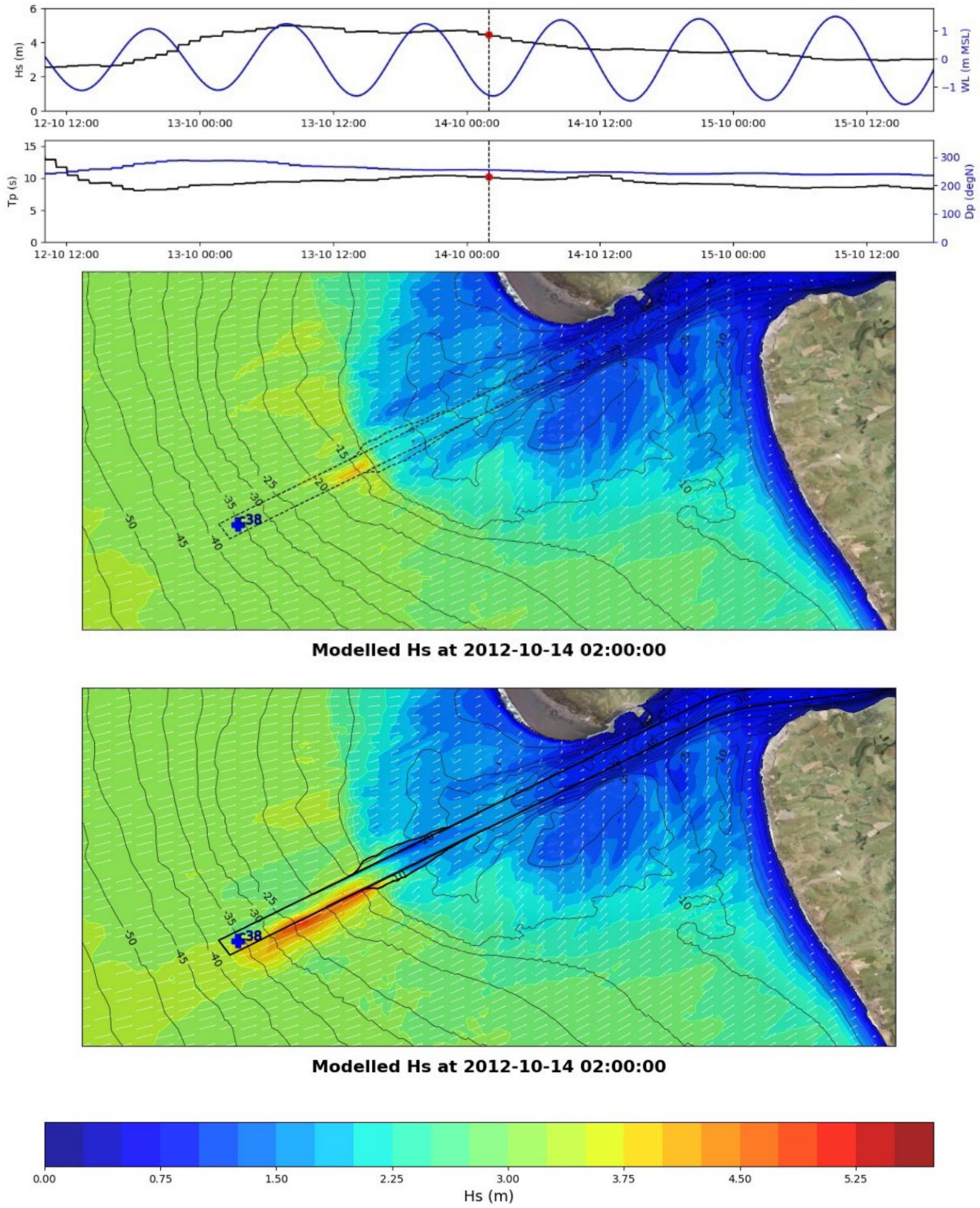

Figure 5.3: Example of modelled wave heights over the bar for the existing (top) and with the design SW channel (lower) during a wave event and outgoing tide

5.4 Sediment transport

Changes in the sediment transport regime are driven by the changes in wave and current processes described above. Figure 5.4 shows mean sediment transport during high energy wave conditions and conceptual sediment transport pathways for the dredged navigation channel compared to the existing and Figure 5.5 shows the change in bed level for the same event. These plots both show a similar process with increased sediment transport offshore beyond the current terminal lobe, likely due to the increased ebb tidal flows. Slightly increased sediment transport occurs on the bar adjacent to the channel likely due to the wave focussing adjacent to the channel.

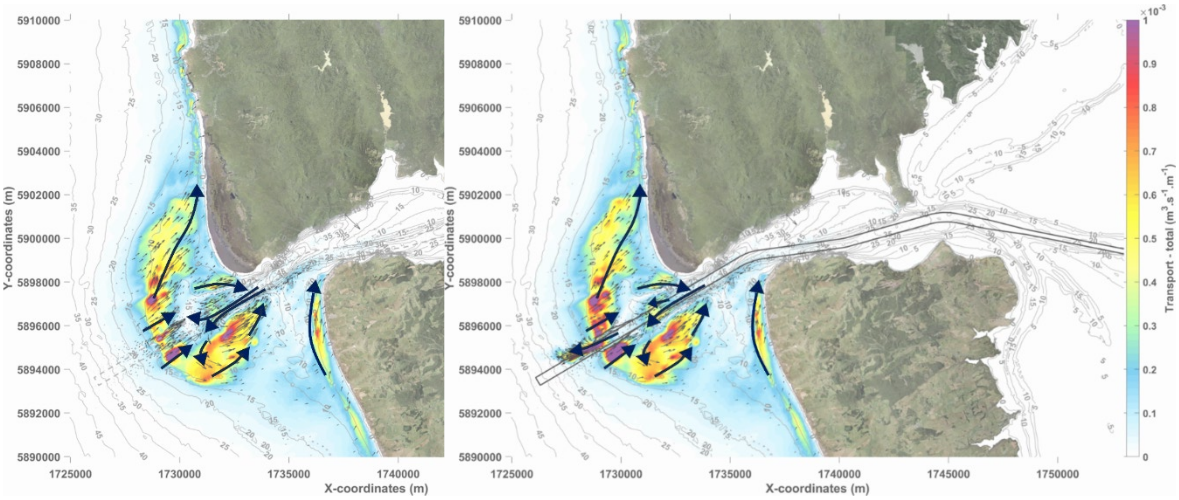

Figure 5.4: Mean sediment transport during large wave conditions with conceptual sediment transport pathways overlaid in blue arrows for the existing conditions (left) and with the dredged navigation channel (right) (source TWP 03c)

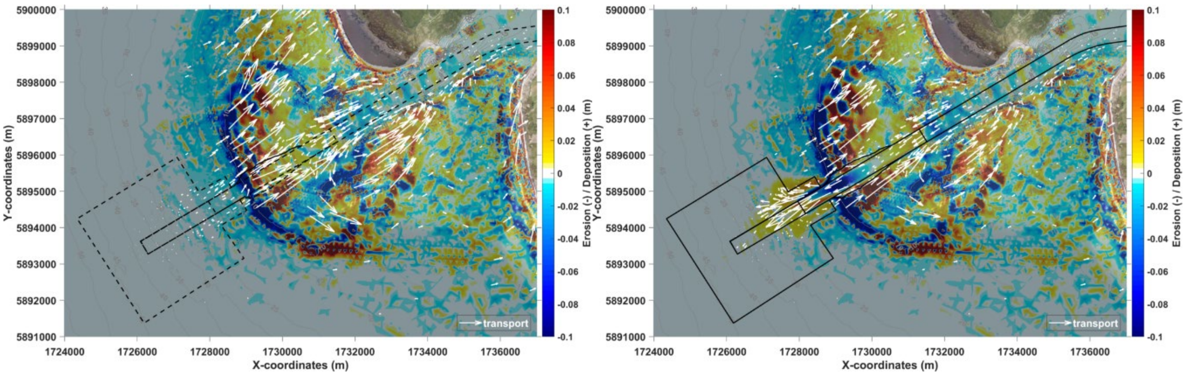

Figure 5.5: Comparison of bed level change following a large wave event between the existing and with the dredged navigation channel

The exact deposition patterns within the channel are complex. Figure 5.6 shows the deposition within the navigation channel above the design depth following a 10 day synthetic storm event. During this event, waves increased to reach 7 m (an approximately annual wave height) before reducing. Results (Figure 5.6 and Figure 5.7) indicate that deposition occurs in specific locations, at the landward and seaward ends of the channel and along the side batter slopes. In the centre of the dredged channel erosion occurred. This pattern of bar development is similar to a typical formation of ebb and flood deltas, with material scoured within the narrow constriction (i.e. when the bar on either side is relatively higher) and deposition as the adjacent bars open up and velocities decrease – a delta system within a delta system.

The deposition above the design depth during this event was approximately 200,000 m^3, whereas the net change was approximately -25,000 m^3 (i.e. total eroded volume wave slightly greater than accumulated). This is similar to findings by Ford (*TWP03a*) based on survey data for Manukau Bar and Pearson (2022) for the Ameland Inlet in Holland that gross changes (the sum of erosion and deposition) are significantly larger on these systems than net changes (the difference between erosion and deposition).

It is likely, though not certain, that the material being deposited within the channel is derived from the material being eroded and so the rapid rate of change observed in modelling may reduce over time as this erosion reaches a more stable 'quasi-equilibrium' depth.

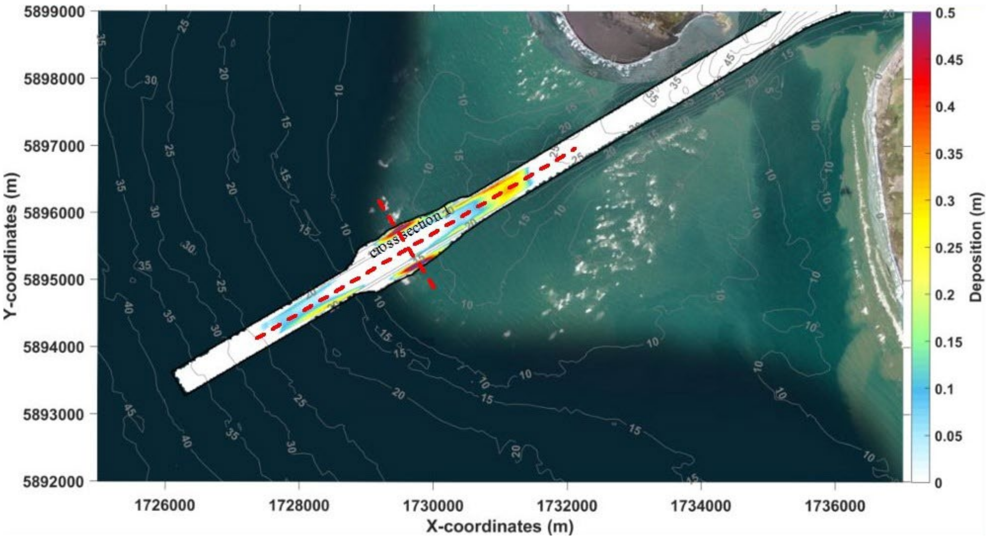

Figure 5.6: Deposition above the design depth following a synthetic storm event with the dredged channel

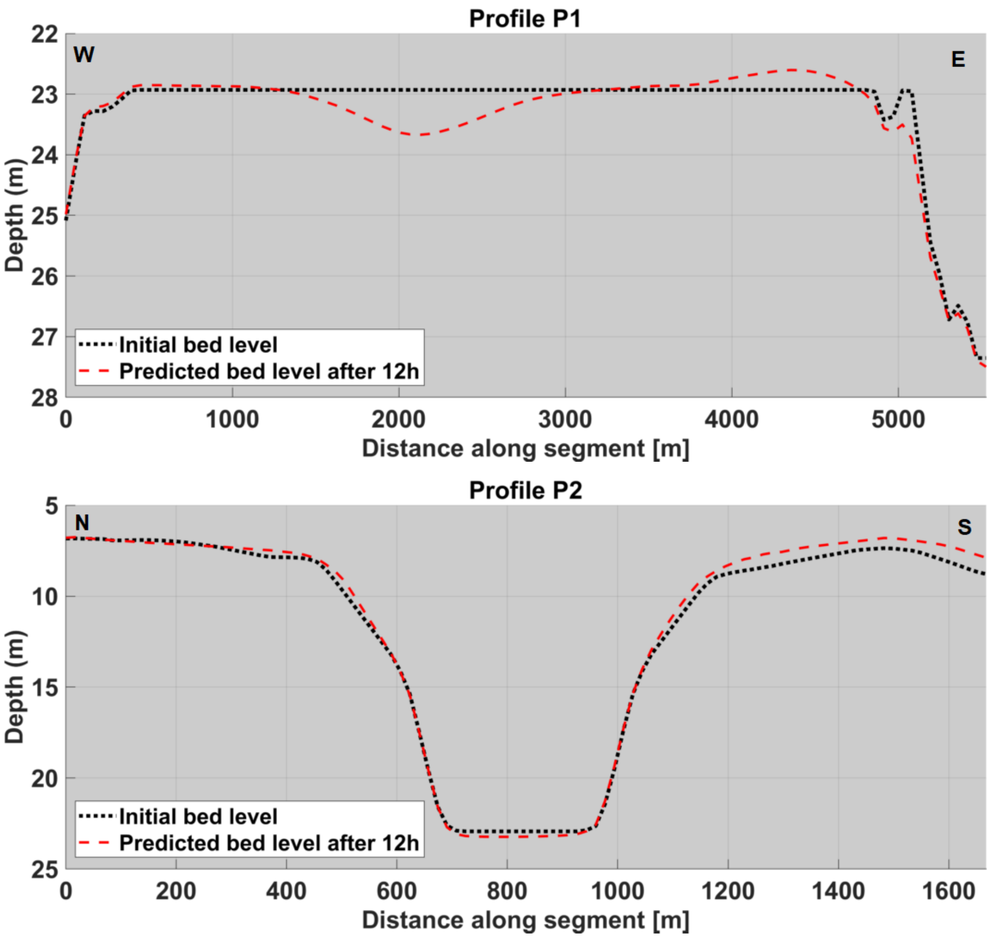

Figure 5.7: Changes in profile along the dredged channel (top) and across the channel (bottom) following a synthetic storm event

Changes to sediment transport processes within the harbour as a consequence of dredging are driven by the modification of seabed bathymetry and resulting changes in hydrodynamics. Changes in sediment transport therefore primarily relate to infilling (i.e. within the footprint of dredging itself) and localised effects upstream and downstream of dredged channel areas.

Deepening of the upper Papakura Channel will reduce bed levels to those typical of the lower Papakura Channel (Figure 6.4). This will likely increase flood tidal transport of fine to medium sands from the lower channel into this area. Changes in bed material from predominantly silt to sand, means that tidal currents become more influential on sediment transport along channels in these areas, which are comparatively higher in volume rather than the more gradual deposition of fine silt over very limited slack low tides.

6 Maintenance implications

6.1 Sediment infill on bar

As previously discussed, sedimentation patterns in the dredged navigation channel are not regular and include both areas of erosion and deposition (Figure 5.7). However, areas of decreased depth are hazardous for navigation whereas areas of erosion do not affect navigation. Therefore, the sediment deposition above the design depth (shown in red in Figure 6.1) from the base of the channel and side batter slopes has been considered in isolation in determining likely infill volumes that will require removal.

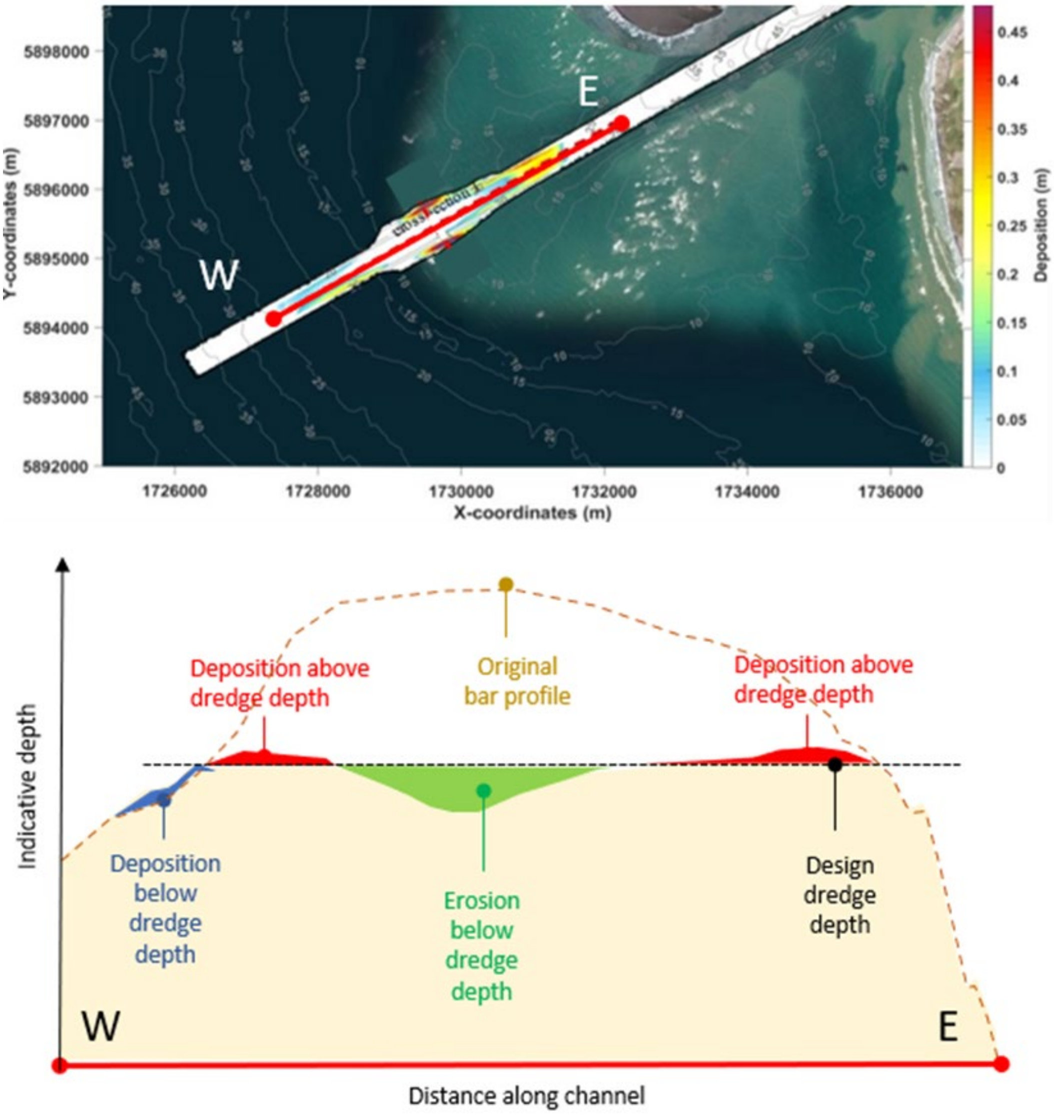

Figure 6.1: Schematic showing definition of areas used to calculate infill volumes

The following process, illustrated in Figure 6.2, was taken to estimate total infill volumes into the dredged navigation channel. Refer to *TWP03c Sediment Transport* for detail:

1 Sediment transport models are run for specific wave (Hs, Tp, Dp) events (an *Input Reduction* run matrix). These simulations include a 12 hour spin up period and then a 12 hour simulation period to ensure a complete tidal cycle.

2 Sediment accumulating with the dredged channel and surrounding batter slopes above the design depth or profile (red area shown in Figure 6.1) at the conclusion of the simulation period is recorded.

3 Using the long-term wave hindcast and a 4D interpolation function, the sediment accumulation is interpolated for each 12 hr time step.

4 The resulting sediment accumulation hindcast can be analysed to extract annual rates of infill.

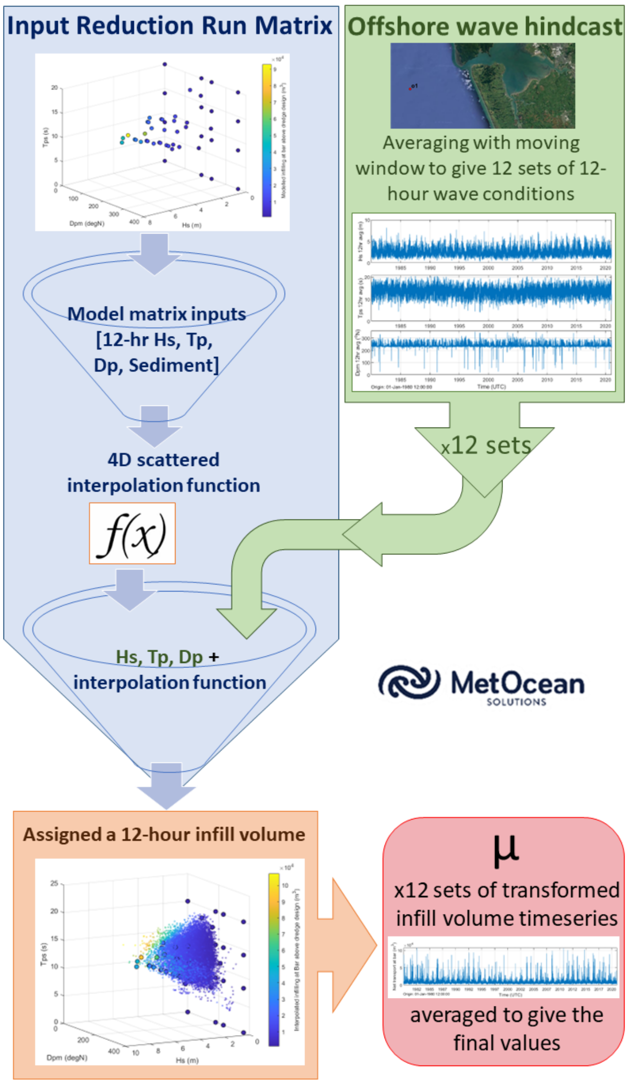

Figure 6.2: Input reduction approach to determining sediment infill rates

Rates of deposition above the design depth are found at between +5.03M to +7.68M m^3/year with an average rate of 6.55 M m^3/year. Including a 5% increase in wave height due to climate change by 2070 (refer Section 3.3.1), increase volumes by approximately 10%. A smaller annual net change of between -0.33M to -1.33M m^3/year suggests that while there is a high volume of sediment moving within the channel, the total change is relatively lower, as indicated in Figure 5.7.

This total deposition volume exceeds the ~2M m^3/year that was found to be moving into the channel from the south (Section 2.6.3) and driving the channel to the north. It is likely this total deposition includes this material depositing on the side batter slopes, as well as the material accumulating within the base of the channel.

Table 6.1 Annual infill volumes[1] above the design depth and net infill rates[1]

	Annual infill[2] volume above design depth at the bar (m^3)	Annual infill volume above design depth at the bar (m^3) including +5% wave height for climate change (2070)	Annual net volume change at the bar (m^3)[3]
Max	7,680,000	8,380,000	-330,000
Min	5,030,000	5,360,000	-1,330,000
Mean	6,550,000	7,060,000	-800,000

[1]Values rounded to the nearest 10,000 m^3

[2]Infill volumes are the deposition above the design dredge depth only (i.e. area shown in red in Figure 6.1)

[3]Net volumes are infill (deposition) minus scour (erosion)

As discussed in Section 5.4, it is likely, though not certain, that the material being deposited in the channel is derived from the material being eroded and, over time, this eroded area may achieve a deeper and more stable, quasi-equilibrium, reducing the material available to accumulate. An additional sensitivity run was undertaken where the bathymetry following the 10 day synthetic storm event was modified to remove the deposited material and a subsequent wave event (control 7) was run. The results indicated that the deposition reduced by around 10% compared to the initial 'flat channel' bathymetry and erosion reduced by around 5%. These results indicate that deposition may reduce over time, however, present modelling has not allowed thorough investigation of this longer-term process and so it is prudent to assume that following dredging the navigation channel resets back to a design depth. Improved understanding of this process during future design stages presents an opportunity to reduce assessed maintenance dredge requirements.

6.2 South Channel

A limited assessment of infill rates for a southern channel was undertaken. This channel is located in the lower energy flood channel, or 'South Channel' and required a substantially longer length of dredging. Results for a single high energy event (Figure 6.3) indicated less infill into the base of the channel compared to the South-West Channel (likely due to lower flows and less reshaping of the bed within the channel), but much higher infill onto the side batters owing to their longer length. The resultant infill for this single event was around 60% higher than the South-West Channel. Is it worth noting that the majority of this infill was on the side batters and may be reduced with steeper batters (increasing hydraulic efficiency along the channel) or a slight realignment of the channel and batters.

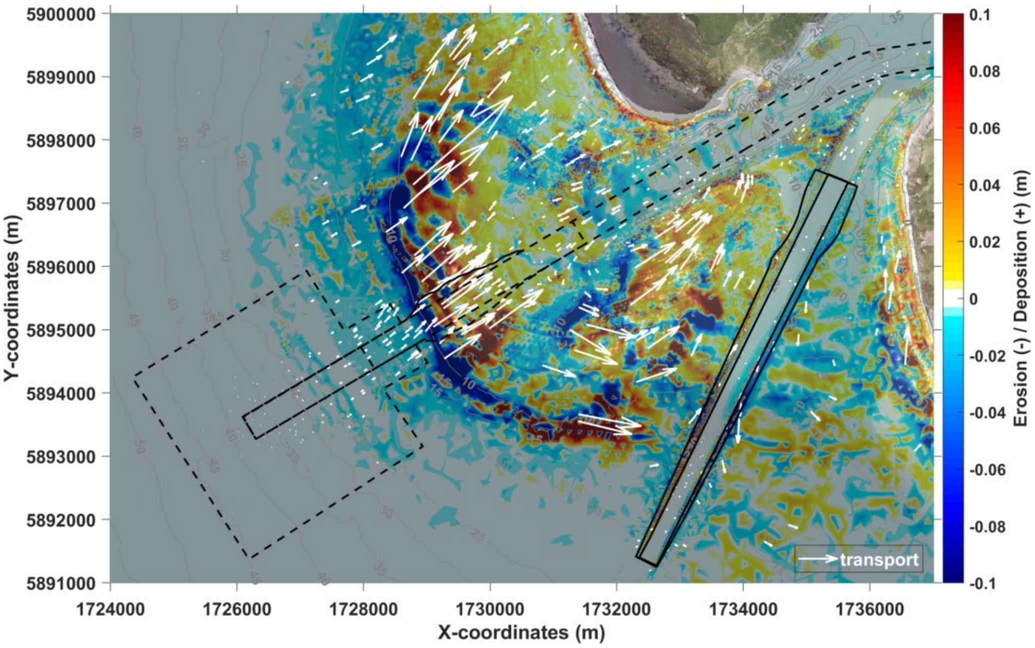

Figure 6.3: Infill of the South Channel during the Control 3 wave event

6.3 Infill in harbour

Section 2.5.1 discusses sediment sources in the inner harbour area. New sediment sources into the harbour primarily comprise silty material from shoreline erosion, terrigenous runoff from freshwater tributaries and resuspension of fines on intertidal flats. A large volume of sand sediment within the harbour sediments date back to early origins and infilling of the Manukau Basin, however limited new sources exist of this material in the inner harbour. Sandy material is notable in areas of the intertidal areas and transported.

Channels in the open reaches of the inner harbour serve as conduits and temporary repositories of fine sediment. They are conduits in the sense that they convey fines back-and-forth between intertidal flats and the coastal ocean. They are also temporary repositories in the sense that sediments scoured from intertidal flats by episodic waves or delivered intermittently from freshwater sources during floods, can deposit on channel bottoms at slack water, but generally energetic currents resuspend these sediments and they are then fed either back up onto the flats or out to sea.

Maintenance implications associated with infill in this section consider silt and sand transport separately noting the different processes by which they are transported.

6.3.1 Silt infill

Section 3.5.1 discusses sediment transport in the inner harbour area. This discusses how fine sediment that becomes suspended near to tidal channels during the ebb tide, either due to wind waves or run-off is likely to be transported out of the harbour with only limited sedimentation occurring when tidal currents recede over low tides.

Channel deepening is likely to lower current speeds in these areas, lengthening the period over slack tide when deposition might occur. Slack water in the channels is limited in duration, thus not allowing much time for deposition or consolidation which would otherwise reduce erodibility. This accounts for small changes in channel currents in response to dredging. Applying Reed’s 5 mm/yr SAR estimate to the inner harbour channels gives us an estimate of 5,000 m^3 of silt accumulation per year. Acknowledging that this SAR is derived from comparatively more sheltered depositional environments in the upper harbour, and due to only small increases in silt infill over dredged areas, we can treat this as an upper bound for silt accumulation in the lower harbour channels.

Areas such as a port basin (layout yet to be discussed) will likely be much more affected by silt-sized deposition where currents are likely to remain low throughout tidal stages.

6.3.2 Sand infill

Sediment infill of the dredged channel base and side batter slopes has been assessed using the coupled wave-flow-sediment transport model with several model runs undertaken for different tidal and wind conditions. Based on similar criteria of deposition above the design depth and a look-up based on % of tide and wind conditions, infill is estimated at around 400,000 to 450,000 m^3/year. Much of this accumulation is likely to be along the sides of the dredged channel with the channel batter slopes adjusting to a more stable, potentially slightly steeper angle. This sediment is expected to comprise medium to fine sand transported via flood tide from the lower Papakura Channel, and sand transported via ebb tide from upper extents of Papakura Channel.

Challenges in the estimation of this volume relate to the limited source of sandy material from the upper Manukau Harbour, likely leading to some conservatism (likely over-estimation) in the accounting of ebb-tidal transport from these areas. This sand being composed of quartz and feldspar, pumiceous sands/gravels and broken shell material is likely to be of a lower overall density to sand at the open coast which has not been factored into modelling and may further reduce maintenance dredging estimates.

Deepening of the upper Papakura Channel will reduce bed levels to those comparable with those of the lower Papakura Channel (Figure 6.4). This will likely increase flood -tidal transport of fine to medium sands from the lower channel into this area.

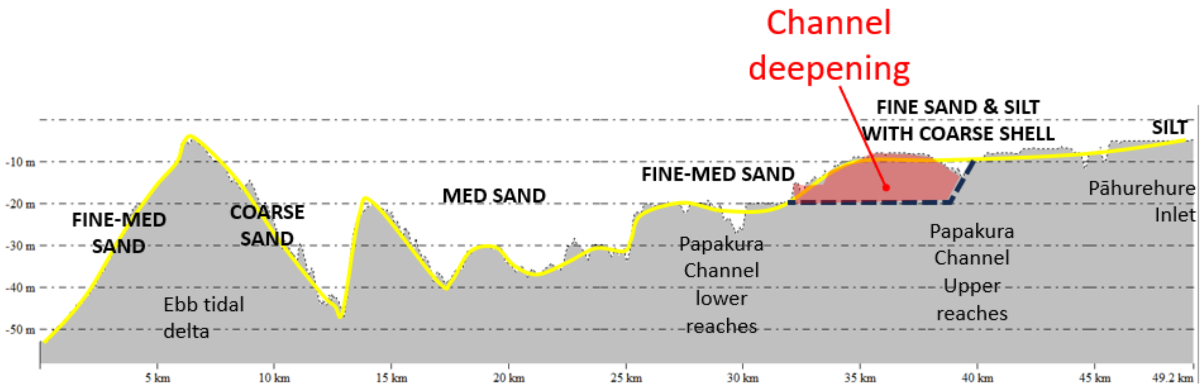

Figure 6.4 Changes in bathymetry due to channel dredging of the upper Papakura Channel

6.4 Cumulative infill with dredging

An exercise has been undertaken to assess the cumulative change in infill rate and sedimentation depth within the channel assuming dredging activities are undertaken when conditions permit. The sedimentation depth is assessed based on the maximum depth of sedimentation (~0.5 m) that occurred during the synthetic storm events (Figure 5.6) which infilled 200,000 m^3 into the channel (around 25 mm for every 10,000 m^3 infilled).

Figure 6.5 presents a time series of the 12-hour averaged wave height and 3 month moving average of wave height and 12-hour infill and dredge rate over the hindcast period. Seasonal fluctuations are evident along with years of higher and lower energy. A 20% factor of safety based on previous sensitivity testing has been applied to the infill rates. Figure 6.6 and Figure 6.7 present the resultant cumulative infill volume and depth with various assumptions made around dredge workability (Hs threshold) and daily production rate.

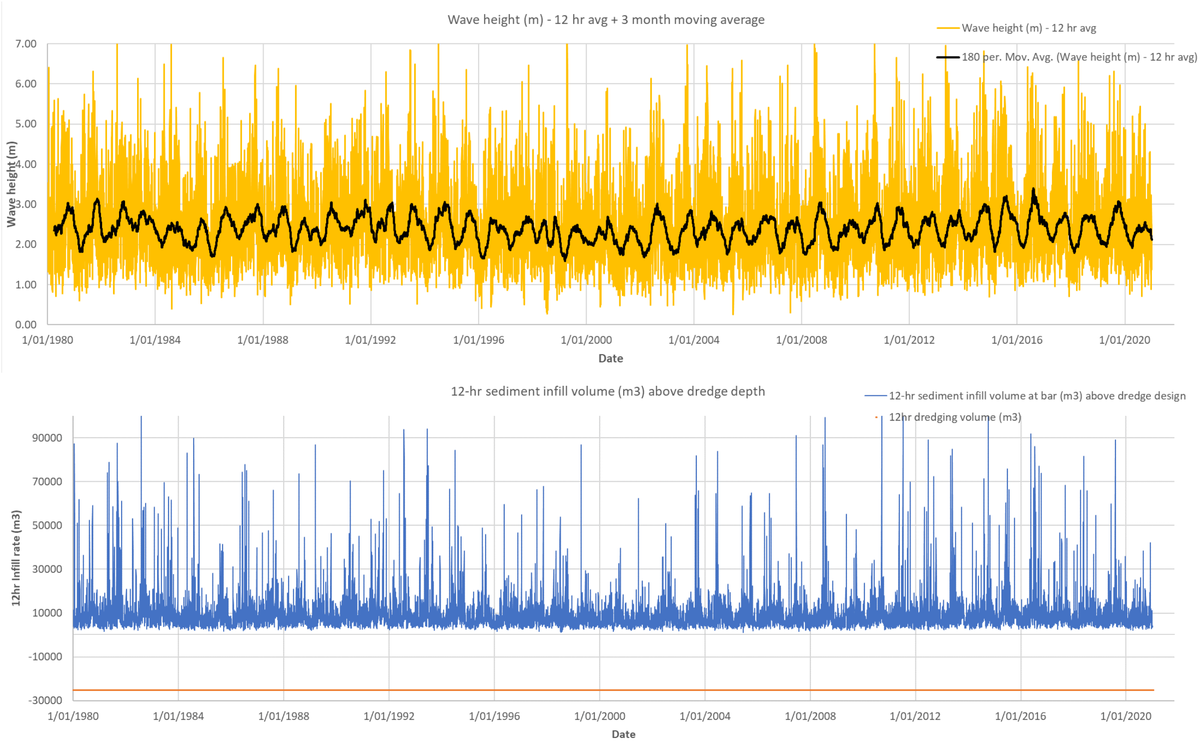

Figure 6.5: Hindcast of wave height and 12hr infill rates

Results indicate that with the adopted wave height threshold of Hs < 3 m and daily production of 50,000 m^3 the channel can be kept reasonably clear, with an average of 1.4 events per year where the depth exceeded a 1 m threshold (a nominal threshold that could relate to an over-dredge scenario or tidally restricted navigation), although often it takes until well into spring or even summer to remove the infill completely. With a lower wave height threshold of Hs < 2.5 m and daily production of 40,000 m^3 the channel is harder to keep dredged and can infill above the threshold for multiple seasons before being cleared. Note that this is a highly simplified scenario with dredging often able to occur in more sheltered locations during higher waves and depths based on very limited, extrapolated scenarios. It gives some indication, however, of the sensitivity of the cumulative infill volumes and depths within the channel to dredging workability.

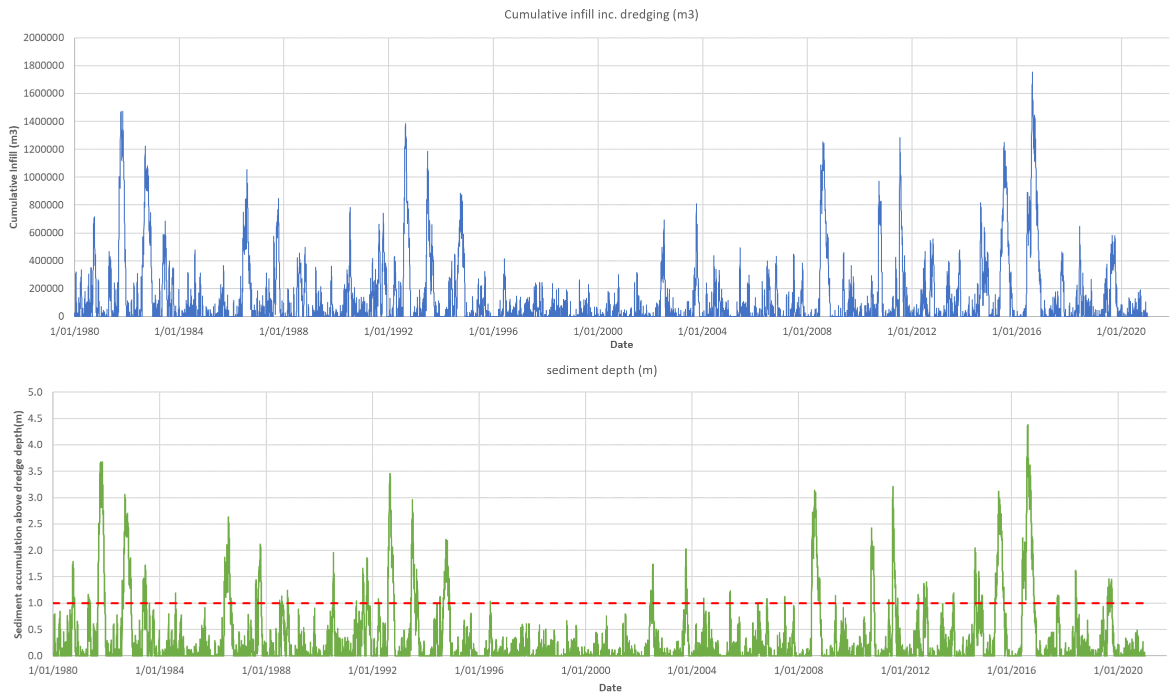

Figure 6.6: Cumulative infill and average seabed depth for a dredge working threshold of Hs = 3m and working rate of 50,000 m^3/24hrs.

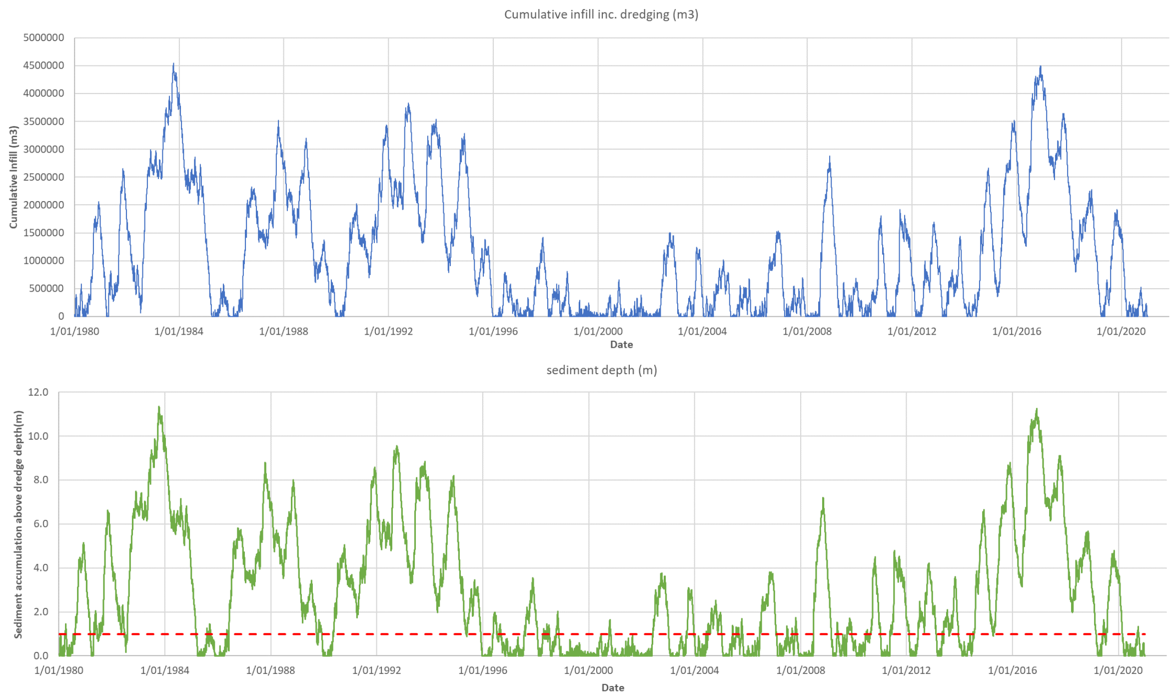

Figure 6.7: Cumulative infill and average seabed depth for a dredge working threshold of Hs = 2.5m and working rate of 40,000 m^3/24hrs.

6.5 Assumptions and accuracy

As discussed in Section 6.1, this approach to determining rates of infill assumes that material that accumulates in the bar each timestep is removed (i.e. the bathymetry or morphology is not updated in the model). This is a reasonable assumption in the long-term as navigation depths must be maintained at a design depth, however, it is unlikely that dredging would occur during a major storm and therefore total infill could differ if the bathymetry were updated (i.e. due to the morphological feedback on hydrodynamics). To test the sensitivity of this on modelled infill rates, a 10 day model run was undertaking using a synthetic storm as described previously with morphology updated every 12 hours. The results of this compared to the event-based *Input Reduction* approach with results indicating the *Input Reduction* approach may overestimate infill by 20% during an event.

Sensitivity assessments were also undertaken using a range of sediment sizes at the bounds of sediment grading. Sediment infill using a finer sediment was substantially higher than using the adopted mean size and, when adjusting for the likely percent component of fine sediment, infill rates may underestimate infill by up to 20%. Infill in the channels within the harbour were also likely over-predicted as they assume an unlimited sediment source.

In terms of overall model accuracy, verification data for the sediment transport is limited. Comparison between modelled and measured sediment flux in a single sample found very close agreement, however, the sample is for a single point and time and during relatively low concentration, so some caution should be exercised. Comparison of longshore sediment transport on the open coast between the coupled numerical model and empirical formula found larger differences, with empirical values being 1.5 to 2 times higher than the coupled numerical model. This does not provide guidance as to which model (if either) is more accurate as field verification data is not available, but can provide an indication of the ranges of prediction using the different models. Likewise, these longshore predictions do not directly relate to predicted infill rates on the bar as they are driven by different processes. Assuming an error of -0.08 for the sediment flux comparison and 2.0 for the longshore transport comparison, and assuming independence of errors, the resultant RMS error is 1.56, or around 50%.

Overall, the results of sensitivity runs undertaken indicate that variations in adopted infill rates in the order of ± 20% is reasonable. If stress testing is undertaken, adopting a ± 50% to account for uncertainty in model accuracy due to the lack of verification data and long-term system behaviour is likely prudent at this stage of assessment.

7 Effects on geomorphology

7.1 Ebb tidal delta

Previous assessments of the geomorphology of the Manukau ebb tidal delta indicates significant, large-scale changes in channel and bar configuration on an approx. 30 year timescale (refer Section 2.6.3). The effects of dredging a channel on waves, currents and sediment transport processes is described in Section 5 and include development of a shallower bar further offshore (i.e. the terminal lobe of the delta is moving offshore in response to the increased tidal flows) and along the inner portion of the channel along with deposition on the side batter slopes.

Ongoing maintenance dredging is intended to maintain the deeper channel in a fixed alignment and thus prevent a return to its current form and process. The placement of spoil (maintenance dredge material) will affect the geomorphology of the bar. If this material (~7M m^3/year) is removed from the bar system, the overall bar volume (assessed by Hicks and Hume, 1991, at 1250M m^3) may decrease over time. While this annual dredge volume is in the order of 0.4 to 0.5% of the total ebb tidal delta volume, over 50 years this becomes more significant. A reduction in the ebb tidal delta volume, leading to a reduction in bar elevation and extent, may have adverse effects on adjacent coastlines and/or the flood tide delta as sand is 'sourced' from elsewhere to bring the system back to equilibrium (based on the relationships between tidal prism and ebb tidal delta volume - Hicks and Hume, 1996). Placement of dredge material should therefore be designed to maintain the existing sediment transport circulation patterns on the bar and generally keep processes in balance.

While historically in the order of ~2M m^3/year was moved from the southern bar into the channel, during certain stages of the channel and bar evolution, large volumes of sediment (several M m^3) are forced by waves and currents from the south bank across the proposed channel alignment (Figure 2.33). However, these changes are likely dependent on sufficient material accumulating on the southern banks to interrupt the strong tidal flows once they are pushed into the channel and force the channel to the north. By selective placement of the maintenance dredge spoil the accumulation of sediment can be likely managed and this process controlled. Therefore, additional volume as a result of morphological movement of the bar has not been added to the calculated infill rates.

If this was not the case and sediment continued to accumulate on the south bank and be forced into the channel, either rapid dredging would be required (ideally before the event), or potentially managed by training structures. However, the use of such structures is discussed in Section 8.1 and would not likely be suitable in this environment due to the very large scale of the area and dynamic and high energy environment.

7.2 Open coast

The net longshore transport has been assessed (Section 3.5.2) as being from south to north. Therefore, it can be inferred that changes to the bar are unlikely to result in changes to the beach system to the south of the ebb tidal delta. However, beaches to the north of the ebb tidal delta are fed by material moving off the bar and onto the beach (Blue and Kench, 2016). Changes to the bar, in particular to the cyclic processes of channel and bar movement to the north and breakthrough to the south, have the potential to alter sediment supply to the beaches and processes of erosion and accretion.

The proposed maintenance dredge volumes (~7M m^3/year) are substantially larger than the calculated longshore transport rates on adjacent beaches (in the order of 1.7M m^3/year south of the Manukau Bar). If all the dredged material was placed downdrift of the ebb tidal delta then it may have the potential to affect adjacent coastal processes with very large volumes of sand. Careful placement of dredged material will therefore be required to maintain overall volumes on the bar and to provide sufficient supply to the beaches to the north.

7.3 Movement of placed material

The ability to maintain existing sediment transport circulation patterns will be dependent on dredged materials being placed in sufficiently shallow water to propagate onto the bar and open coast beach in a reasonable (months rather than years) timeframe. While a full analysis of the movement of a placed dredge material is outside the scope of this assessment, the potential for this material to be retained in the littoral system has been assessed using closure depth definition. The depth of closure indicates the likely limit of sediment exchange with the nearshore (Nielson and Lord, 1993).

Commonly used predictors include those of Hallermeier (1981, 1983) which establish inner and outer closure depths. The inner closure depth refers to the seaward boundary of significant sediment transport caused by waves in a typical year. The outer closure depth defines the limit in which significant waves can entrain sediment and cause transport.

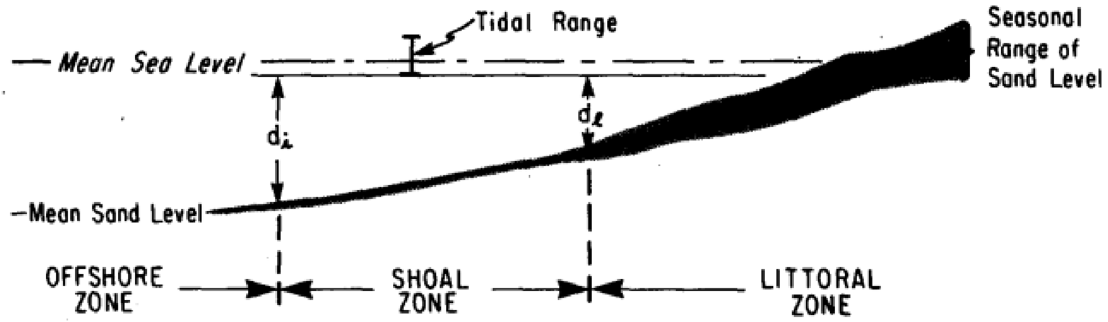

Figure 7.1: Inner and outer closure depths to define the shoal and offshore zones (source: Hallermeier, 1981)

The formulas for inner and outer closure depth are given below:

$$h_{inner} = 2.28H_s - 68.5\left(\frac{H_s^2}{gT^2}\right) \quad \text{(Eqn 7.1)}$$

Where H_s is the wave height seaward of the breaker zone that is exceeded 12 hours per year, T is the period corresponding to H_s and g is acceleration due to gravity.

$$h_{outer} = (\overline{H}_s - 0.3\sigma)\overline{T}_s\sqrt{\frac{g}{5000\,D}} \quad \text{(Eqn 7.2)}$$

Where H_s is significant mean wave height, σ is the standard deviation of significant waves, T_s is significant wave period, D is median grain size and g is acceleration due to gravity.

Based on wave characteristics for site O1 offshore of the Manukau Bar set out in TWP03b, the inner closure depth is estimated at 13.6 m and the outer closure depth at 83m. This indicates that sediment placed beyond 13.6 m may be mobilised under waves but is not necessarily part of the inner profile.

Table 7.1: Wave parameters and closure depth definitions

Parameter	Value	Parameter	Value
Hs-12hr	6.6 m	g	9.81 m/s
Tp-12hr	14.4m	D_{50}	0.25 mm
Hs-mean	2.4m	h_{inner}	13.6 m
Tp-mean	14s	H_{outer}	83 m

While these definitions are derived for open coast beach profiles and may not be applicable to this high energy, offshore bar environment, the findings are generally supported by sediment transport modelling. Figure 3.18 of Section 3, and in more detail, Figure 4.2 to 4.8 of TWP03c suggests that during high energy events (Hs = 5 m), while there is some sediment movement out to around -20 m CD depth, onshore sediment transport primarily occurs seaward of around -10 m CD depth. Further investigation would be required to determine whether sediments can be placed in such a way that they can migrate onto the bar and remain in the littoral system. This may require part loading of TSHDs to reduce loaded draft and minimise allowable placement depths, use of smaller dredgers to double handle material in order to place within the inner closure depth, or placement within the deeper entrance channel and tidal currents are relied upon to re-distribute sediment into the system, although this may lead to greater ongoing maintenance volumes. Placement of dredge material back into the active coastal system is complex and needs further work as part of an effects assessment to determine whether a dynamic equilibrium can be achieved to avoid adverse effects to the bar and adjacent shorelines.

7.4 Inner harbour

Sections 5.1 and 5.2 indicate changes to the tidal propagation into Manukau Harbour and the tidal currents within the dredged channel and on the adjacent intertidal flats. These physical changes are typically considered to be proportionally small in magnitude, but large in spatial extent.

As discussed in Section 6.3.2, deepening of the upper Papakura Channel will reduce bed levels to those comparable with those of the lower Papakura Channel (Figure 6.4). This will likely increase flood tidal transport of fine to medium sands from the lower channel into this area, modifying bed form sediments from being predominantly silty, to sandy material.

8 Engineering mitigations

8.1 Intent

Maintenance dredging is assumed to occur to remove sediments deposited into the dredged navigation channel (refer Section 6).

A range of engineering measures can be employed to either:

1. Reduce the volume that needs to be dredged,
2. Provide a greater capacity for infill to occur before dredging needs to occur, or
3. Train the channel if migration of the sand bars cannot be controlled by dredging alone.

This section discusses potential measures including a description of the measure and its likely effectiveness in this environment.

8.2 Identifying options

8.2.1 Control structures

Coastal structures such as groynes, breakwaters and training walls can be used for a variety of purposes including breaking wave energy to provide a sheltered environment, training flows to stabilise entrances and reduce movement of bars and shoals or to trap sediment, preventing it from moving alongshore. These various approaches are relatively well tested and commonly used in New Zealand and internationally, i.e. Figure 8.1.

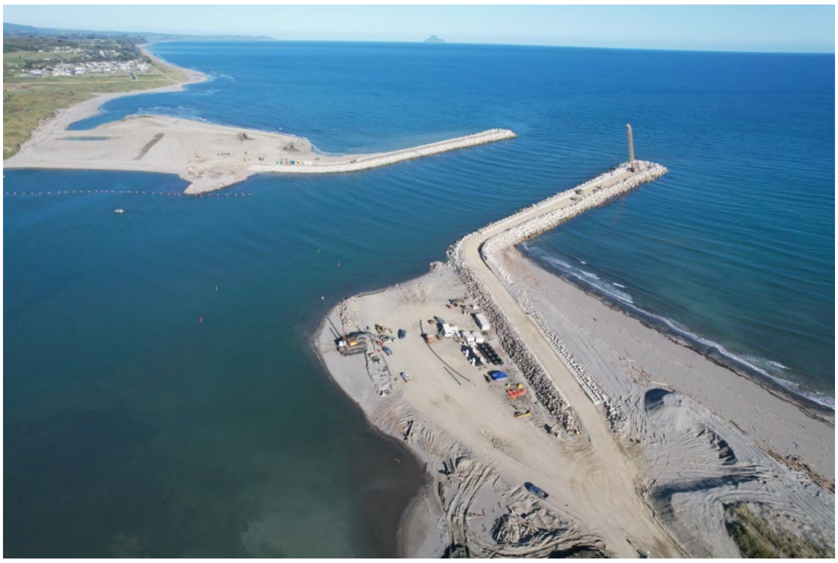

Figure 8.1: Example of training walls built to control the river Waioeka River entrance at Ōpōtiki (source: Ōpōtiki District Council)

Some unique challenges of using such measures at the Manukau Bar include the very large scale of the area with the dredged area extending some 4 km across the bar, the high offshore wave climate requiring very large armouring units (likely greater than 30 tonnes), the high tidal flows and mobile bar morphology that the structure foundations must accommodate.

Structures intended to control sediment entering a channel would usually be placed along the lateral margins of the channel (i.e. Figure 8.1). The effectiveness of such structures in reducing sediment infill within the channel is, however, likely limited as modelling indicates that most material is being transported onshore and offshore under wave and tidal processes (Figure 5.4) with lateral movement typically out of the channel and onto the shallow adjacent bars. Therefore, any structures placed along the lateral margins are unlikely to reduce the sediment infilling the dredged channel, or provide any greater capacity for infill to occur before dredging needs to occur. The structures may provide benefit in reducing the wave climate for vessels once they navigate into the channel, however the navigational operability due to weather restrictions (*TWP05*) is not a limiting factor.

There is potential, as discussed in Section 7.1, that sediment continues to accumulate on the south bank and is forced intermittently into the channel. If this accumulation and/or the movement of this sediment into the channel cannot be managed by maintenance dredging, a structure along the southern channel margins could provide benefit. However, the previously mentioned challenges of implementing such a structure remain and preference would be to manage such accumulation through maintenance dredging.

Overall, control structures are not likely to provide sufficient benefit to justify the cost of construction and have not been considered further.

8.2.2 Sand bypassing system

Sediment bypass systems work by fluidising and extracting sand from one, generally fixed location, pumping the sediment to another location and discharging. Examples of sand bypassing systems set up to reduce dredging of a navigable entrance while maintaining longshore sediment transport are at Tweed Heads in northern New South Wales and at the Gold Coast seaway (Figure 8.2). Both of these systems utilise jetties constructed updrift of an entrance with jet pumps extracting a sand slurry which is then pumped below the entrances and discharged at outlets to the north.

Figure 8.2: Sand bypass system on a jetty structure adjacent to the Gold Coast Seaway (source: Gold Coast Waterways Authority)

These systems work by interrupting the flow of sediment before it can move into a channel, reducing the dredging requirements. However, in this environment a sand bypass system is unlikely to be effective as the majority of sediment accumulating in the channel is moving onshore or offshore under waves and tides rather than laterally (Figure 5.4). Therefore, a bypass system would need to be placed across the channel, which would not be feasible if raised and would likely be subject to very high tidal currents and scour if located on the seabed. A bypass system could be effective in transferring sediment from the southern open coast to the north if the intent was to reduce the volume of the ebb tidal bar, but that is likely to have large-scale environmental impacts and not greatly benefit maintenance dredge volumes for several decades.

Overall, a sand bypass system is not likely to provide sufficient benefit to justify the cost of construction and has not been considered further.

8.2.3 Dredged sediment traps

A dredged sediment trap is a dredged area into which sediment accumulates/infills before that sediment reaches the main navigation channel. The sediment trap may be adjacent to the channel or may be below the design depth (i.e. over-dredging). While this system does not reduce the total infill volume as the trap needs to be periodically emptied by dredging, the system will allow greater infilling to occur before the main channel is affected and provides a buffer for very large infilling episodes which could otherwise close the navigation channel.

Based on sediment transport and deposition processes (refer Figure 5.6 and Figure 5.7), the location where a sediment trap would provide most benefit would be at the inner 1.5 km of the dredged channel over the bar. Over-dredging, for example an additional 1 m depth along the inner 1.5 km of the dredged channel, would decrease the number of episodes per year where sedimentation may become problematic for navigation. This option could be further investigated and the cost-benefit evaluated at a detailed design stage.

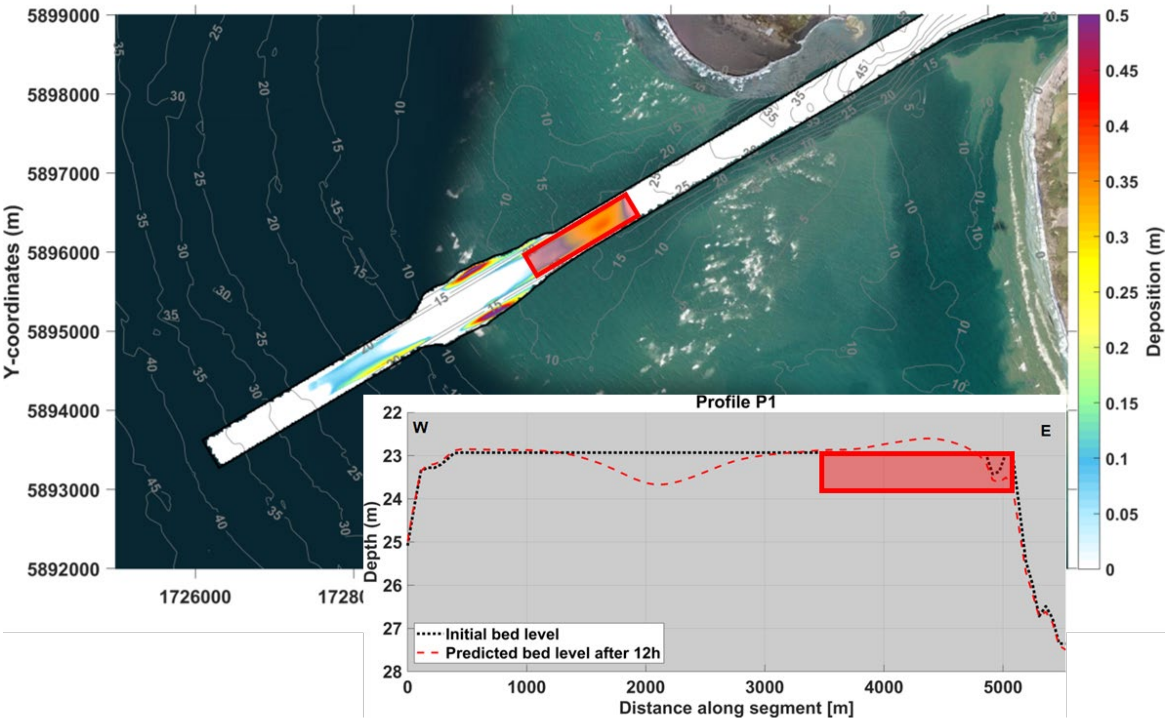

Figure 8.3: Potential over-dredge area or sediment trap (red polygon) to provide more space for sediment deposition before removal is required

8.3 Summary

Engineering measure	Effectiveness in reducing total infill	Effectiveness in accommodating greater infill volumes	Effectiveness in maintaining channel alignment	Likely cost	Suitability
Control structures	Unlikely effective	Unlikely effective	Likely effective	Very high	Unlikely suitable
Sand bypassing system	Unlikely effective	Unlikely effective	Unlikely effective	Very high	Unlikely suitable
Dredged sediment trap	Unlikely effective	Likely to decrease episodes of problematic infill	Unlikely effective	Moderate	Likely suitable for further investigation

9 Natural hazards

New Zealand in general and the Auckland region, including Manukau Harbour in particular, are exposed to numerous natural hazards. The potential exposure and level of impact to establishing and operating a port in the Manukau Harbour is set out below.

9.1 Climate change

9.1.1 Sea level rise

The recent release of the IPCC 6th Assessment Report (IPCC, 2021) includes revised rates of sea level rise for each scenario. The report shifted to a new core set of future representative scenarios, based on Shared Socio-economic Pathways (SSPs). Following the release of the IPCC 6th Assessment Report, the Ministry for the Environment released an interim guidance on the use of the new sea-level rise projections (MfE, 2022). In the interim, guidance published by MfE also recommends the consideration of Vertical Land movement (VLM) with the SSP SLR projections. Vertical land movement is the average long-term rate of change over multiple years or decades on the land surface and can include processes such as tectonic movements and subsidence that cause land to move up or down. This can impact relative sea level rise at any particular location. The NZSeaRise website suggests that the vertical land movement (VLM) rate around Manukau Harbour is in the order of 0 to -3 mm/year (hence subsiding) (Figure 9.1). The SLR projections for each SSP in the present day, in 2080 years and in 2130 including VLM are given in Table 9.1 for the 50% with the 83rd percentile values also provided for the high emission scenario (SSP5-8.5). These projections use a baseline of 1995-2014 with a mid-point (zero) at 75 approx. 2005.

Table 9.1: Sea level rise predictions for the five IPCC projection scenarios including VLM for Manukau Harbour

Time frame	Emission scenario				
	Projections to 2150 – medium confidence				
	SSP1-1.9	SSP1-2.6	SSP2-4.5	SSP3-7.0	SSP5-8.5
2020	0.12	0.11	0.11	0.11	0.11 (0.141)
2080	0.53	0.57	0.65	0.73	0.79 (0.971)
2130	0.90	0.90	1.20	1.46	1.61 (2.071)

[1] 83rd percentile

The potential effects of this sea level rise on the ability to establish and operate a port in the Manukau Harbour include the potential for an increased tidal prism with more water entering and leaving the harbour as the intertidal sand banks become relatively deeper. This has the potential to increase the size and volume of the ebb tide delta (Hicks & Hume, 1991) potentially increasing volumes being transported and requiring maintenance dredging. The increased tidal prism may lead to higher currents within the harbour, which could lead to either greater volumes of sediment being transported into the channel or improved scouring of the channels. These effects are likely to be subtle and provide opportunity to gradually increase dredging regimes and are therefore, unlikely to pose a major issue for port operation. Furthermore, the increased sea levels will result in relatively deeper channels, potentially decreasing the requirement for dredging to maintain navigation depths.

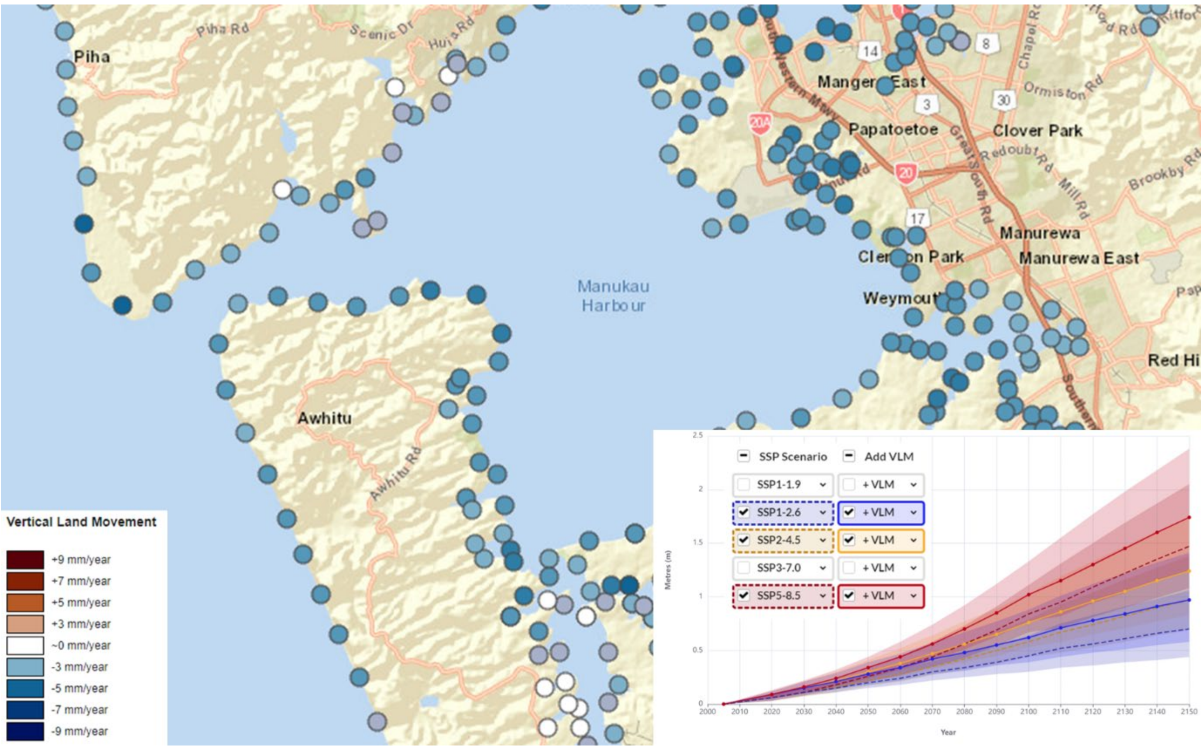

Figure 9.1: Projected sea level rise scenarios for Auckland including the effects of vertical land movement (source: https://searise.takiwa.co/)

9.1.2 Metocean conditions

Climate change projections for New Zealand (Mullan et al., 2011) suggest that westerly flow will increase in frequency in spring (up to 20%) and winter (up to 70%), and to decrease in summer and autumn (up to 20%). Mullan et al. (2011) suggest a 2.4% averaged increase in the maximum wind speed, in the period 1961-2100 relative to 1961-2000 (refer *TWP 03b*). This may marginally increase the height of waves generated within Manukau Harbour, especially with high sea levels reducing the effectiveness of shallow intertidal areas in dissipating wave height.

Climate change is expected to change wave height on the open coast. Albuquerque et al. (2022) predicts wave height and peak period to increase along the west coast of New Zealand throughout this century with Hemer et al. (2013) and Rouse et al. (2017) suggesting wave height increases in the order of 5% for 2070–2099 for parts of New Zealand exposed to Southern Ocean swell. While there is little information on the change of storm wave climate, studies of global wave height measured by satellite altimeter ((Young, Zieger, & Babanin, 2011)) indicates that extreme waves (1% exceedance) would experience larger increases than mean conditions.

9.1.3 Changes in sediment supply and transport processes

Changes in rainfall may result in changes to sediment transported to the harbour from the catchment. However, such changes are highly uncertain and the effects of fine sediment on channel infill generally low (refer Section 6.3), therefore are unlikely to significantly affect dredging regimes. Sediment supply from catchment to harbour – uncertain.

The effects of changes in the mean wave climate on sediment infill rates have been assessed (refer *TWP03c*) and indicate an increase in infill rates in the order of 10% by 2070-2099. Similar to the effects of sea level rise, these changes are likely to be subtle and gradual providing opportunity to gradually increase dredging regimes or navigational operations and are therefore unlikely to pose a major issue for port operation.

9.2 Tsunami

As a coastal city, Auckland could potentially be affected by a tsunami. Tsunami waves are generated by the sudden displacement of water (caused by a submarine landslide, volcanic eruption or earthquake). Areas that may be at risk to tsunamis are often overtaken by the destructive tsunami overland flow path, and lives, property and infrastructure are exposed.

Recent modelling of tsunami hazard carried out for Auckland Council (Borrero, 2022) show that west coast tsunami hazard is less than on the east coast, with lower predicted tsunami heights from large magnitude events (Mw 9.3 to 9.6) from around the Pacific Rim than those predicted from earlier studies (Power, 2013). The more recent modelling shows the maximum tsunami height of 2.9 m for around a 2,500 year return period event at Manukau Heads, 3.1 m at Clarks Beach and 1.2 m at Onehunga (Borrero, 2022). This suggests that tsunami amplification is possible within the harbour at high tide levels particularly towards the southern part of the harbour. The tsunami evacuation zones shown in Figure 9.2 were therefore set on a topographic level of 2 m above MHWS for the red zone, the aggregation of around 22 model runs from South America and north and western Pacific for the Orange Zone (to develop around a 500 year return period timeframe), and the maximum of all simulations for the Yellow Zone (around 2,500 year return period timeframe).

The high velocities resulting from the tsunami are likely to result in large scale movements within the sandy systems of the nearshore, ebb tide delta, coastline, and inner harbour. Specifically scouring of the narrower parts of the inlet throat with deposition both in deeper water seaward and landward of the inlet in the present-day situation. Even in the present-day situation this is likely to require inspection of the channel and inlet to confirm the safe operability of vessels accessing the port and it is likely that some maintenance dredging may be required to resume operability. However, this is unlikely to result in prolonged closure due to the large amount of maintenance dredging being undertaken and dredging equipment on hand.

While tsunami wave modelling has not been carried out for this assessment, it can be expected that the dredged channel area through the delta could be subject to both rapid deposition and erosion in different locations (similar to the effects of tidal processes). Any dredge disposal areas may also experience greater rates of localised change with higher forces exerted on the seabed than typically occur from extreme storm events.

Given the location of any port will be in the Coastal Marine Area, the risk of tsunami will need to be considered in the design and site-specific modelling and design considerations will be required. It is likely design criteria set out in NZTA|Waka Kotahi Bridge Manual (3rd ed.) for IL4 structures as well as international guidance would be used (Till, 2022).

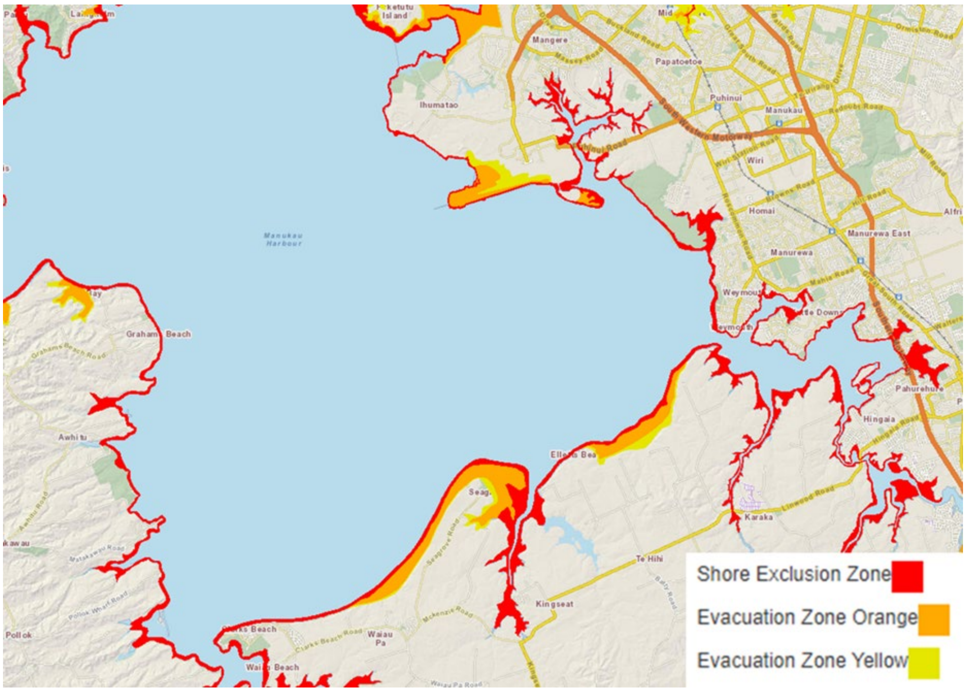

Figure 9.2: Tsunami evacuation zones (Source: AC Geomaps)

9.3 Earthquake

Earth shaking, ground displacement, and liquefaction can be experienced during seismic events and can cause damage and losses to infrastructure, property and lives as well as the economy and environment.

Auckland lies in a less seismically active part of the country. However, earthquakes have been felt in Auckland in the past (see Figure 9.3). The Auckland region lies upon a small number of active faults such as Wairoa North, Drury and Glenbrook faults. More shaking is forecast in the south of the Auckland region. Overall, shaking is forecast to be lower than nationwide. However, anywhere in New Zealand can experience earthquakes and regions can be affected by earthquakes from far away.

The National Seismic Hazard Model (NSHM - GNS, 2020) combines the best available scientific knowledge to estimate future earthquake shaking in Aotearoa New Zealand. The NSHM considers possible earthquakes that could affect a location and then estimates the severity of the related shaking that might occur. Figure 9.4 shows low ground accelerations in the southern Auckland region, including Manukau Harbour for an event with a 2% probability of exceedance in 50 years.

Given the location of any port will be in the Coastal Marine Area, the risk of earthquake impacts will need to be considered in the design and site-specific modelling and design considerations will be required. It is likely design criteria set out in NZTA|Waka Kotahi Bridge Manual (3rd ed.) for IL4 structures. Assessment of the seismic stability of the dredged navigation side slopes indicates these are generally stable with some limited lateral movement possible within the harbour.

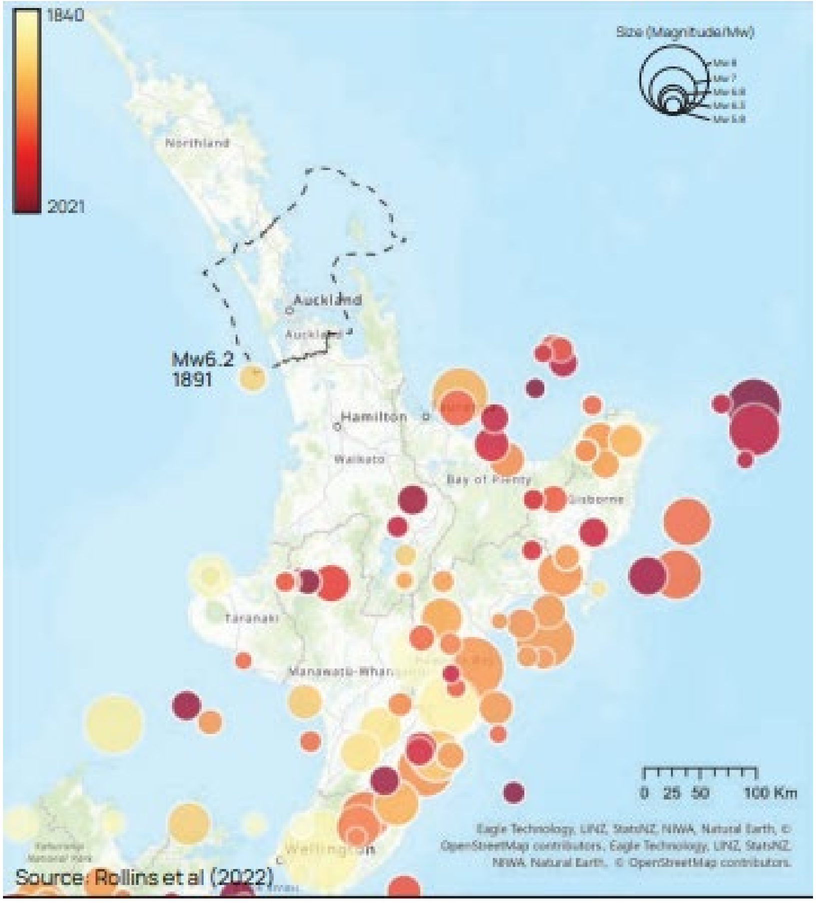

Figure 9.3: Significant past earthquakes which have affected the North Island (Source: (Rollins, 2022))

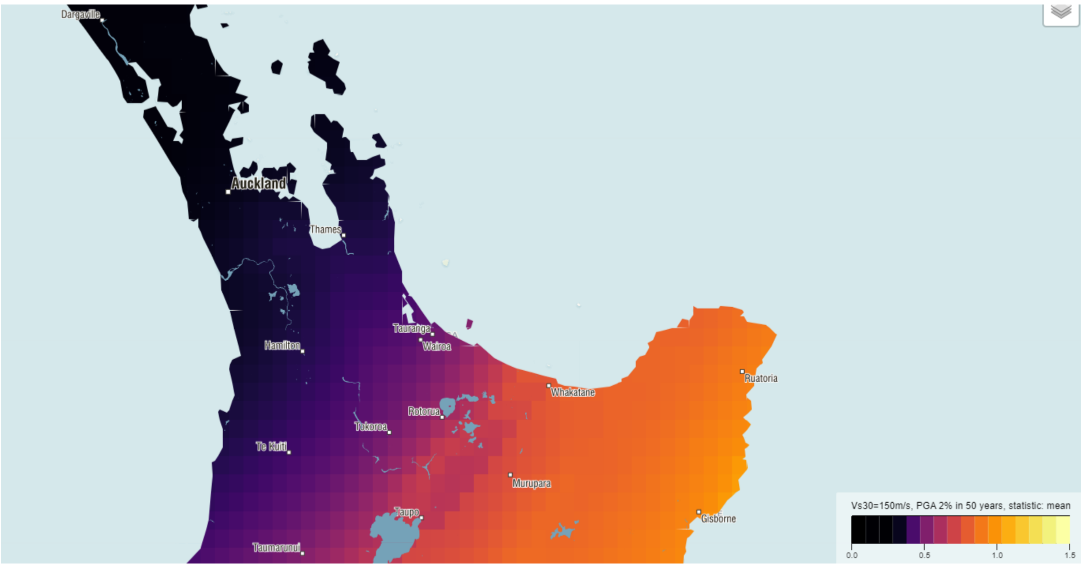

Figure 9.4: Hazard map for Auckland and central North Island showing the mean peak ground acceleration for an event with a probability of exceedance of 2% in 50 years (Source: GNS NSHM maps)

9.4 Volcano

The Auckland Volcanic Field (AVF) is located in the central part of the Auckland region and is an active volcanic centre. The last eruption occurred approximately 600 years ago at Rangitoto, although as shown in Figure 9.5, the return periods between past events has ranged from tens to thousands of years (CDEM and AC, 2015). The AVF is largely monogenetic, meaning that the location of the next volcanic eruption cannot be predicted and will probably occur in a new location and could occur at any time in the future.

Any eruption in Auckland will likely cause significant widespread disruption to the region, possibly for an extended time although the initial phase of the activity is likely to be the most catastrophic (CDEM and AC, 2015). The primary hazard zone extends around 3 km from any vent and all hazards could occur within this zone including base surges, volcano formation, ash-fall, lava, gas, ballistics, shockwaves, earthquakes, lightning and tsunami. People and animals within this zone may be severely injured or killed. Infrastructure is likely to be severely damaged or destroyed. Underground infrastructure may be damaged from heat exposure, ground deformation or high-velocity ballistic impacts. The secondary hazard zone extends 2 km around the primary hazard zone and represents an area of moderate hazard including base surges, ash-fall, lava, gas, ballistics, shockwaves, earthquakes and lightning. People and animals located in this zone may be injured or suffer significant health effects. Infrastructure on the surface may be severely damaged. Beyond these zones ash-fall could extend as far as 30 km from the secondary hazard zone (CDEM and AC, 2015).

Consideration of volcanic hazard risk would need to be carried out in detailed design.

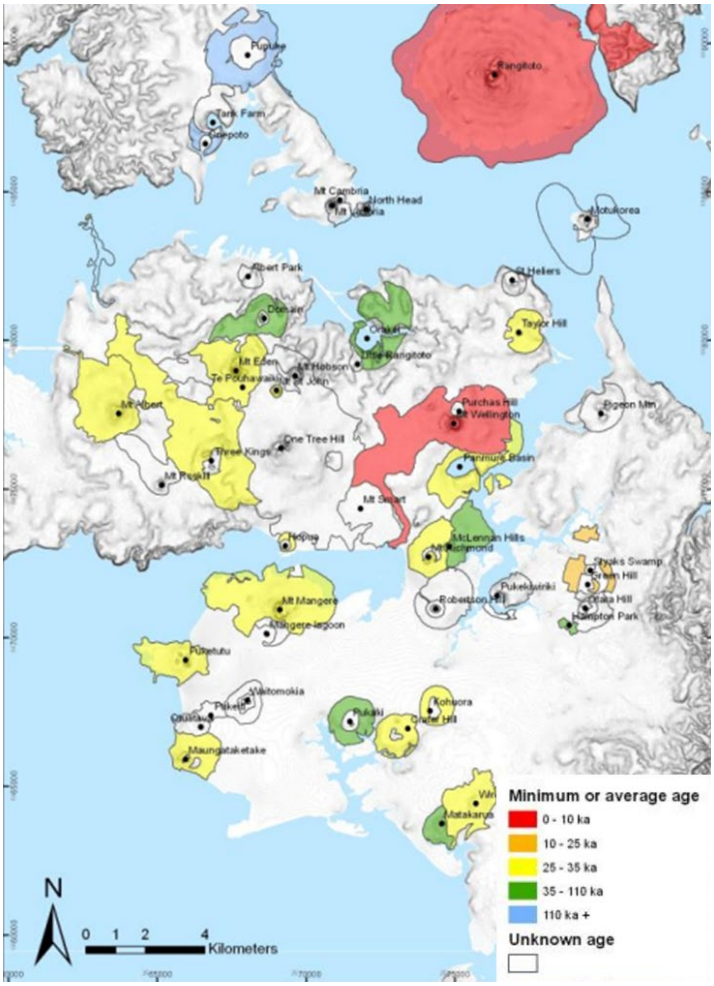

Figure 9.5: The Auckland Volcanic Field best age estimate (Source: CDEM and AC, 2015)

10 Applicability

This report has been prepared for the exclusive use of our client Ministry of Transport | Te Manatū Waka, with respect to the particular brief given to us and it may not be relied upon in other contexts or for any other purpose, or by any person other than our client, without our prior written agreement.

Tonkin & Taylor Ltd
Environmental and Engineering Consultants

Report prepared by: Authorised for Tonkin & Taylor Ltd by:

....

Dr Tom Shand
Technical Director - Coastal

Richard Reinen-Hamill
Project Director

Peter Quilter
Senior Coastal Engineer

Seth Smith
Coastal Engineer

Report reviewed by:

Dr Malcom Green
Principal Scientist – RMA Science

TDS
t:\auckland\projects\1018198\issueddocuments\final report\final (final) word\twp03 (tt) - coastal.docx

11 References

Alburqrque, J., Antolinez, J. A., Goramn, R. .., Fernando J, M., & Coco, G. (2021). Seas and swells throughout New Zealand: A new partitioned hindcast. *Ocean Modeling*(168).

Anderson, I. (2006). *Manukau Harbour: Geography.* Retrieved from New Zealand Geographic: https://www.nzgeo.com/stories/manukau-harbour/

Auckland Council. (2021). *A Synthesis of State of the Environment Monitoring in the Manukau Harbour.* Auckland: Auckland Council.

Ballance, P. (2009). *New Zealand Geology: An illustrated guide.* Geoscience Society of New Zealand.

Bell, R., Hume, T., Dolphin, T., Green, M., & Walters, R. A. (1997). Characterisation of hysical environment factors on an intertidal sandflat, Manukau Harbour, New Zealand. *New Zealand Journal of Marine and Freshwater Research*, 11-31.

Blue, B., & Kench, P. (2016). Multi-decadal shoreline change and beach connectivity in a high-energy sand system. *ew Zealand Journal of Marine and Freshwater Research*, 406-426.

Borrero, J. S. (2022). *Tsunami inundation modelling and development of draft evacuation maps for Auckland Region.* Auckland: eCoast.

CDEM and AC. (2015). *Auckland Volcanic Field Contingency Plan.* Auckland, New Zealand: Civil Defence and Emergency Management and Auckland Council.

Duder, J., & Senior, A. (2010). *The Manukau Harbour Bar: a 200+ years perspective.*

eCoast. (2020). *Numerical modelling of the Manukau Harbour Entrance: High-Level estimates of dredged entrance channel infilling.*

Edbrooke, S. W. (2001). *Geology of the Auckland Area.* Institue of Geological & Nuclear Sciences.

Ernst & Young (EY). (2016). *Consultants report to the Port Future Study. Prepared for Auckland Council.*

FitzGerald, D. M. (1988). Shoreline erosional-depsitional processes associated with tidal inlets. In D. Aubrey, & L. Weishar, *Hydrodynamics and sediment dynamics of tidal inlets* (pp. 186-225). Springer.

FitzGerald, D. M., Kraus, N. C., & Hands, E. B. (2000). *Natural Mechanisms of Sediment Bypassing at Tidal Inlets. ERDC/CHL CHETN-IV-30.* US Army Corps of Engineers.

Ford, M., & Dickson, M. (2018). *Detecting ebb-tidal delta migration using Landsat imagery.*

Green, M. (2008). *Southeastern Manukau Harbour / Pahurehure Inlet Contaminant Study. Predictions of sediment, zinc and copper accumulation in southeastern Manukau Harbour / Pahurehure Inlet under future development scenario 1. Prepared for Auckland Council.* NIWA.

Green, M. O., & Coco, G. (2013). Review of wave-driven sediment resuspension and transport in estuaries.

Green, M., Bell, R., Dolphin, T., & Swales, A. (2000). *Silt and sand transport in a deep tidal channel of a large estuary (Manukau Harbour, New Zealand).*

Gregory, M., Blacksmore, N., Glasby, G., & Burrows, M. (1994). *Manukau and Waitemata Harbours sediments.* New Zealand: Oceanographic Institute.

Heath, R., Greig, M., & Shakespeare, B. (1977). Circulation and hydrology of Manukau Harbour, New Zealand. *Journal of Marine and Freshwater Research*, 589-607.

Hicks, D. M., & Hume, T. M. (1996). Morphology and Size of Ebb Tidal Deltas at Natural Inlets on Open-sea and Pocket-bay Coasts, North Island, New Zealand. *Journal of Coastal Research*.

Hume, T., Snelder, T., Weatherhead, M., & Liefting, R. (2007). A controlling factor approach to estuary classification. *Journal of Ocean and Coastal Management, 50*(11-12).

J. B. Rowntree Collection. (1964). *Aerial view of the Pahurehure Inlet, 1964.* Retrieved from https://kura.aucklandlibraries.govt.nz/digital/collection/photos/id/89906/

Jacobs in association with AECOM and McMillen Jacobs Associates. (2017). *Central Interceptor Main Project Works Detailed Design - Geotechnical Interpretative Report.* Auckland: Watercare Services Ltd.

Kelly, S. (2008). *Environmental condition and values of Manukau Harbour. Prepared by Coast and Catchment Ltd for Auckland Council. Auckland REgional Council Technical Report 2008/059.*

Kelly, S. (2008). *Environmental condition and values of Manukau Harbour. Prepared by Coast and Catchment Ltd for Auckland Regional Council.*

Kenny, J., Lindsay, J., & Howe, T. (2012). *Post-Miocene faults in Auckland: insights from.*

Macdonald, W. (1986). Cliff Erosion and Coastal Porcesses on the West Coast of the Awhitu Penisula. Masters Thesis. The University of Auckland.

Pegman, A. P. (2005). Plant succession and dune dynamics on actively prograding dune, Whatipu Beach, northern New Zealand. *New Zealand Journal of Botany*.

Power, w. (2013). *Review of tsunami hazard in New Zealand (2013 update).* Lower Hutt, New Zealand: GNS Science Consultancy Report No. 2013/131.

Reed, J., Swales, A., Ovenden, R., Buckthought, D., Rush, N., Wadhwa, S., & Ikey, M. (2008). *Southeastern Manukau Harbour / Pahurehure Inlet Contaminant Study. Harbour Sediments.* NIWA for Auckland Regional Council.

Rollins, C. R. (2022). *The magnitude-frequency distributions of earthquakes in the greater New Zealand region and along the Hikurangi-Kermadec and Puysegur subduction zones, and their uncertainties with application to the 2022 New Zealand National Seismic Hazard Model.* Lower Hutt, New Zealand: GNS Science Report 2022/48.

Smith, M. J., Stevens, C., Gorman, R., McGregor, J., & Neilson, C. (2001). Wind-wave development across a large shallow intertidal estuary: a case study of Manukau Harbour, New Zealand. *NZ Marine Freshwater Research, 35*, 985-100.

Stephens, S., Wadhwa, S., Gorman, R., Goodhue, N., Pritchard, M., Ovenden, R., & Reeve, G. (2016). *Coastal inundation by storm-tides and waves in the Auckland region. Prepared by the National Institute for Water and Atmospheric Research, NIWA and DHI Ltd for Auckland Council. Auckland .*

Till, H. M. (2022). A review of internatinal guidance for tsunami loading on buildings. *New Zealand Society for Earthquake Engineering* (p. 7). University of Auckland.

Tonkin & Taylor Ltd. (1986). *Manukau Harbour Resources Study - Report 6678 for Maritime Harbour Authority.* Auckland.

Tonkin & Taylor Ltd. (2023). *Manukau Harbour Port Feasibility Inception Report. Prepared for Te Manatu Waka | Ministry of Transport.*

Young, I., Zieger, S., & Babanin, A. (2011). Global trends in wind speed and wave height. *Science 332 (6028)*, 451-455.

Appendix A Previous borehole investigations

Central Interceptor borehole investigations across Mangere Inlet

A number of boreholes and associated soil testing were undertaken across the Mangere inlet channel as part of geotechnical investigations for the Watercare Central Interceptor project. (Jacobs in association with AECOM and McMillen Jacobs Associates, 2017)

Surface materials comprising Tauranga Group and Recent Alluvium in the Watercare central interceptor geotechnical report (coloured green in the cross section below) are described as:

"Tauranga Group alluvium represents locally derived stream and coastal alluvium and minor fan deposits. It typically consists of up to 20m thick unconsolidated to very soft thinly to thickly bedded, yellow grey to orange brown clay, silt, sand and gravel with local silty peat and pumiceous beds. The undifferentiated Tauranga Group is sometimes referred to as undifferentiated Pliocene to Pleistocene Alluvium. Since the end of the last ice age (the Holocene) the most recent deposits in Auckland have been laid down. In lowland areas of Auckland these comprise floodplain, lacustrine and coastal alluvial deposits, while estuarine sand and silt occur in harbours and bays. The majority of the material along the proposed alignment in this category is found at the Manukau Harbour, although there are small pockets associated with other watercourses."

At depths of between 10 and 20 m ECBF rock was encountered, typically dense (SPTN >50).

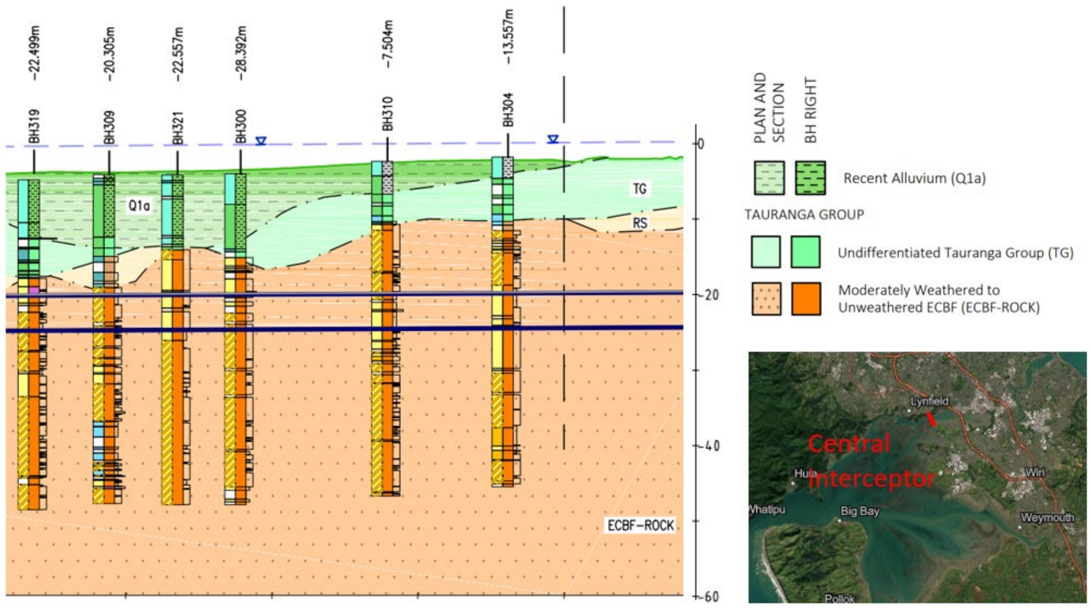

Figure Appendix A.1: Geological section along the central interceptor alignment crossing the mouth of the Mangere inlet showing variable thicknesses of recent Holocene-aged alluvium overlying undifferentiated Tauranga group. At depths between 10 and 20 m weathered ECBF rock is encountered

Airport boreholes over reclaimed land

Two boreholes undertaken in areas of the runway extension over reclaimed land put down to depths between 20 m and 30 m depth. Despite being within several hundred metres apart, the depth and thickness of materials differed considerably, indicating variable thicknesses of interbedded sands and silts. SPTN values did not exceed 50 (taken as ECBF rock in Central Interceptor investigations described in Section 3.1) at any depth within these boreholes.

Figure Appendix A.2: Location of airport boreholes

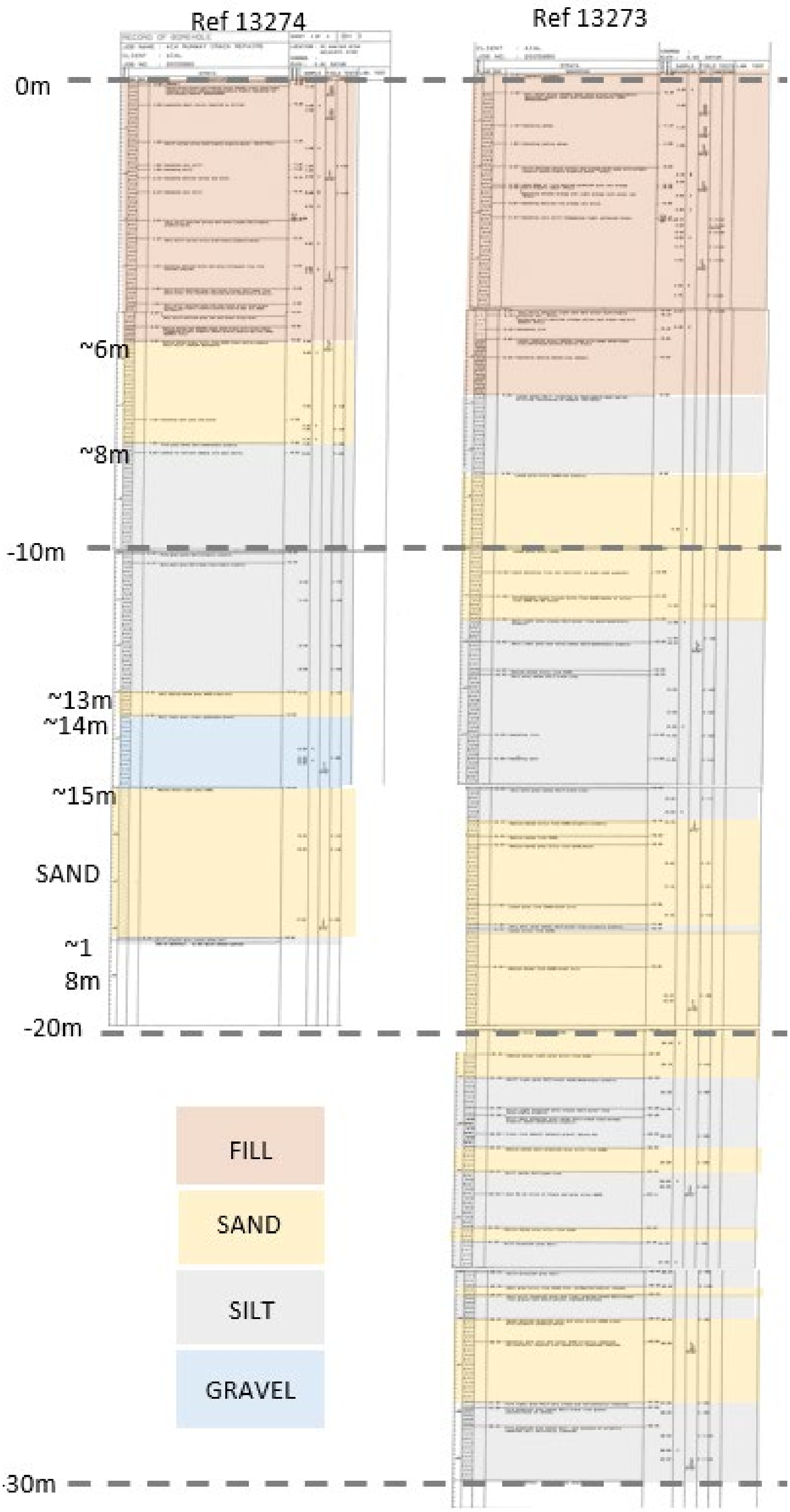

Figure Appendix A.3: Although difficult to read, colours indicate major soil constituents. This reveals highly variable (silts and sands) making up recent alluvial deposits between the two adjacent airport boreholes located several hundred metres apart

1988 Beca Boreholes

A series of machine boreholes were undertaken in 1988 within Manukau Harbour and surrounds for the Auckland Regional Authority (Figure A-4). Relevant to the proposed dredge include M13 being located within Papakura Channel in -3.1m depth and M7 and M8 being located on sand banks to the south of the channel at +0.5 and +1.5m.

BH M13 indicates fine sand becoming more silty to a depth of -15m CD, becoming silt and then clay to a depth of -20m CD. BH M7 indicates layered fine sands and silts in 2-3m layers to -7m CD and BH M8 indicates sandy silt with some clays to -8.5m CD becoming fine to medium sand.

While there are no known marine boreholes within the entrance, reference has been made to nearby land-based boreholes at Hamilton’s Gap on the Awhitu Peninsula at an elevation of 3m (i.e., just behind the beach). This showed fine sand with clay layers and traces to -5m CD, layered find sands, silts and clays to -18m, and dense fine to medium sands below this.

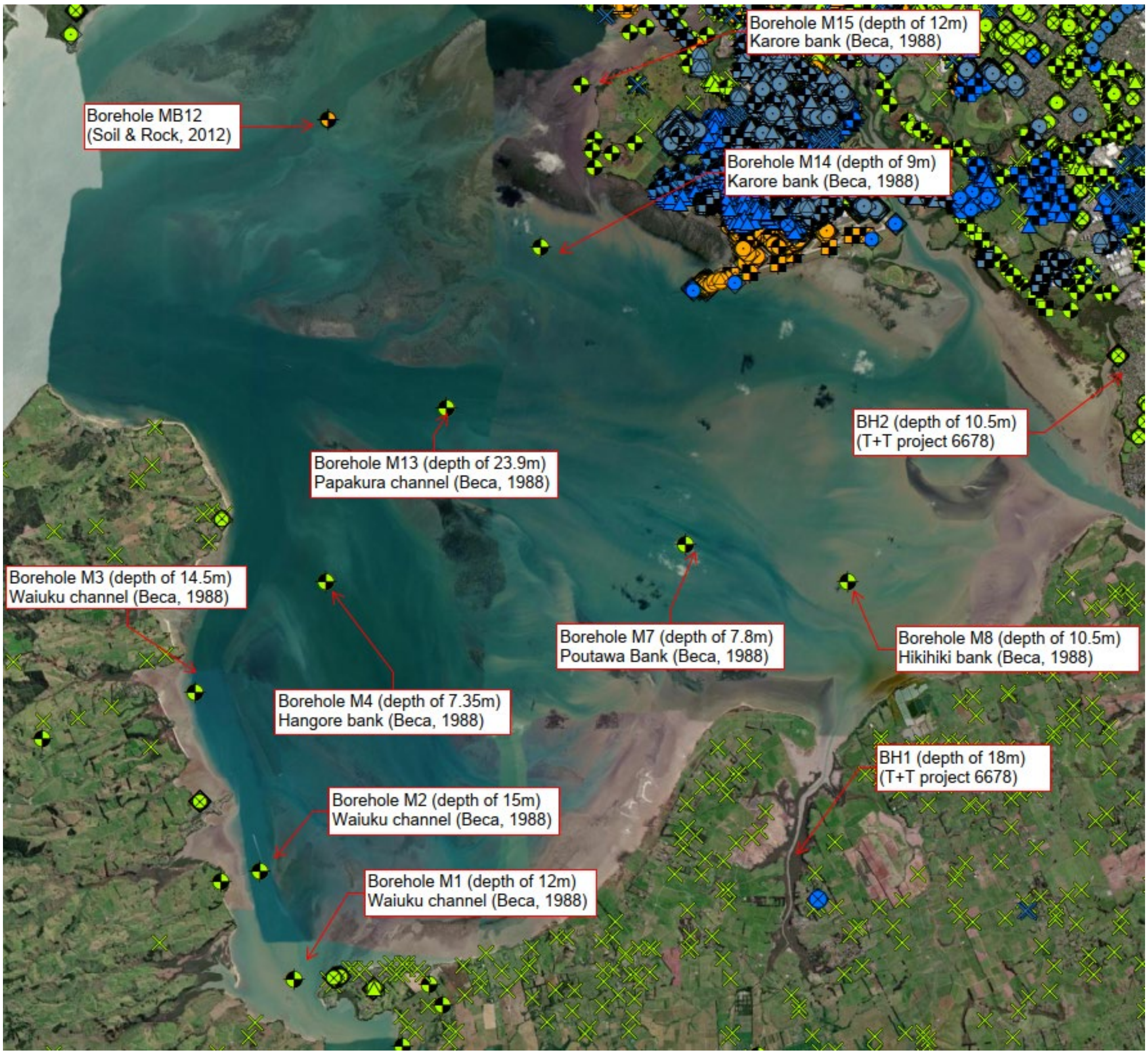

Figure Appendix A.4: Manukau Harbour known historic boreholes locations

Appendix A Table 11.1: Manukau Harbour borehole information (inner harbour)

Borehole	Easting (NZTM)	Northing (NZTM)	Depth below surface (m)	Approx. surface RL (m CD)	Notes
M1	1749458	5888598	12	-7.6	
M2	1748806	5890658	15	-11	
M3	1747574	5894042	14.5	-2	
M4	1750057	5896145	7.35	-1.7	Suspect wrong location, should shift toward the east.
M7	1756887	5896842	7.8	0.5	
M8	1759964	5896150	10.5	1.5	
M12	1750102	5904918	n/a	-5	Suspect wrong location, was for a road development in Mangere.
M13	1752342	5899438	3.10	-21	
M14	1754137	5902495	9	1.6	
M15	1754904	5905550	12	3.4	

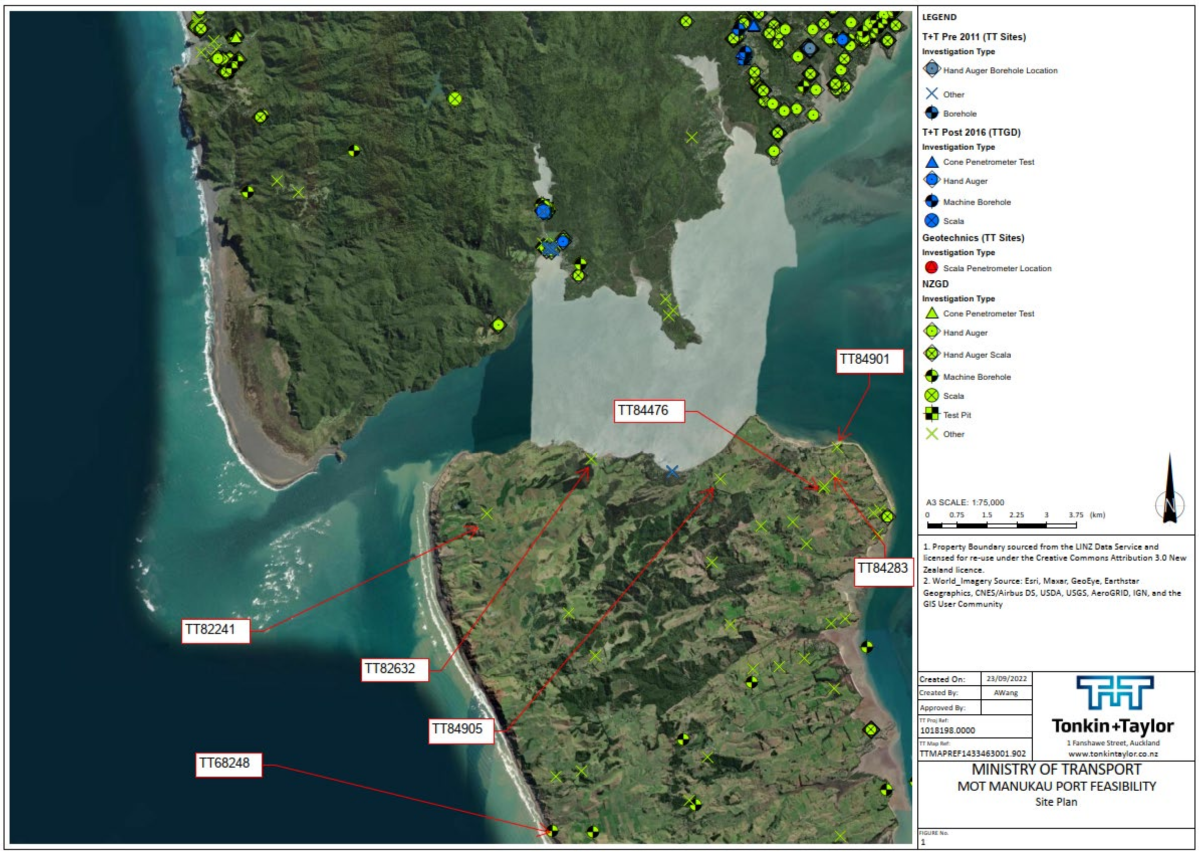

Figure Appendix A.5: Manukau Harbour entrance, known historic borehole locations

Appendix A Table 11.2: Manukau Harbour borehole information (harbour entrance)

Borehole	Easting (NZTM)	Northing (NZTM)	Depth below surface (m)	Approx. surface RL (m CD)
TT82241	1738002	5897409	256.61	199
TT82632	1740628	5898782	61.0	33
TT84283	1746760	5893360	60.10	52
TT84476	1746470	5898050	60.0	48
TT84901	1746820	5899080	316.0	8
TT84905	1743880	5898278	346.7	53
TT68248	1739641	5889437	66.25	5.5

Appendix B Geotechnical Information

- **B1 Existing side slopes**
- **B2 Slope stability outputs**

B1 Existing side slopes

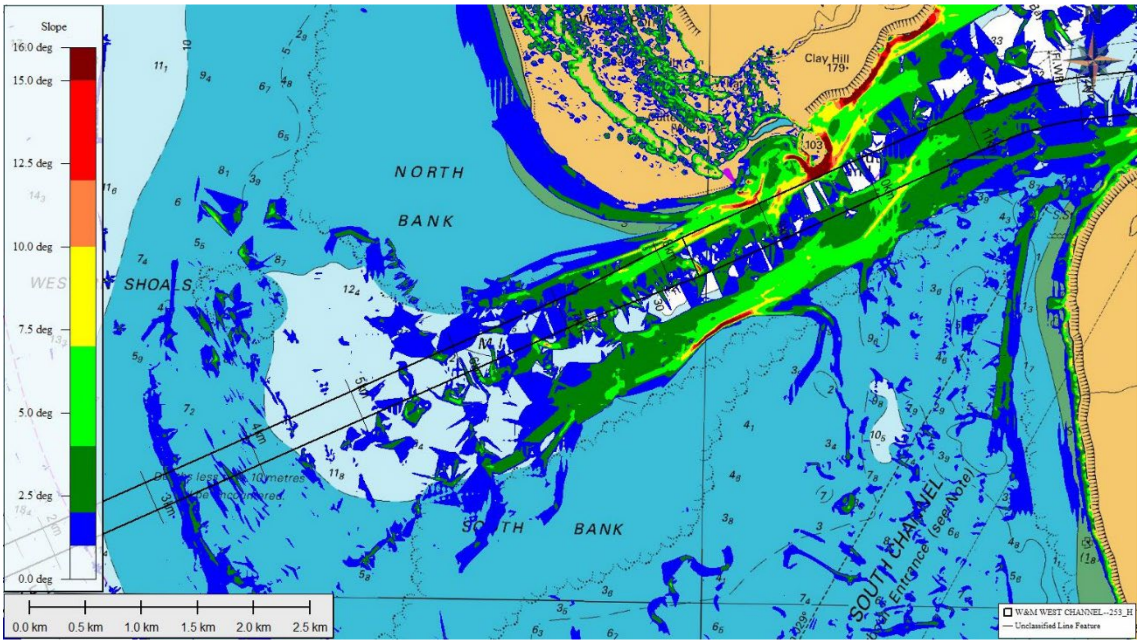

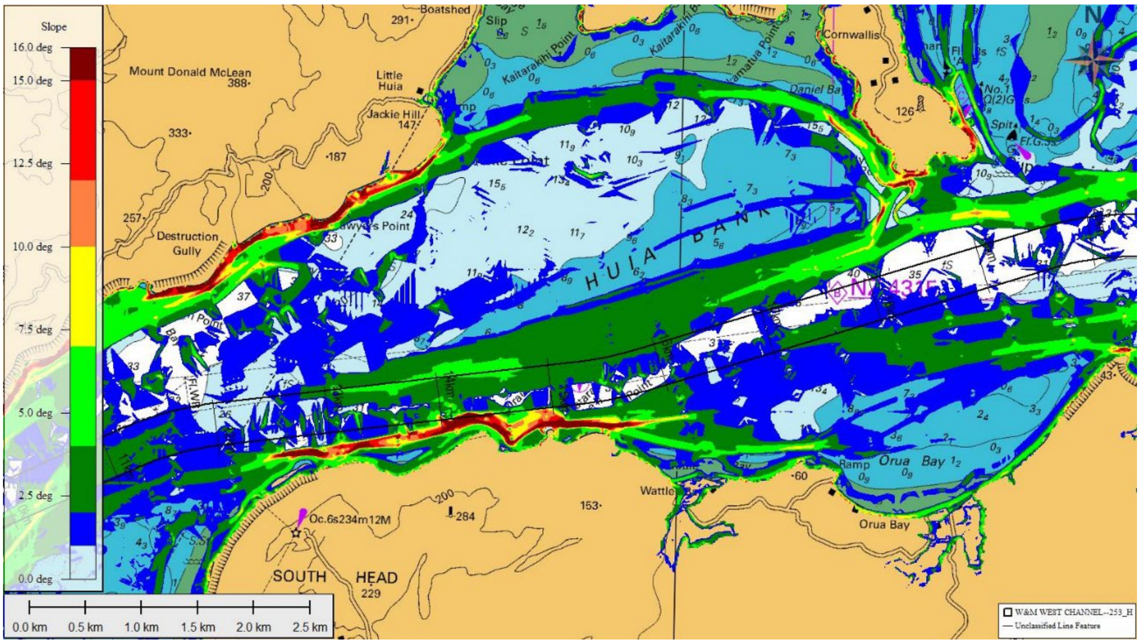

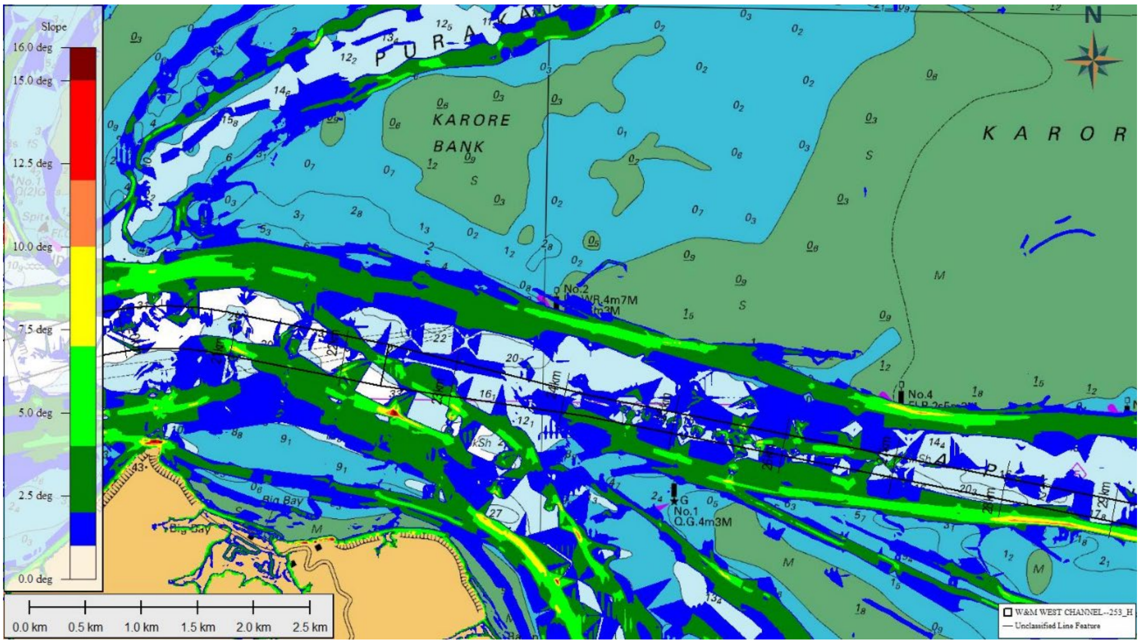

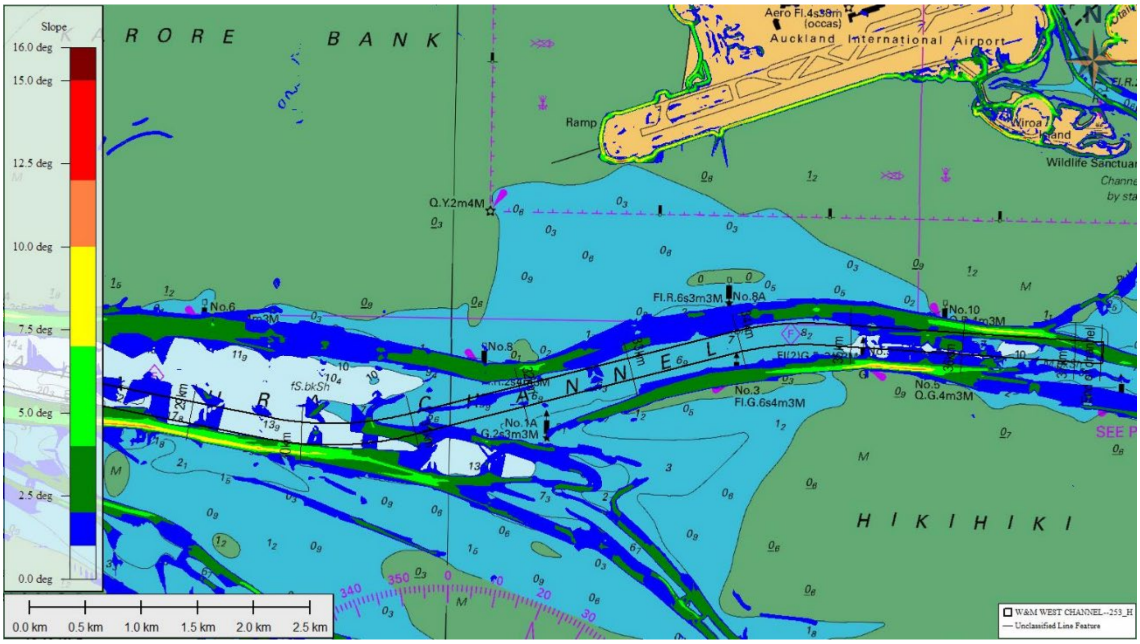

Appendix B Table 11.3: Side slopes along the existing channel alignment

Distance (Km) from seaward end of RH indicative channel	RH channel section	Channel depth required (m CD)	Average excavation depth (m)	Existing Side Slope angle (of nearest channel side) - degrees		
				Above -10m CD	Below - 10m CD	Notes
0	I	-20.5	0.0	N/A	0.5	Offshore slope - likely wave controlled
1	I	-20.5	0.0	N/A	0.5	Offshore slope - likely wave controlled
2	I	-20.5	3.2	N/A	0.5	Offshore slope - likely wave controlled
3	I	-20.5	9.6	1		Offshore slope - likely wave controlled

Distance (Km) from seaward end of RH indicative channel	RH channel section	Channel depth required (m CD)	Average excavation depth (m)	Existing Side Slope angle (of nearest channel side) - degrees		
				Above -10m CD	Below - 10m CD	Notes
4	I	-20.5	14.9	1		slope on back of bar = wave/current controlled
5	I	-20.5	10.2	1		slope on back of bar = wave/current controlled
6	I	-20.5	4.9	1		north side
7	I	-20.5	2.6	2	1.5	north side
8	I	-20.5	0.0	3	6	Steep channel on north side adjacent Whatipu
9	I	-20.5	0.0	8	5	Steep channel on north side adjacent Whatipu
10	I	-20.5	0.0	4	4	Steep channel on north side adjacent Whatipu
11	I	-20.5	0.0	N/A	2	
12	II	-19.1	0.0	N/A	2	
13	II	-19.1	0.0	10	7.5	Steep channel on sth side adjacent Awhitu
14	II	-19.1	0.0	8	8	Steep channel on sth side adjacent Awhitu
15	II	-19.1	0.0	15	15	Steep channel on sth side adjacent Awhitu
16	II	-19.1	0.0	3.5	2.5	North side
17	II	-19.1	0.0	2	3	North side
18	II	-19.1	0.0	1.5	4	North side
19	II	-19.1	0.0	N/A	4	north side
20	II	-19.1	0.0	N/A	3	north side
21	III	-17.7	0.0	1.5	3.5	North side
22	III	-17.7	0.0	1.5	2.5	South side
23	III	-17.7	0.0	1.5	2.5	north side
24	III	-17.7	0.0	3	3	North side
25	III	-17.7	0.0	3.5	1.5	North side
26	III	-17.7	0.0	2	1.5	North side
27	III	-17.7	0.0	5	3	North side
28	III	-17.7	0.0	3	2.5	North side
29	III	-17.7	1.9	2.5	1.5	North side - seems like accumulation of material in lower parts of slope
30	III	-17.7	3.2	4	4	South side
31	III	-17.7	8.5	3	1.5	south side
32	III	-17.7	10.0	2	N/A	north side
33	III	-17.7	10.3	2	N/A	
34	III	-17.7	10.0	3	N/A	south bank (north ~2 deg)
35	III	-17.7	9.0	4	N/A	south bank (north ~2 deg)
36	III	-17.7	9.2	3	N/A	both sides
37	III	-17.7	12.7	1.5	N/A	both sides

Shading	No dredging	dredging required

B2 Slope stability outputs

Color	Name	Slope Stability Material Model	Unit Weight (kN/m³)	Effective Cohesion (kPa)	Effective Friction Angle (°)	Piezometric Surface
	Dense SAND	Mohr-Coulomb	18	0	38	1
	Loose SAND	Mohr-Coulomb	17	0	30	1

5 to 1 scale distortion

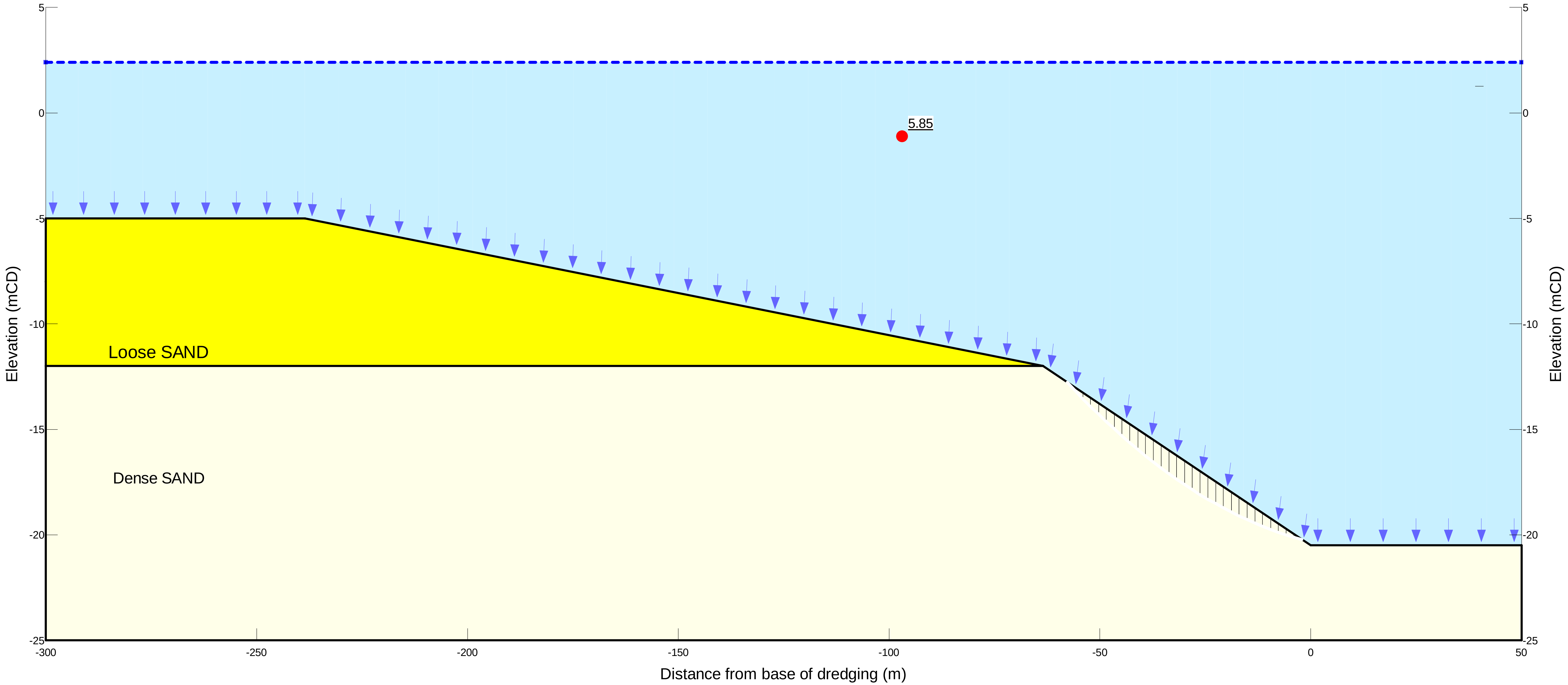

Tonkin+Taylor

Project: Manukau_Port_Bar_Crossing_270724.gsz	
Project Number: 1018198	
A3 Scale: 1:1,000	Vertical Exaggeration: 5
Analysed by: Andrew Langbein	Checked By: Andrew Langbein

Analysis Details:
1. Scenario: 1.a. Proposed Profile - deep slip
2. Method: Morgenstern-Price
3. Direction of movement: Left to Right
4. Slip Surface Option: Entry and Exit
5. PWP Conditions: Piezometric Surfaces
6. Optimization: No
7. Tension Crack Option: (none)
8. F of S Calculation Option: Constant
9. Horizontal Seismic Load:

Analysis Description:
1(vert):25(horiz) above -12 mCD
1(vert::7.5(horiz) below -12mCD

Directory: P:\1018198\WorkingMaterial\B_Coastal_processes_and_engineering\06_Geotech\01 Slope Stability\02 Slope Stability\

Color	Name	Slope Stability Material Model	Unit Weight (kN/m³)	Effective Cohesion (kPa)	Effective Friction Angle (°)	Piezometric Surface
	Dense SAND	Mohr-Coulomb	18	0	38	1
	Loose SAND	Mohr-Coulomb	17	0	30	1

5 to 1 scale distortion

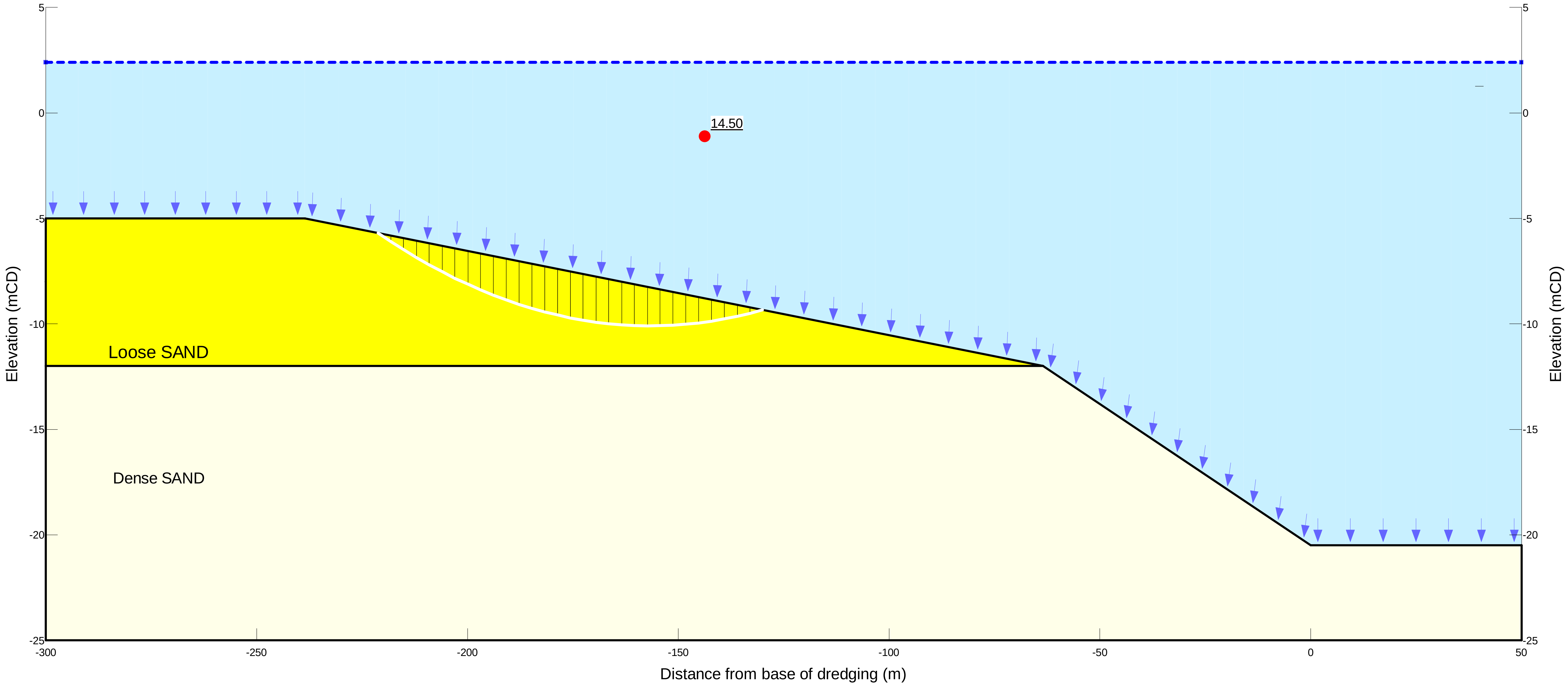

Tonkin+Taylor

Project: Manukau_Port_Bar_Crossing_270724.gsz	
Project Number: 1018198	
A3 Scale: 1:1,000	Vertical Exaggeration: 5
Analysed by: Andrew Langbein	Checked By: Andrew Langbein

Analysis Details:
1. Scenario: 1.b. Proposed Profile - shallow slip
2. Method: Morgenstern-Price
3. Direction of movement: Left to Right
4. Slip Surface Option: Entry and Exit
5. PWP Conditions: Piezometric Surfaces
6. Optimization: No
7. Tension Crack Option: (none)
8. F of S Calculation Option: Constant
9. Horizontal Seismic Load:

Analysis Description:
1(vert):25(horiz) above -12 mCD
1(vert::7.5(horiz) below -12mCD

Directory: P:\1018198\WorkingMaterial\B_Coastal_processes_and_engineering\06_Geotech\01 Slope Stability\02 Slope Stability\

Color	Name	Slope Stability Material Model	Unit Weight (kN/m³)	Effective Cohesion (kPa)	Effective Friction Angle (°)	Cohesion R (kPa)	Phi R (°)	Piezometric Surface
	Dense SAND	Mohr-Coulomb	18	0	38	0	0	1
	Loose SAND	Mohr-Coulomb	17	0	30	0	0	1

5 to 1 scale distortion

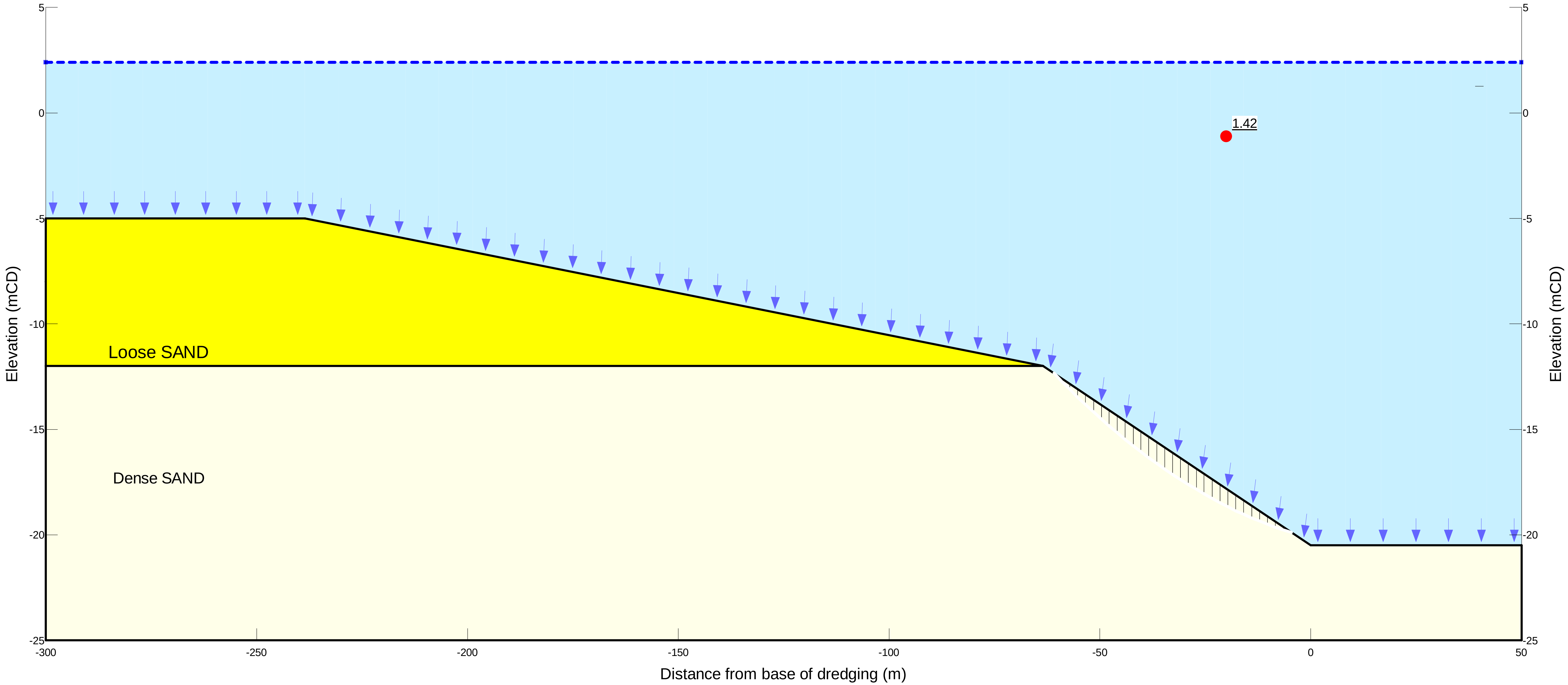

Tonkin+Taylor	Project: Manukau_Port_Bar_Crossing_270724.gsz		
	Project Number: 1018198		
	A3 Scale: 1:1,000	Vertical Exaggeration: 5	
	Analysed by: Andrew Langbein	Checked By: Andrew Langbein	

Analysis Details:
1. Scenario: 1.c. Proposed Profile - seismic
2. Method: Morgenstern-Price
3. Direction of movement: Left to Right
4. Slip Surface Option: Entry and Exit
5. PWP Conditions: Piezometric Surfaces
6. Optimization: No
7. Tension Crack Option: (none)
8. F of S Calculation Option: Constant
9. Horizontal Seismic Load: 0.19

Analysis Description:
1(vert):25(horiz) above -12 mCD
1(vert::7.5(horiz) below -12mCD

Directory: P:\1018198\WorkingMaterial\B_Coastal_processes_and_engineering\06_Geotech\01 Slope Stability\02 Slope Stability\

Color	Name	Slope Stability Material Model	Unit Weight (kN/m³)	Effective Cohesion (kPa)	Effective Friction Angle (°)	Piezometric Surface
(light cream)	Dense SAND	Mohr-Coulomb	18	0	38	1
(yellow)	Loose SAND	Mohr-Coulomb	17	0	30	1
(light green)	Soft SILTS	Mohr-Coulomb	16.5	0	20	1

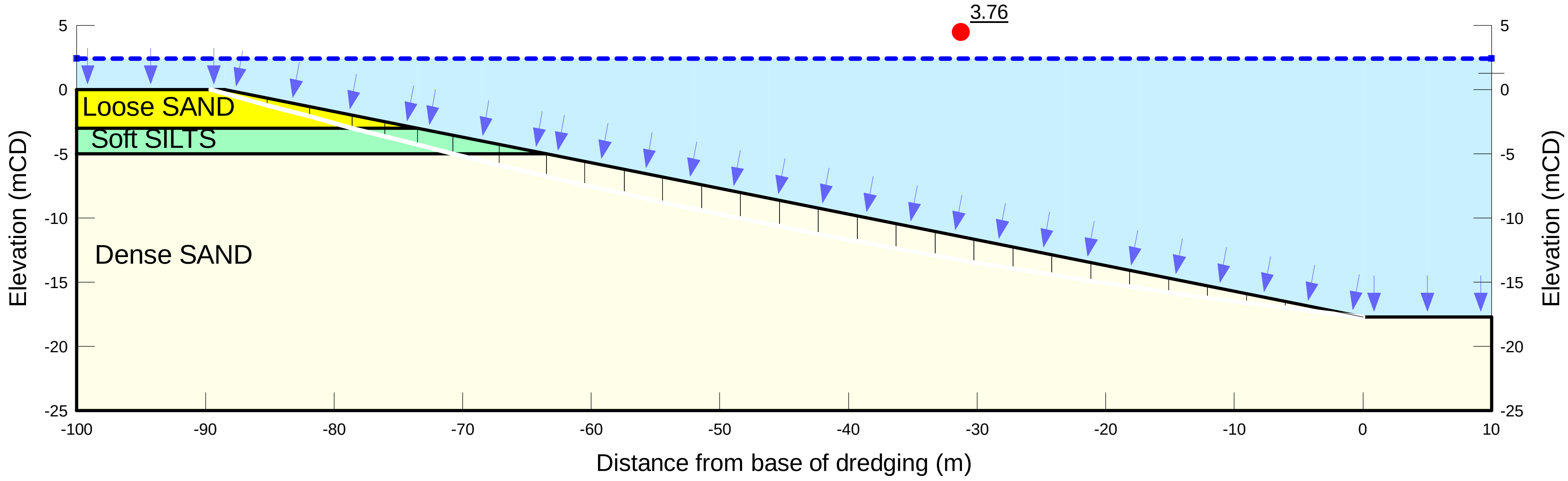

Analysis Description:
M7
1(vert):5(horiz) constant grade above -17.7mCD

Tonkin+Taylor	Project: Manukau_Port_Papakura Channel_270724.gsz	
	Project Number: 1018198	
	A3 Scale: 1:500	Vertical Exaggeration: 1
	Analysed by: Andrew Langbein	Checked By: Andrew Langbein

Analysis Details:
1. Scenario: 1.a. Proposed Profile - deep slip
2. Method: Morgenstern-Price
3. Direction of movement: Left to Right
4. Slip Surface Option: Entry and Exit
5. PWP Conditions: Piezometric Surfaces
6. Optimization: No
7. Tension Crack Option: (none)
8. F of S Calculation Option: Constant
9. Horizontal Seismic Load: 0

Directory: P:\1018198\WorkingMaterial\B_Coastal_processes_and_engineering\06_Geotech\01 Slope Stability\02 Slope Stability\

Color	Name	Slope Stability Material Model	Unit Weight (kN/m³)	Effective Cohesion (kPa)	Effective Friction Angle (°)	Piezometric Surface
	Dense SAND	Mohr-Coulomb	18	0	38	1
	Loose SAND	Mohr-Coulomb	17	0	30	1
	Soft SILTS	Mohr-Coulomb	16.5	0	20	1

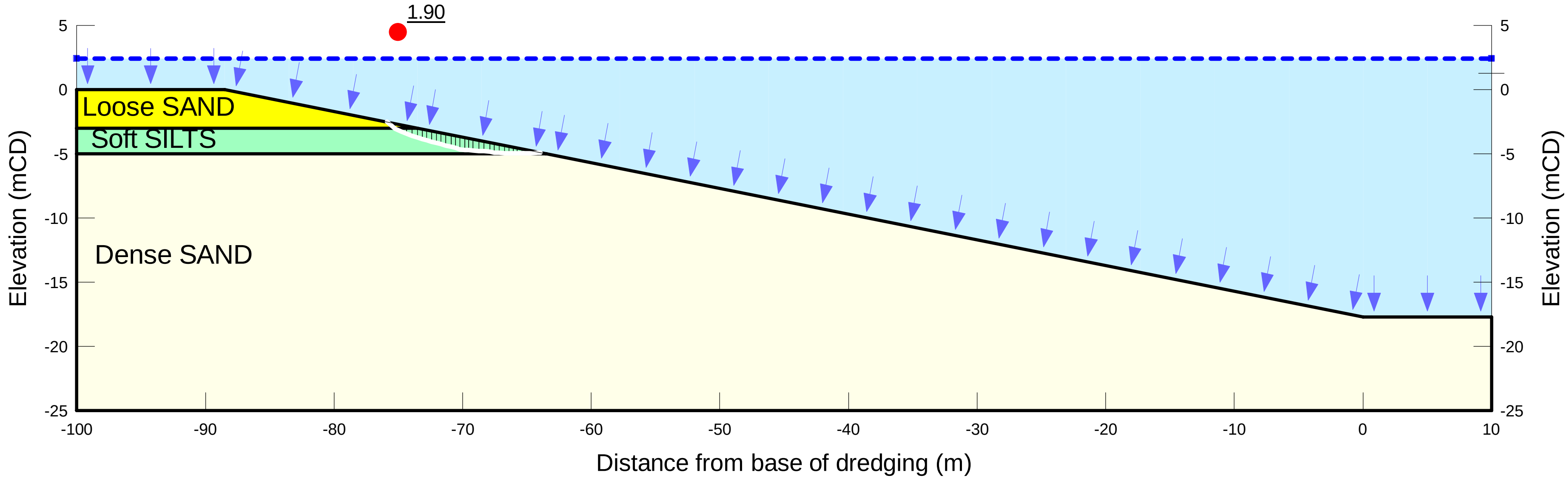

Analysis Description:
M7
1(vert):5(horiz) constant grade above -17.7mCD

Tonkin+Taylor

Project: Manukau_Port_Papakura Channel_270724.gsz	
Project Number: 1018198	
A3 Scale: 1:500	Vertical Exaggeration: 1
Analysed by: Andrew Langbein	Checked By: Andrew Langbein

Analysis Details:
1. Scenario: 1.b. Proposed Profile - mid slip
2. Method: Morgenstern-Price
3. Direction of movement: Left to Right
4. Slip Surface Option: Entry and Exit
5. PWP Conditions: Piezometric Surfaces
6. Optimization: Yes
7. Tension Crack Option: (none)
8. F of S Calculation Option: Constant
9. Horizontal Seismic Load:

Directory: P:\1018198\WorkingMaterial\B_Coastal_processes_and_engineering\06_Geotech\01 Slope Stability\02 Slope Stability\

Color	Name	Slope Stability Material Model	Unit Weight (kN/m³)	Effective Cohesion (kPa)	Effective Friction Angle (°)	Piezometric Surface
	Dense SAND	Mohr-Coulomb	18	0	38	1
	Loose SAND	Mohr-Coulomb	17	0	30	1
	Soft SILTS	Mohr-Coulomb	16.5	0	20	1

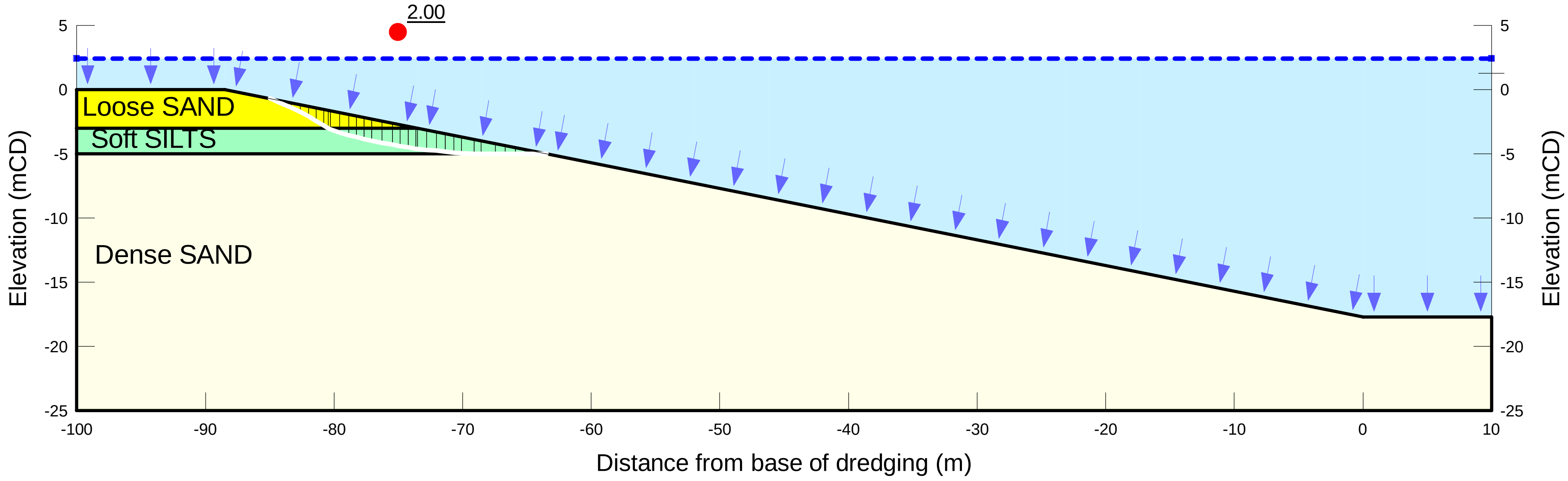

Analysis Description:
M7
1(vert):5(horiz) constant grade above -17.7mCD

Tonkin+Taylor

Project: Manukau_Port_Papakura Channel_270724.gsz	
Project Number: 1018198	
A3 Scale: 1:500	Vertical Exaggeration: 1
Analysed by: Andrew Langbein	Checked By: Andrew Langbein

Analysis Details:
1. Scenario: 1.c. Proposed Profile - shallow slip
2. Method: Morgenstern-Price
3. Direction of movement: Left to Right
4. Slip Surface Option: Entry and Exit
5. PWP Conditions: Piezometric Surfaces
6. Optimization: Yes
7. Tension Crack Option: (none)
8. F of S Calculation Option: Constant
9. Horizontal Seismic Load:

Directory: P:\1018198\WorkingMaterial\B_Coastal_processes_and_engineering\06_Geotech\01 Slope Stability\02 Slope Stability\

Color	Name	Slope Stability Material Model	Unit Weight (kN/m³)	Effective Cohesion (kPa)	Effective Friction Angle (°)	Cohesion R (kPa)	Phi R (°)	Piezometric Surface
	Dense SAND	Mohr-Coulomb	18	0	38	0	0	1
	Loose SAND	Mohr-Coulomb	17	0	30	0	0	1
	Soft SILTS	Mohr-Coulomb	16.5	0	20	0	0	1

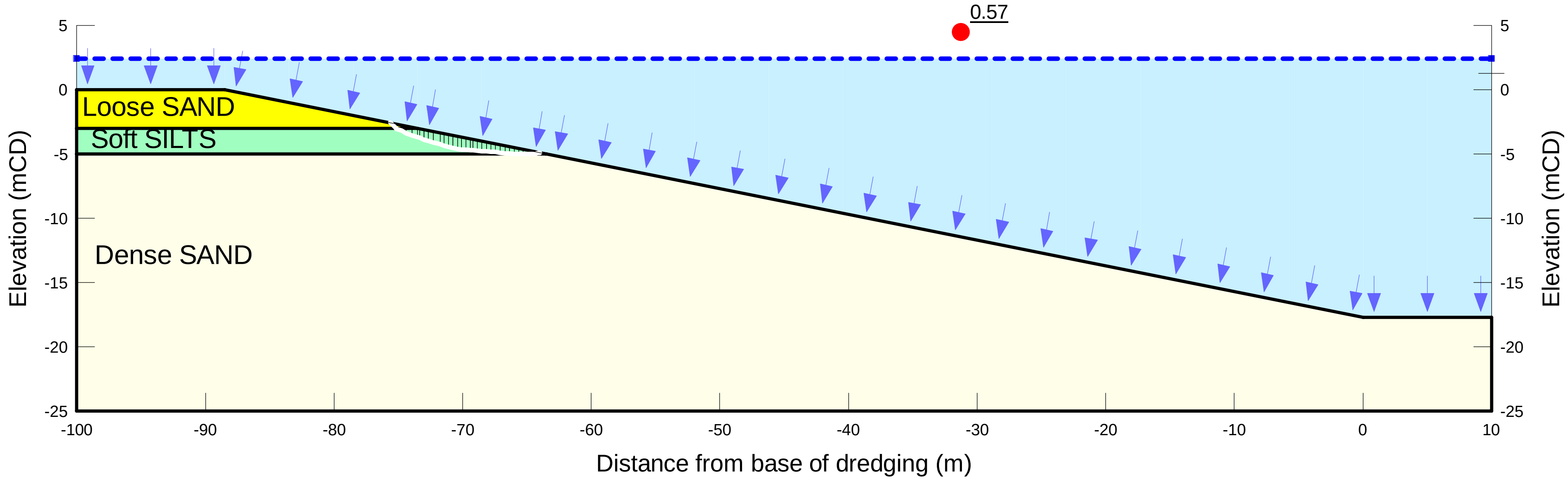

Analysis Description:
M7
1(vert):5(horiz) constant grade above -17.7mCD

Project: Manukau_Port_Papakura Channel_270724.gsz	
Project Number: 1018198	
A3 Scale: 1:500	Vertical Exaggeration: 1
Analysed by: Andrew Langbein	Checked By: Andrew Langbein

Tonkin+Taylor

Analysis Details:
1. Scenario: 1.d. Proposed Profile - seismic
2. Method: Morgenstern-Price
3. Direction of movement: Left to Right
4. Slip Surface Option: Entry and Exit
5. PWP Conditions: Piezometric Surfaces
6. Optimization: Yes
7. Tension Crack Option: (none)
8. F of S Calculation Option: Constant
9. Horizontal Seismic Load: 0.19

Directory: P:\1018198\WorkingMaterial\B_Coastal_processes_and_engineering\06_Geotech\01 Slope Stability\02 Slope Stability\

Color	Name	Slope Stability Material Model	Unit Weight (kN/m³)	Effective Cohesion (kPa)	Effective Friction Angle (°)	Cohesion R (kPa)	Phi R (°)	Piezometric Surface
	Dense SAND	Mohr-Coulomb	18	0	38	0	0	1
	Loose SAND	Mohr-Coulomb	17	0	30	0	0	1
	Soft SILTS	Mohr-Coulomb	16.5	0	20	0	0	1

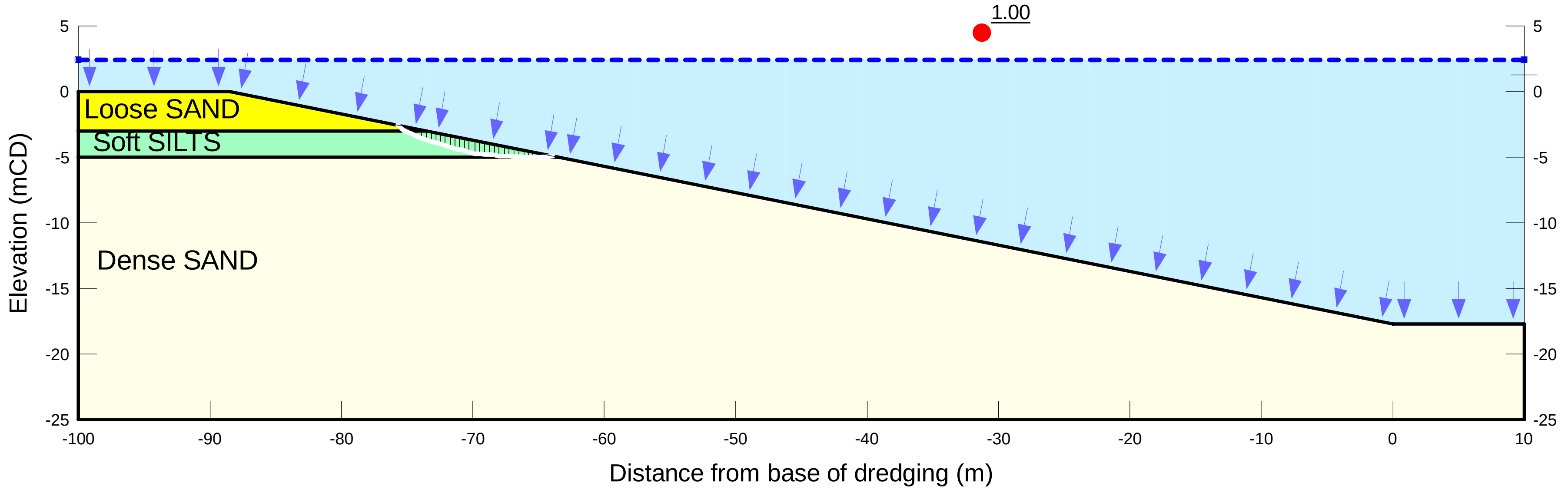

Analysis Description:
M7
1(vert):5(horiz) constant grade above -17.7mCD

Tonkin+Taylor

Project: Manukau_Port_Papakura Channel_270724.gsz	
Project Number: 1018198	
A3 Scale: 1:500	Vertical Exaggeration: 1
Analysed by: Andrew Langbein	Checked By: Andrew Langbein

Analysis Details:
1. Scenario: 1.e. Proposed Profile - yield
2. Method: Morgenstern-Price
3. Direction of movement: Left to Right
4. Slip Surface Option: Entry and Exit
5. PWP Conditions: Piezometric Surfaces
6. Optimization: Yes
7. Tension Crack Option: (none)
8. F of S Calculation Option: Constant
9. Horizontal Seismic Load: 0.074

Directory: P:\1018198\WorkingMaterial\B_Coastal_processes_and_engineering\06_Geotech\01 Slope Stability\02 Slope Stability\

Color	Name	Slope Stability Material Model	Unit Weight (kN/m³)	Effective Cohesion (kPa)	Effective Friction Angle (°)	Piezometric Surface
	Dense SAND	Mohr-Coulomb	18	0	38	1
	Soft SILTS	Mohr-Coulomb	16.5	0	20	1
	Very stiff CLAY	Mohr-Coulomb	17.5	5	30	1

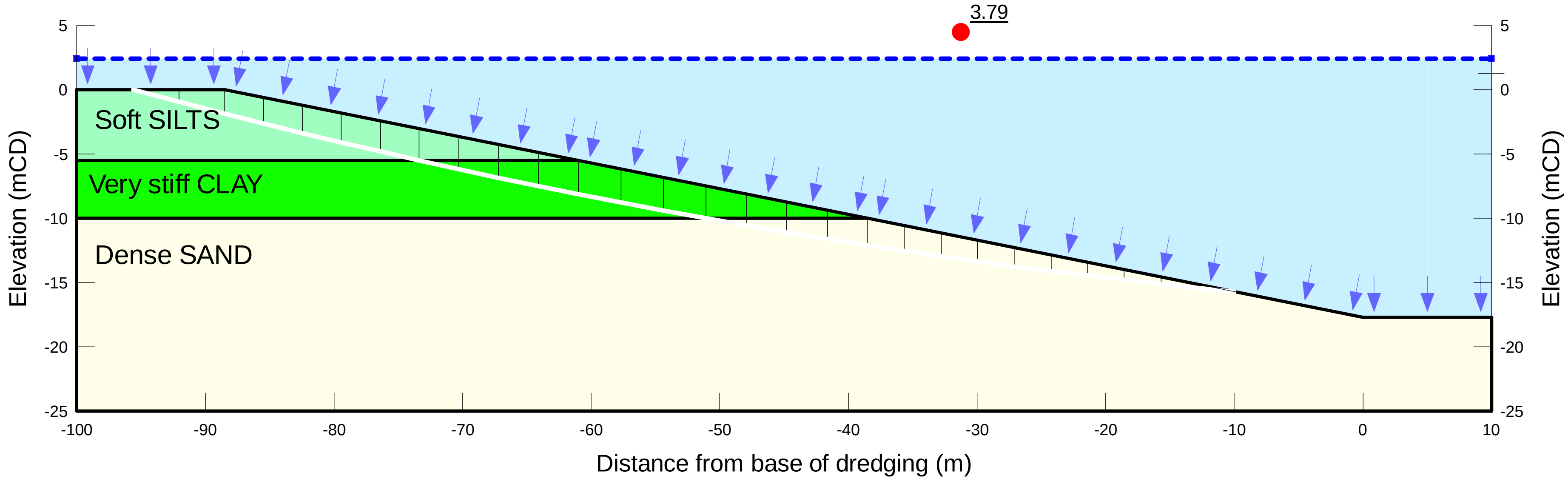

Analysis Description:
M8
1(vert):5(horiz) constant grade above -17.7mCD

Tonkin+Taylor

Project: Manukau_Port_Papakura Channel_270724.gsz	
Project Number: 1018198	
A3 Scale: 1:500	Vertical Exaggeration: 1
Analysed by: Andrew Langbein	Checked By: Andrew Langbein

Analysis Details:
1. Scenario: 2.a. Proposed Profile - deep slip
2. Method: Morgenstern-Price
3. Direction of movement: Left to Right
4. Slip Surface Option: Entry and Exit
5. PWP Conditions: Piezometric Surfaces
6. Optimization: No
7. Tension Crack Option: (none)
8. F of S Calculation Option: Constant
9. Horizontal Seismic Load: 0

Directory: P:\1018198\WorkingMaterial\B_Coastal_processes_and_engineering\06_Geotech\01 Slope Stability\02 Slope Stability\

Color	Name	Slope Stability Material Model	Unit Weight (kN/m³)	Effective Cohesion (kPa)	Effective Friction Angle (°)	Piezometric Surface
	Dense SAND	Mohr-Coulomb	18	0	38	1
	Soft SILTS	Mohr-Coulomb	16.5	0	20	1
	Very stiff CLAY	Mohr-Coulomb	17.5	5	30	1

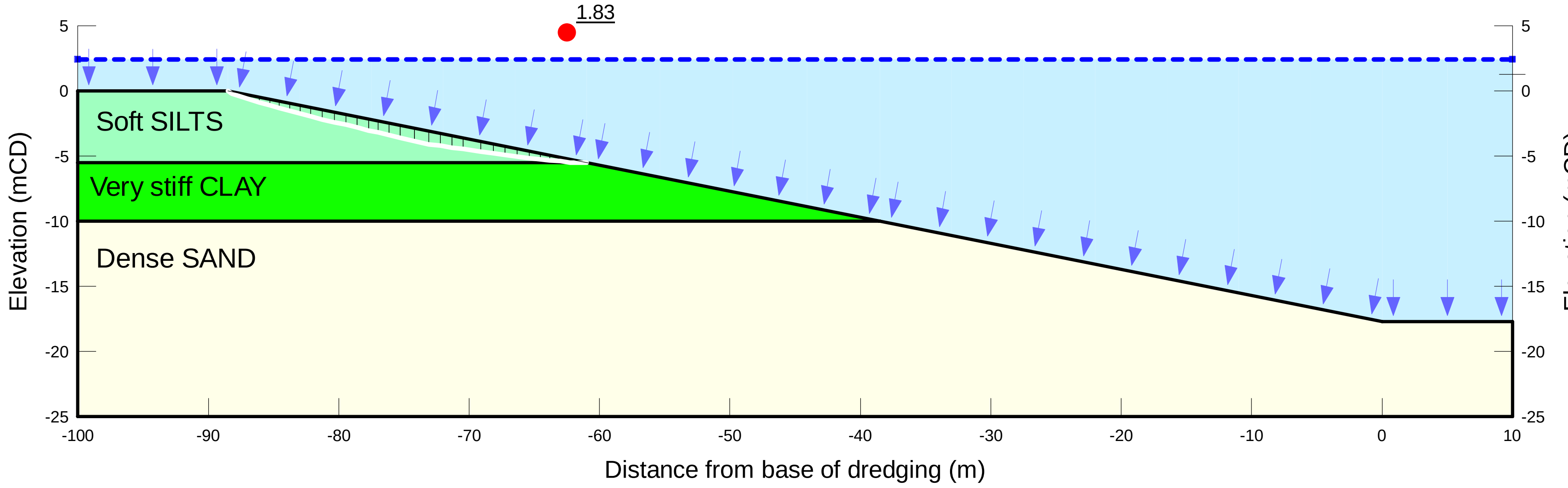

Analysis Description:
M8
1(vert):5(horiz) constant grade above -17.7mCD

Tonkin+Taylor	Project: Manukau_Port_Papakura Channel_270724.gsz	
	Project Number: 1018198	
	A3 Scale: 1:500	Vertical Exaggeration: 1
	Analysed by: Andrew Langbein	Checked By: Andrew Langbein

Analysis Details:
1. Scenario: 2.b. Proposed Profile - shallow slip
2. Method: Morgenstern-Price
3. Direction of movement: Left to Right
4. Slip Surface Option: Entry and Exit
5. PWP Conditions: Piezometric Surfaces
6. Optimization: Yes
7. Tension Crack Option: (none)
8. F of S Calculation Option: Constant
9. Horizontal Seismic Load:

Directory: P:\1018198\WorkingMaterial\B_Coastal_processes_and_engineering\06_Geotech\01 Slope Stability\02 Slope Stability\

Color	Name	Slope Stability Material Model	Unit Weight (kN/m³)	Effective Cohesion (kPa)	Effective Friction Angle (°)	Cohesion R (kPa)	Phi R (°)	Piezometric Surface
	Dense SAND	Mohr-Coulomb	18	0	38	0	0	1
	Soft SILTS	Mohr-Coulomb	16.5	0	20	0	0	1
	Very stiff CLAY	Mohr-Coulomb	17.5	5	30	0	0	1

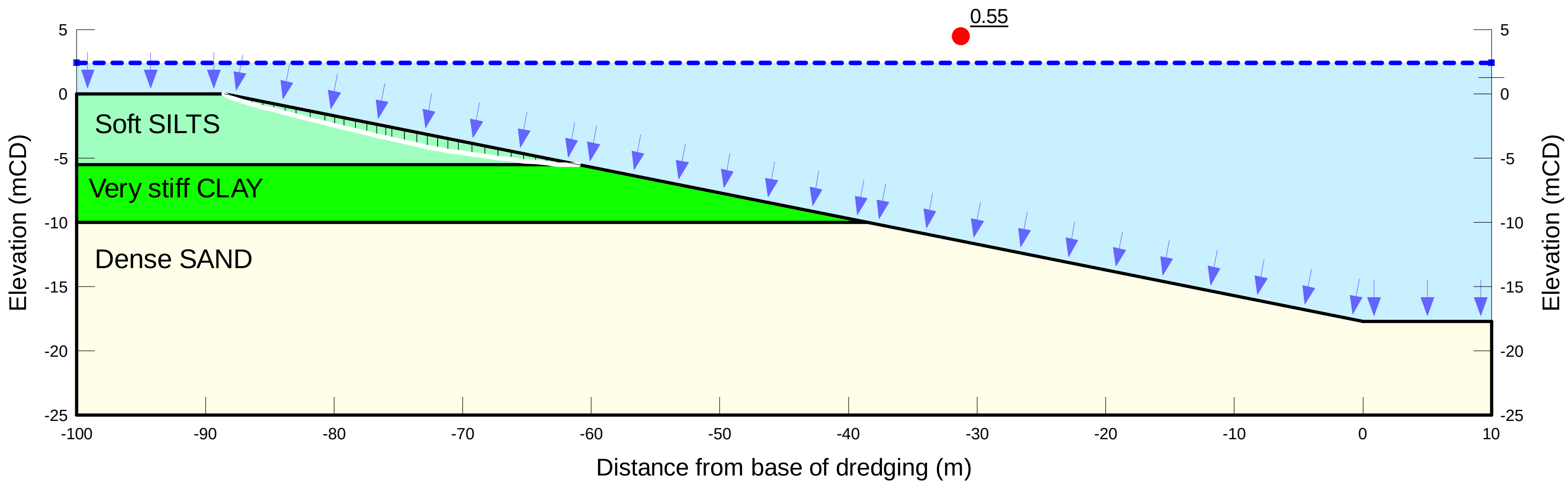

Analysis Description:
M8
1(vert):5(horiz) constant grade above -17.7mCD

Tonkin+Taylor	Project: Manukau_Port_Papakura Channel_270724.gsz	
	Project Number: 1018198	
	A3 Scale: 1:500	Vertical Exaggeration: 1
	Analysed by: Andrew Langbein	Checked By: Andrew Langbein

Analysis Details:
1. Scenario: 2.c. Proposed Profile - seismic
2. Method: Morgenstern-Price
3. Direction of movement: Left to Right
4. Slip Surface Option: Entry and Exit
5. PWP Conditions: Piezometric Surfaces
6. Optimization: Yes
7. Tension Crack Option: (none)
8. F of S Calculation Option: Constant
9. Horizontal Seismic Load: 0.19

Directory: P:\1018198\WorkingMaterial\B_Coastal_processes_and_engineering\06_Geotech\01 Slope Stability\02 Slope Stability\

Color	Name	Slope Stability Material Model	Unit Weight (kN/m³)	Effective Cohesion (kPa)	Effective Friction Angle (°)	Cohesion R (kPa)	Phi R (°)	Piezometric Surface
	Dense SAND	Mohr-Coulomb	18	0	38	0	0	1
	Soft SILTS	Mohr-Coulomb	16.5	0	20	0	0	1
	Very stiff CLAY	Mohr-Coulomb	17.5	5	30	0	0	1

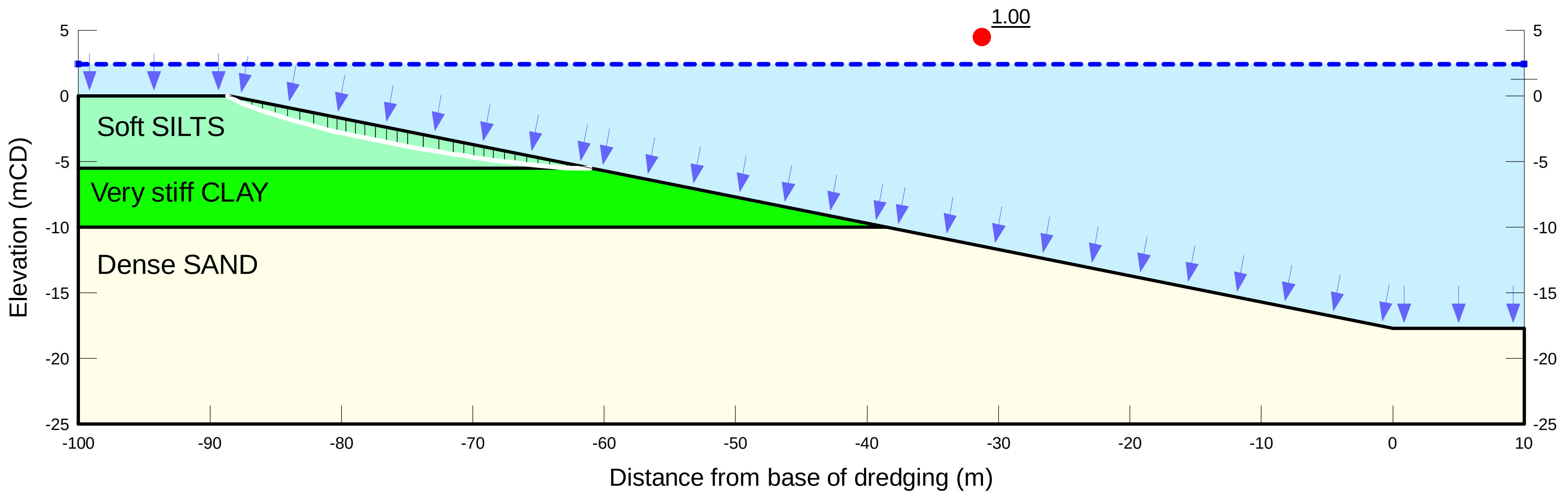

Analysis Description:
M8
1(vert):5(horiz) constant grade above -17.7mCD

Tonkin+Taylor

Project: Manukau_Port_Papakura Channel_270724.gsz	
Project Number: 1018198	
A3 Scale: 1:500	Vertical Exaggeration: 1
Analysed by: Andrew Langbein	Checked By: Andrew Langbein

Analysis Details:
1. Scenario: 2.d. Proposed Profile - yield
2. Method: Morgenstern-Price
3. Direction of movement: Left to Right
4. Slip Surface Option: Entry and Exit
5. PWP Conditions: Piezometric Surfaces
6. Optimization: Yes
7. Tension Crack Option: (none)
8. F of S Calculation Option: Constant
9. Horizontal Seismic Load: 0.068

Directory: P:\1018198\WorkingMaterial\B_Coastal_processes_and_engineering\06_Geotech\01 Slope Stability\02 Slope Stability\